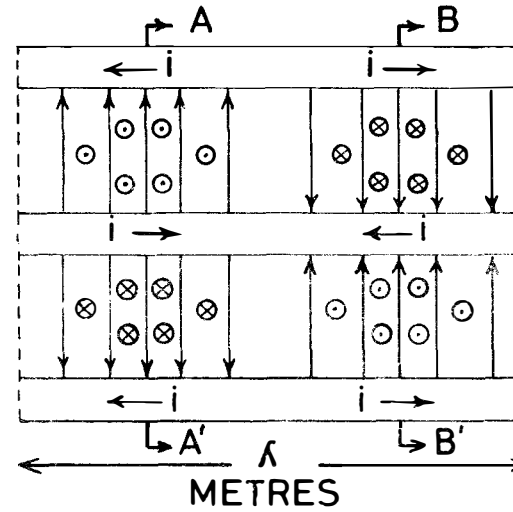
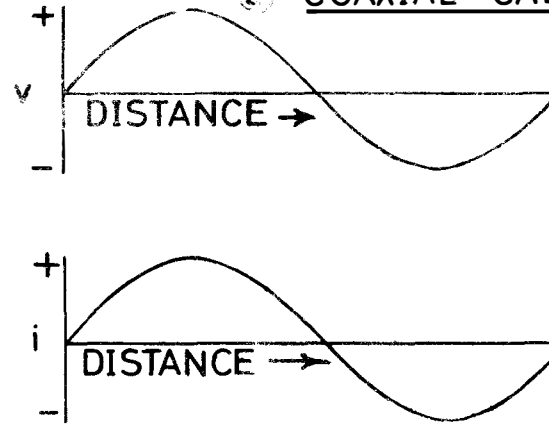


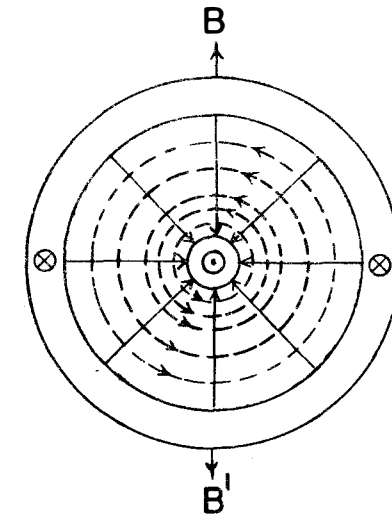
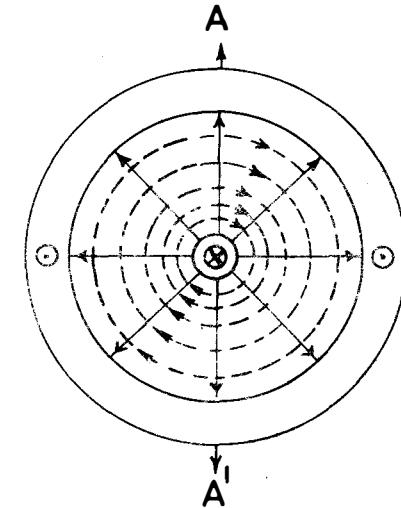
→ ELECTRIC FLUX  
 - - - → MAGNETIC FLUX  
 ⊕ CURRENT ENTERING PLANE  
 ⊙ CURRENT LEAVING PLANE



COAXIAL CABLES

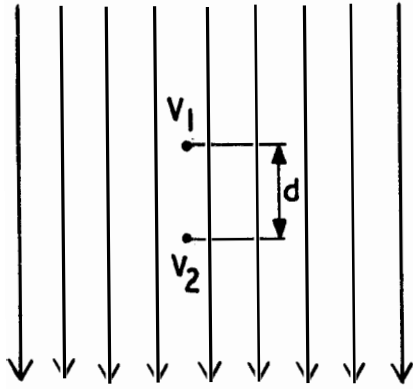


FIELD CONFIGURATIONS

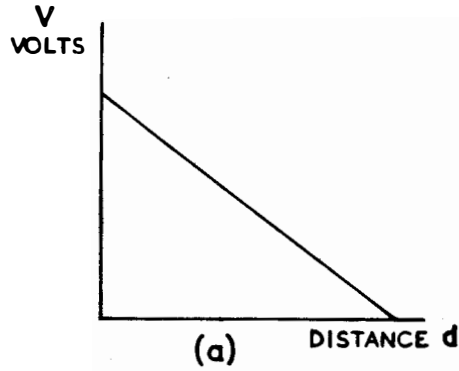


R36659

Fig. 1-1 Field configurations in a Capacitor, 2-Wire Line and Coaxial Cable



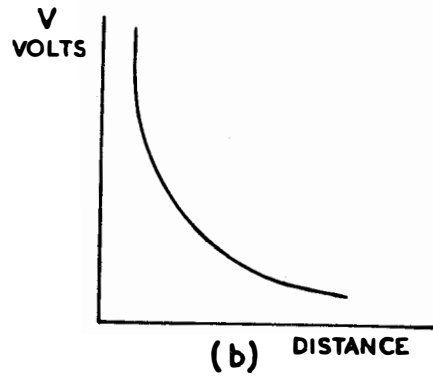
R44739



R43455

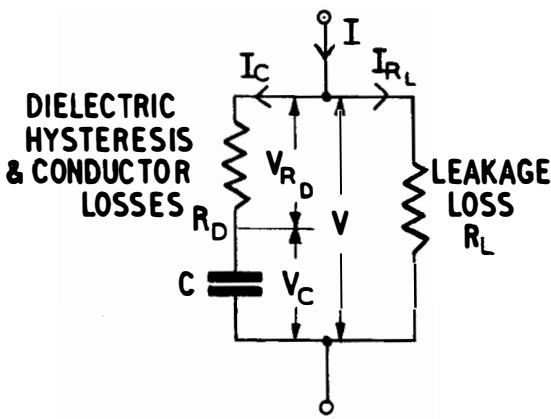
Uniform Field  
 $E = - \frac{V}{d}$

Fig. 1-2 Potential Gradient  
 $E = - \frac{(V_1 - V_2)}{d}$  volts/metre



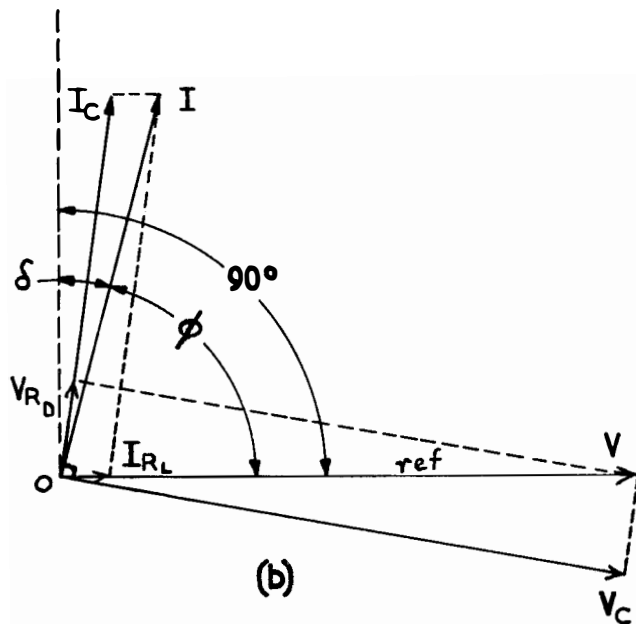
Non-Uniform Field  
 $E = - \frac{\delta V}{\delta d}$

Fig. 1-3



(a)

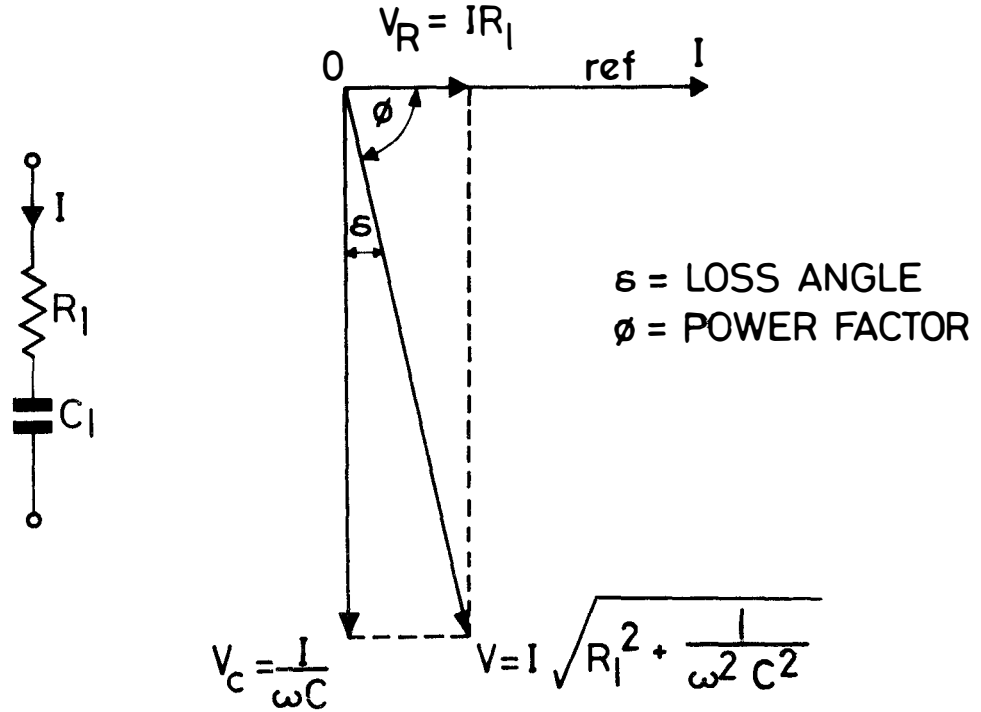
R35027 A



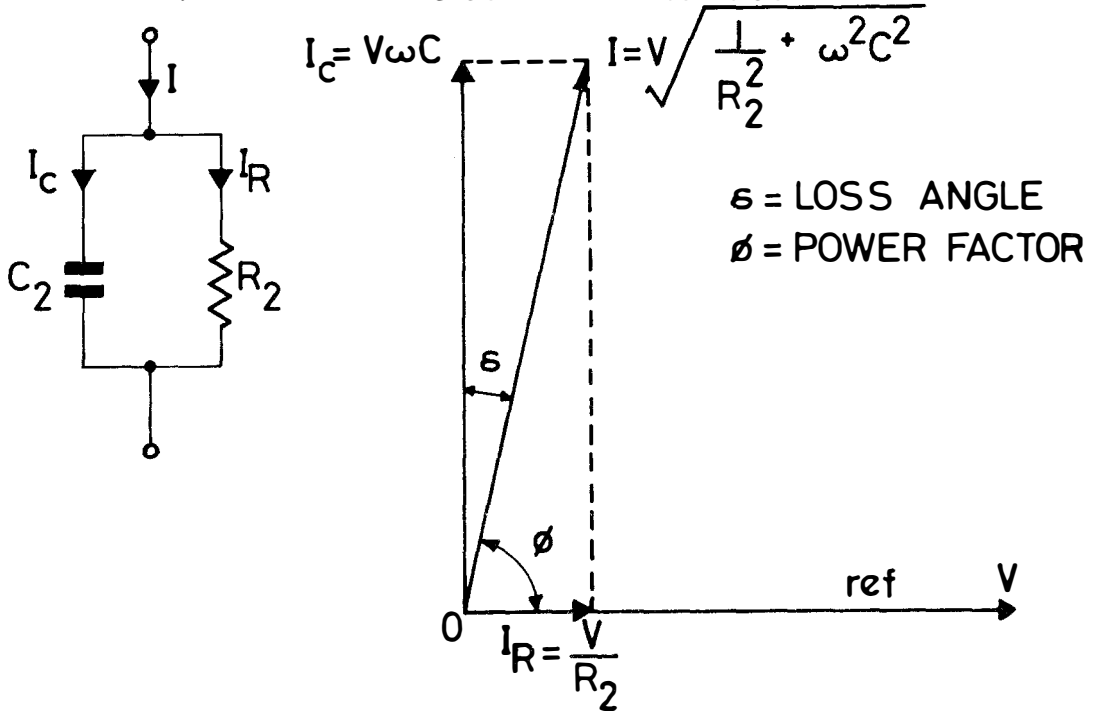
(b)

Fig. 1-4 Capacitor complete equivalent circuit and phasor diagram where  $\phi$  is the phase angle and  $\delta$  is the loss angle

SERIES EQUIVALENT CIRCUIT



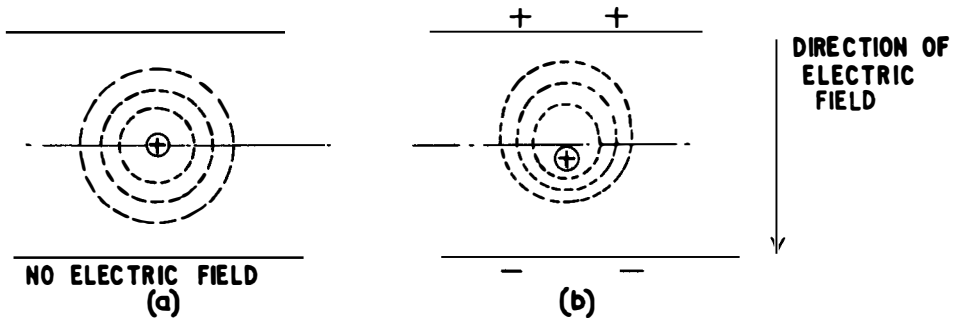
PARALLEL EQUIVALENT CIRCUIT



R36660

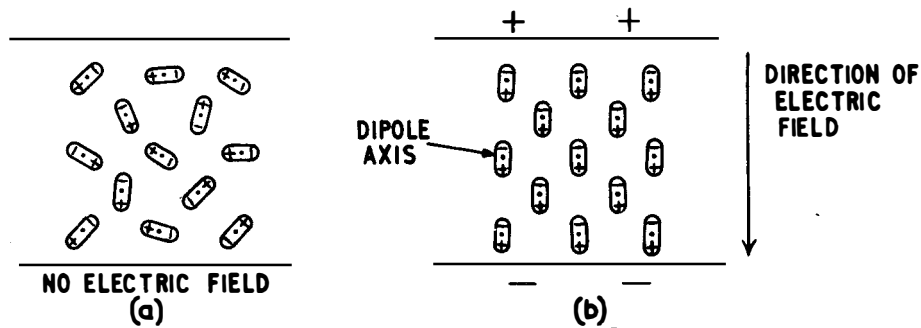
CAPACITOR EQUIVALENT CIRCUITS

Fig. 1-5 Capacitor; series and parallel equivalent circuits



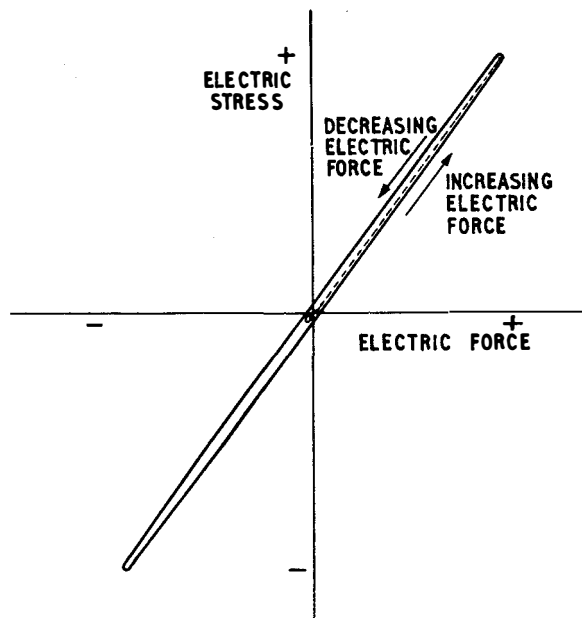
R 35024

Fig. 1-6 Elliptical distortion of an electron orbit by an electric field



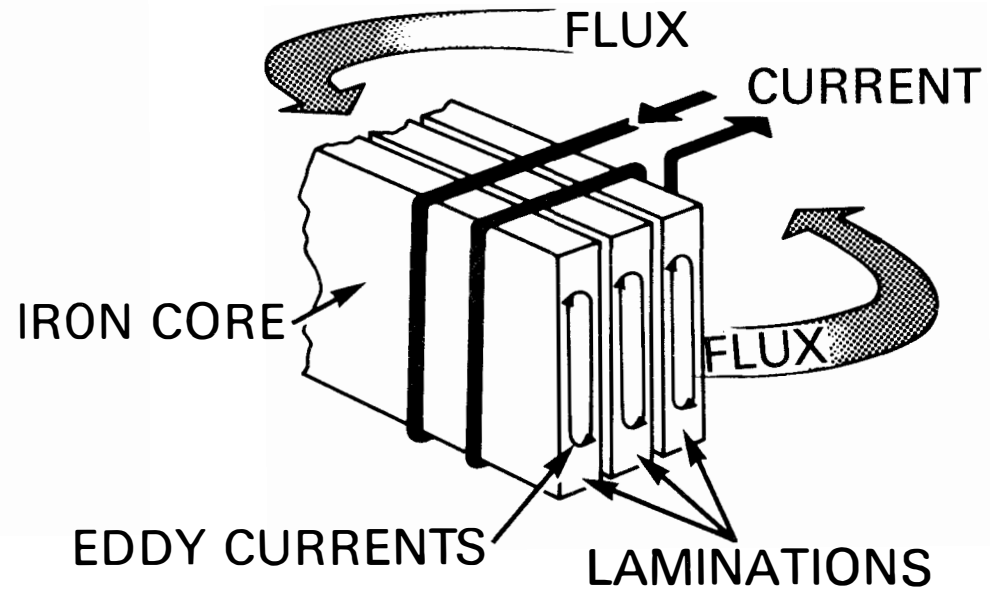
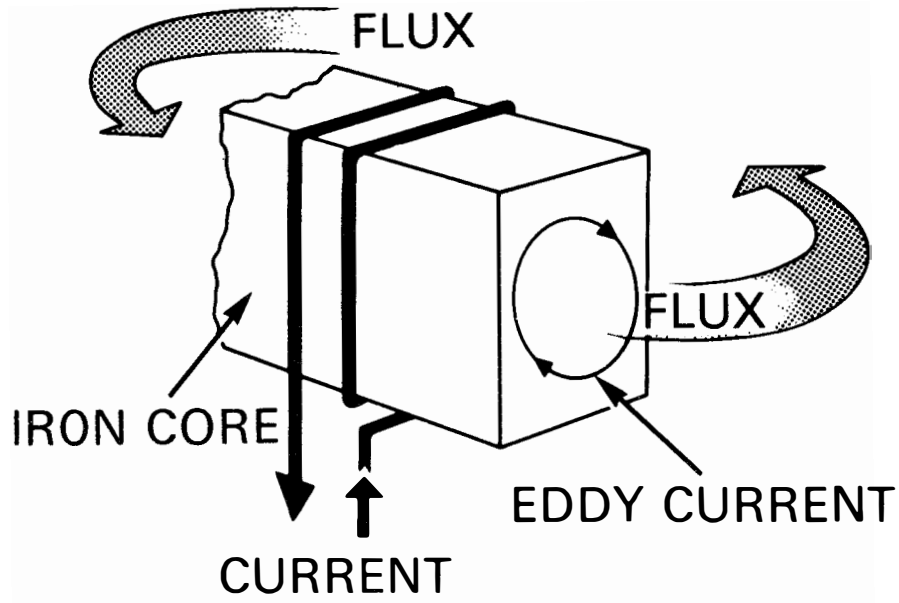
R 35025

Fig. 1-7 Polarization of molecules in an electric field



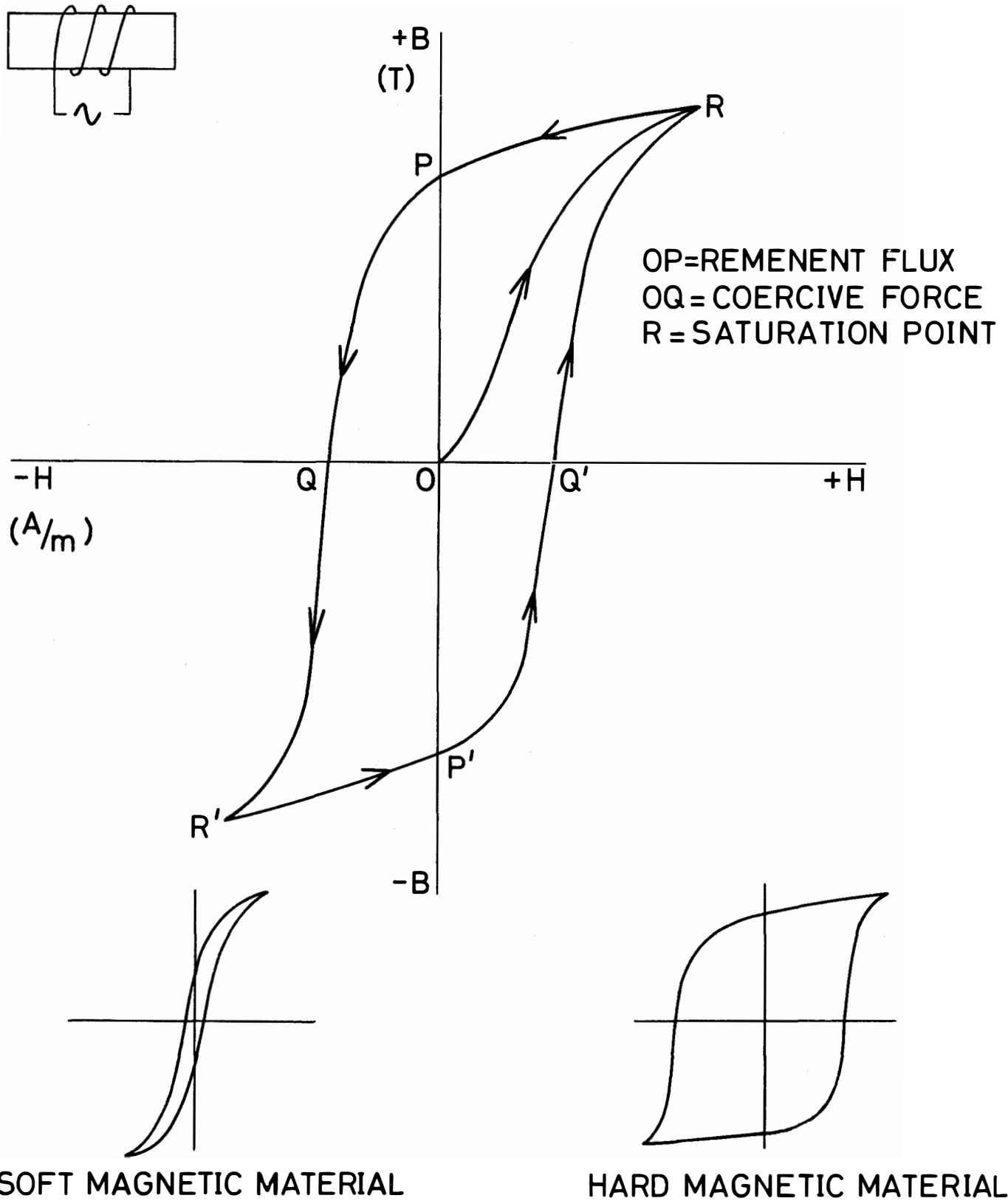
R 35026

Fig. 1-8 Dielectric hysteresis



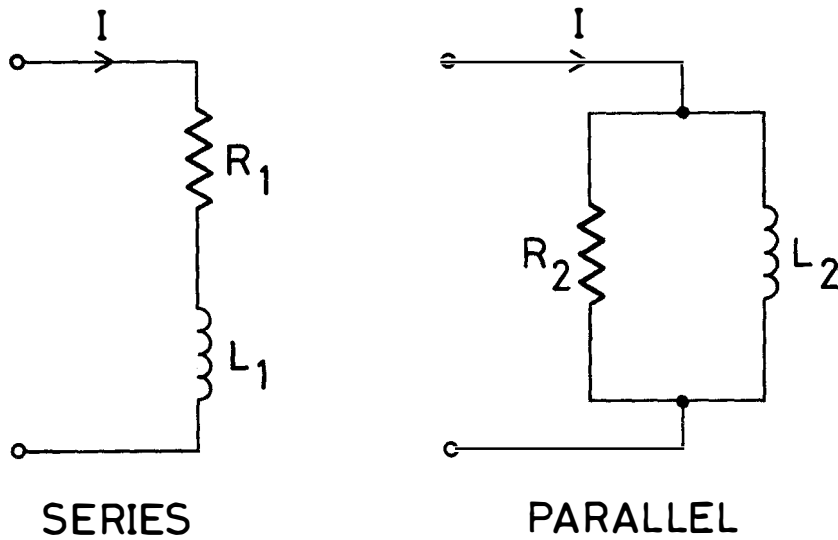
R36661

Fig. 2-1 Reducing Eddy Currents by the use of laminations

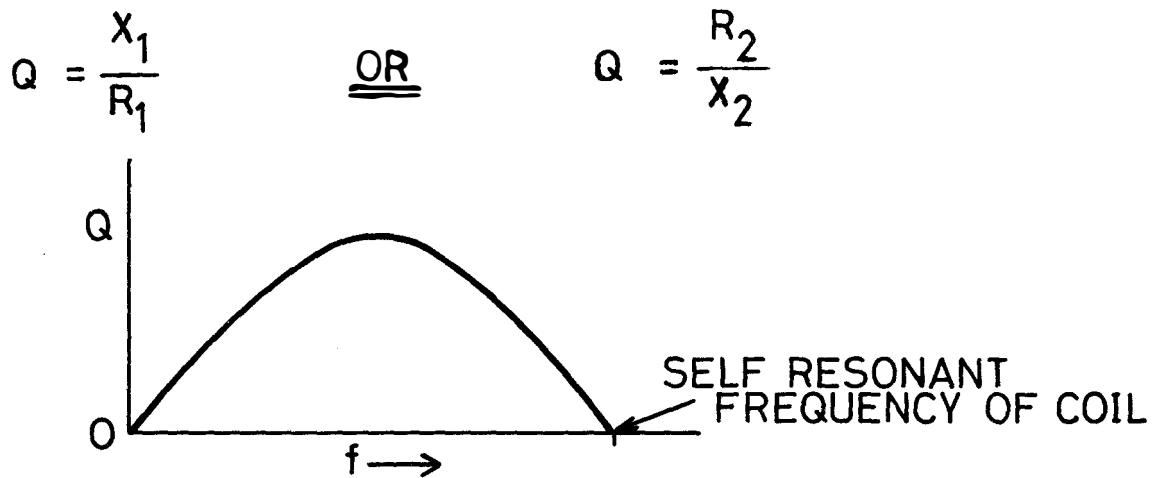


R36662

Fig. 2-2 Hysteresis loops for general, hard and soft magnetic materials



INDUCTOR EQUIVALENT CIRCUIT



VARIATION OF Q FACTOR WITH FREQUENCY

R36663

Fig. 2-3 Inductor Equivalent Circuits and Q Factor

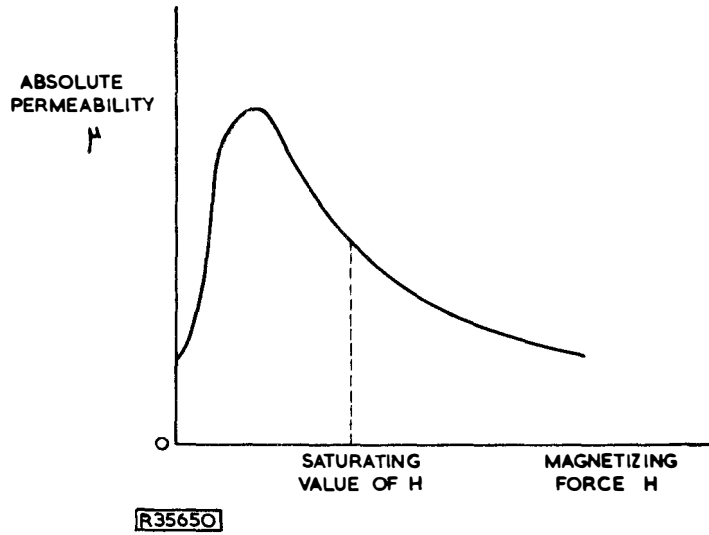


Fig. 2-4 Variation of  $\mu$  with changes in  $H$  in a ferromagnetic material

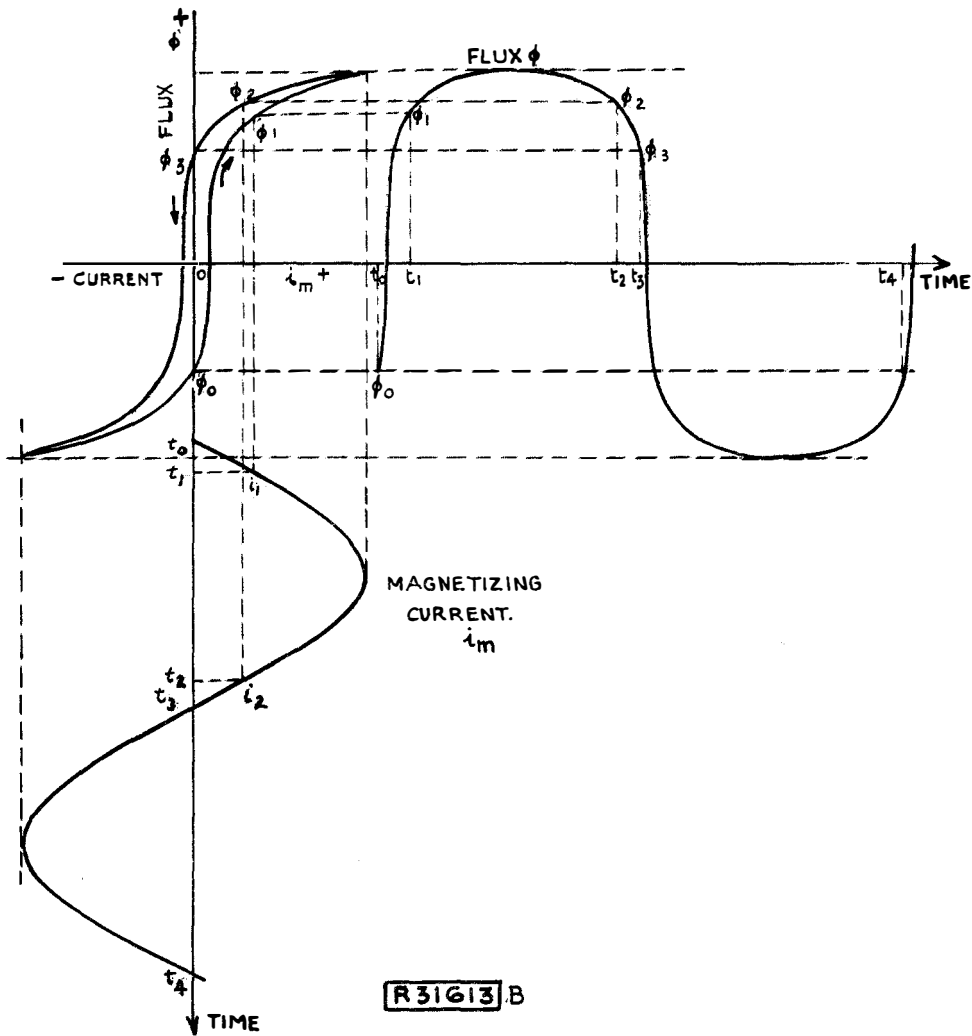
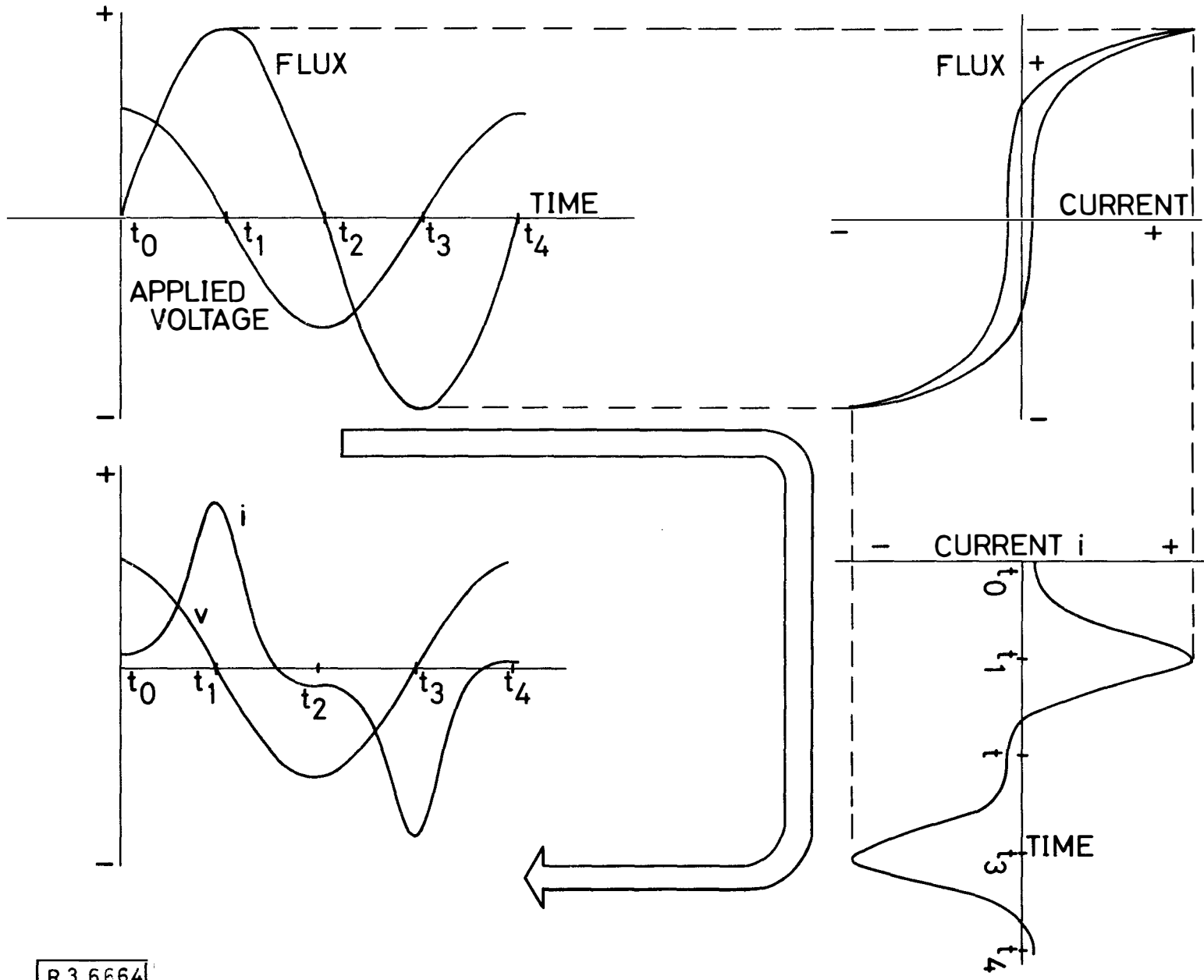


Fig. 2-5 Flux distortion in a saturated iron core





R 3 6664

Fig. 2-6 Current distortion in a saturated iron cored inductor

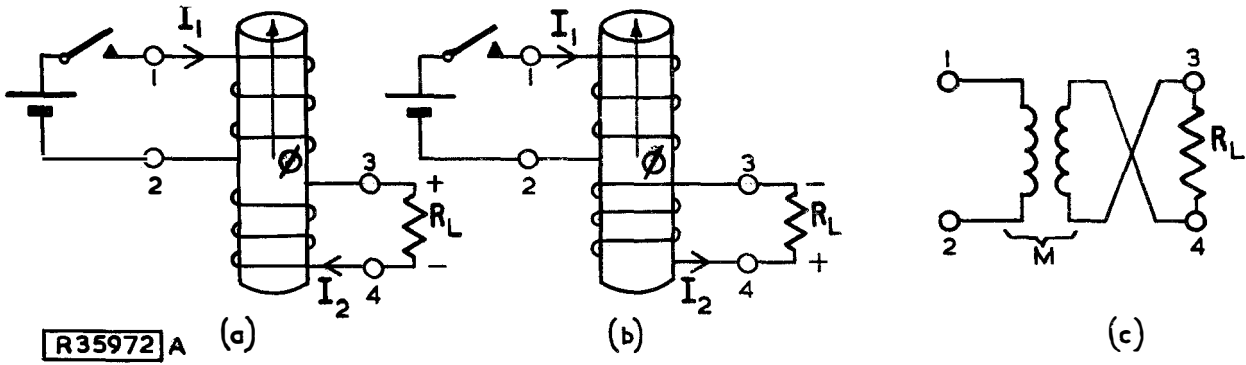


Fig. 2-7 Basic Transformer and direction of induced currents

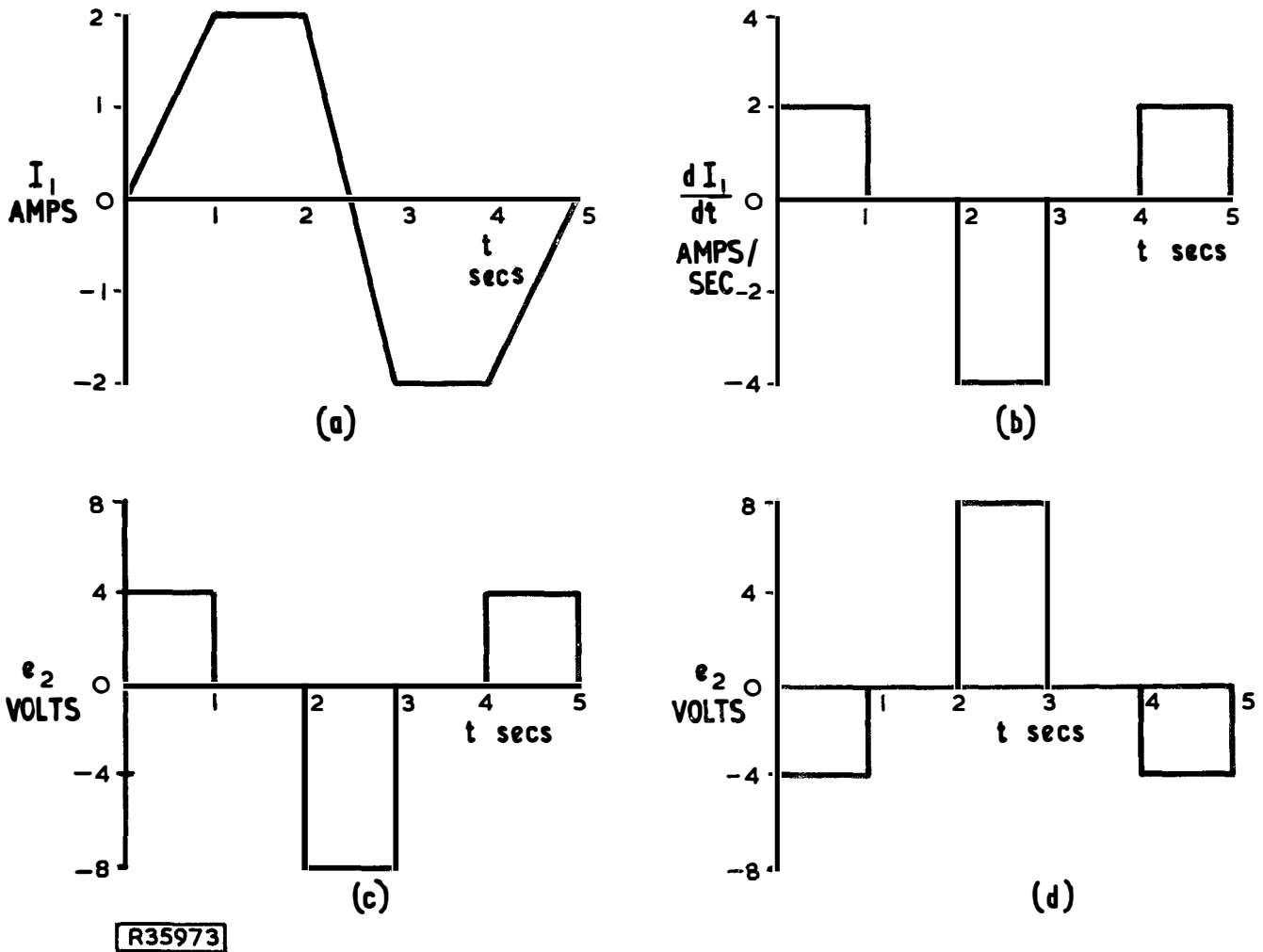
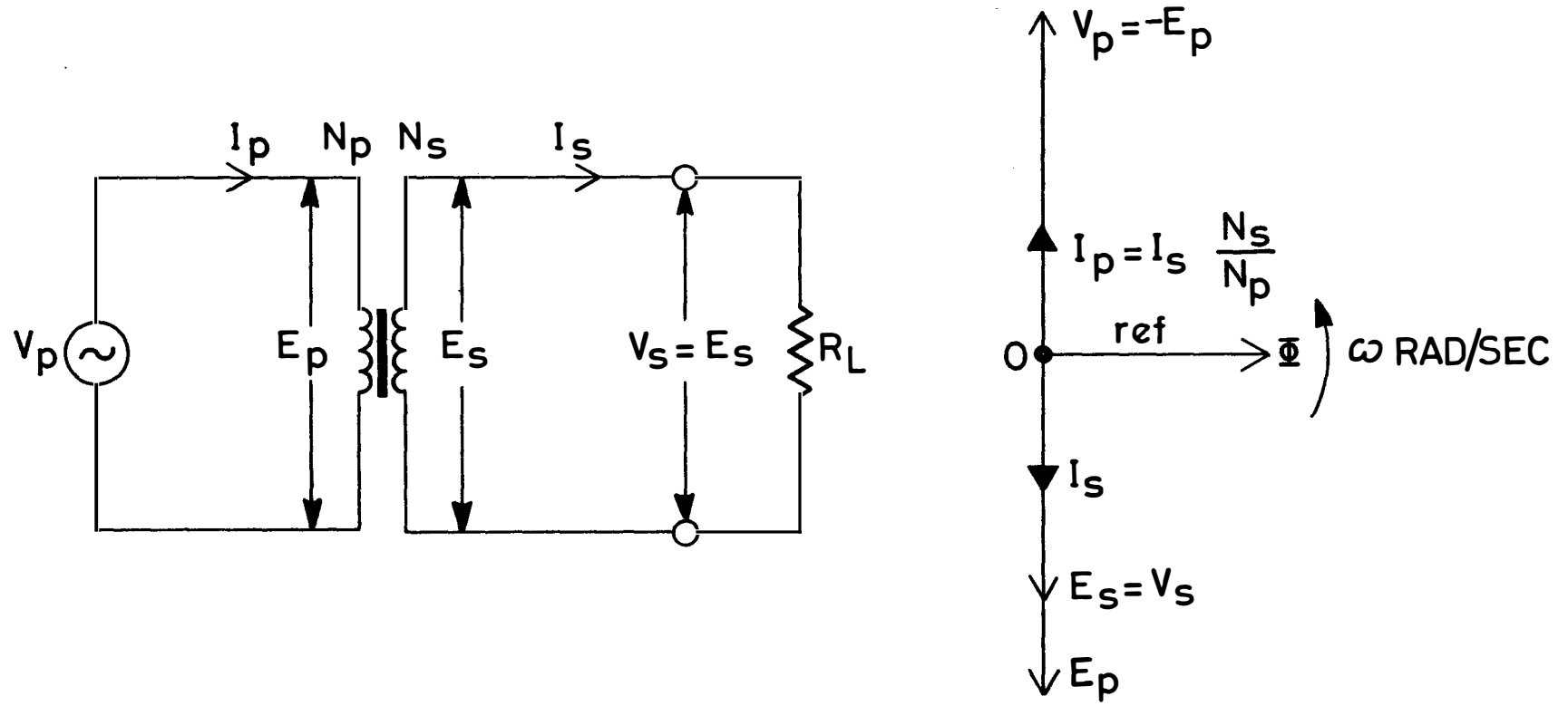
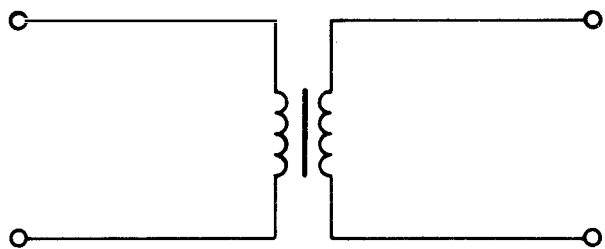


Fig. 2-8 Diagram showing how the secondary induced emf is determined by the rate of change of primary current and the sense of the secondary winding

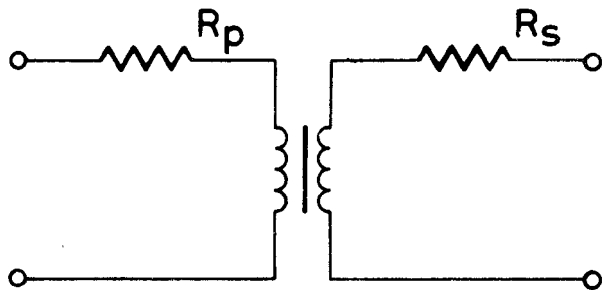


R36665

Fig. 2-9 Phasor diagram for an ideal transformer with a resistive load



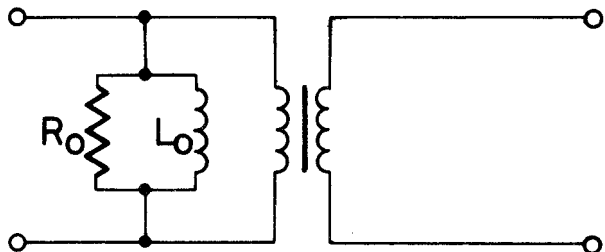
IDEAL TRANSFORMER



COPPER LOSS

$R_p$  = PRIMARY WINDING RESISTANCE

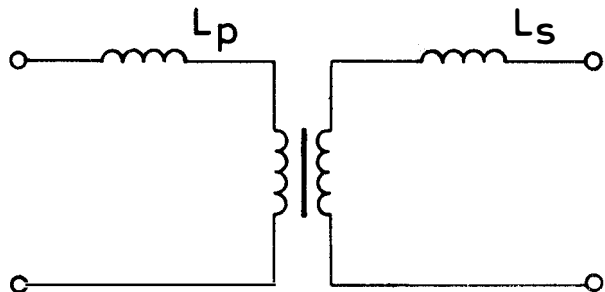
$R_s$  = SECONDARY WINDING RESISTANCE



IRON LOSSES

$R_o$  = EDDY CURRENT AND HYSTERESIS LOSSES

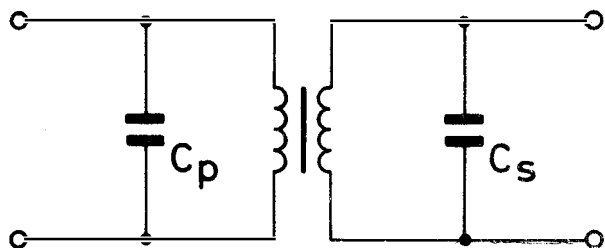
$L_o$  = PRIMARY WINDING INDUCTANCE



LEAKAGE INDUCTANCE

$L_p$  = PRIMARY LEAKAGE INDUCTANCE

$L_s$  = SECONDARY LEAKAGE INDUCTANCE



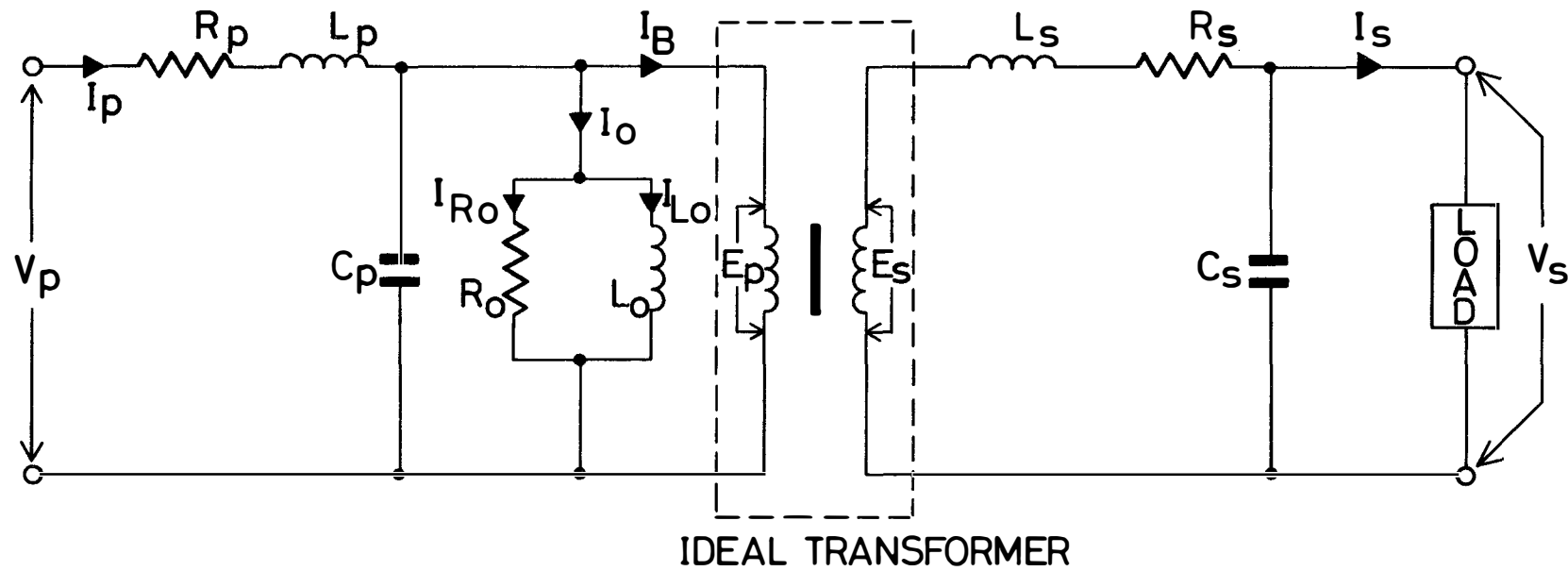
SELF CAPACITANCE

$C_p$  = PRIMARY SELF-CAPACITANCE

$C_s$  = SECONDARY SELF-CAPACITANCE

R 36666

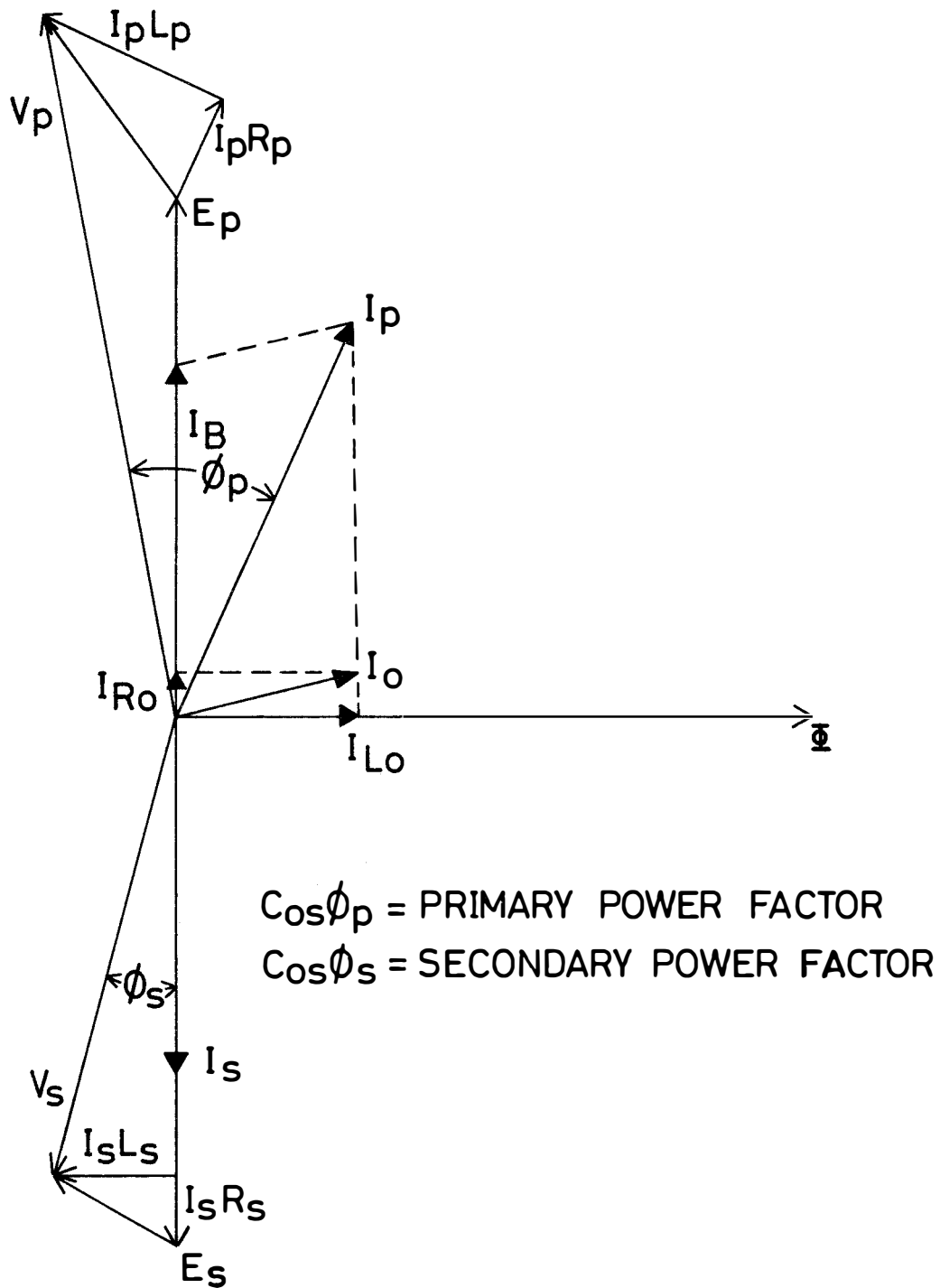
Fig. 2-10 Equivalent circuits of losses inherent in the practical transformer



- |  |                                      |
|--|--------------------------------------|
| $V_p$ = APPLIED VOLTAGE                    | $V_s$ = SECONDARY TERMINAL VOLTAGE   |
| $I_p$ = SUPPLY CURRENT                     | $I_s$ = SECONDARY CURRENT            |
| $R_p$ = PRIMARY RESISTANCE                 | $C_s$ = SECONDARY SELF CAPACITANCE   |
| $L_p$ = PRIMARY LEAKAGE INDUCTANCE         | $R_s$ = SECONDARY RESISTANCE         |
| $C_p$ = PRIMARY SELF CAPACITANCE           | $L_s$ = SECONDARY LEAKAGE INDUCTANCE |
| $I_o$ = NO LOAD CURRENT                    | $E_s$ = SECONDARY VOLTAGE            |
| $R_o$ = EDDY CURRENT AND HYSTERESIS LOSSES |                                      |
| $L_o$ = PRIMARY WINDING INDUCTANCE         |                                      |
| $I_B$ = BALANCING CURRENT                  |                                      |
| $E_p$ = PRIMARY VOLTAGE                    |                                      |

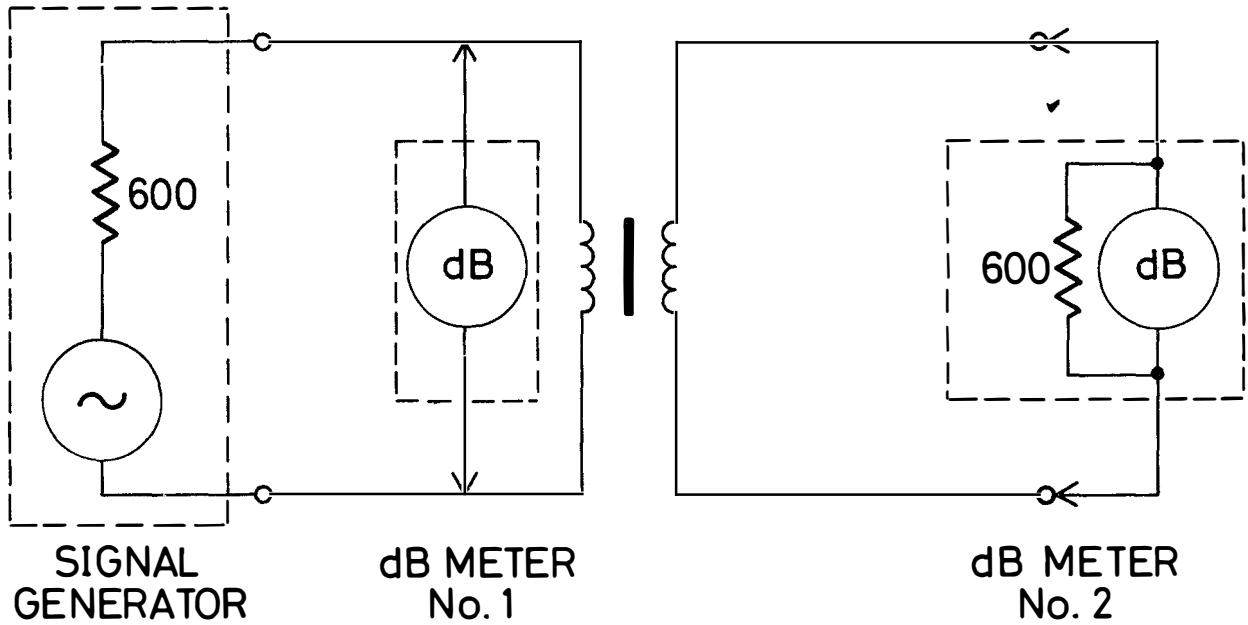
R 36667

Fig. 2-11 Complete transformer equivalent circuit



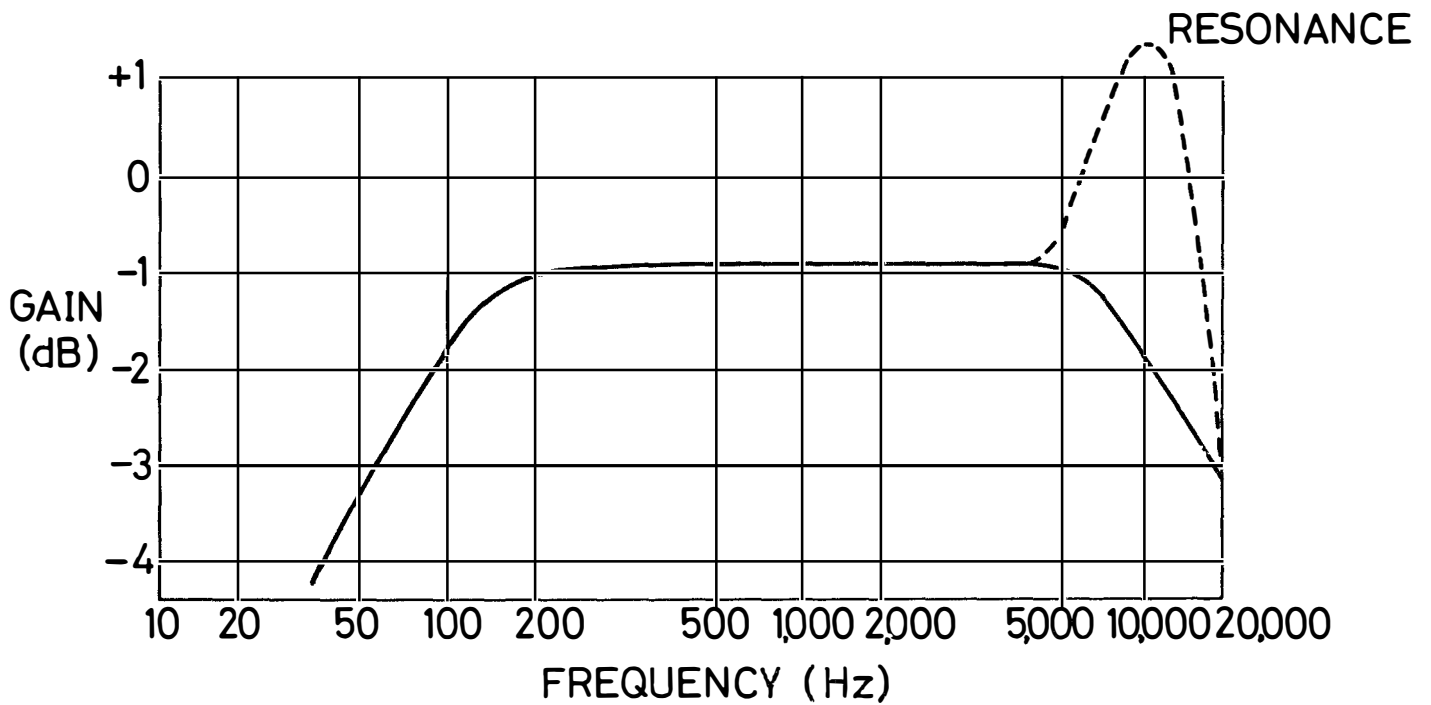
R36668

Fig. 2-12 Phasor diagram for a practical transformer having a 1:1 turns ratio and a resistive load



INPUT LEVEL TO BE MAINTAINED CONSTANT

TYPICAL TEST EQUIPMENT



AUDIO TRANSFORMER FREQUENCY RESPONSE

R 36669

Fig. 2-13 Test equipment used and frequency response obtained when a range of frequencies is passed through an audio transformer

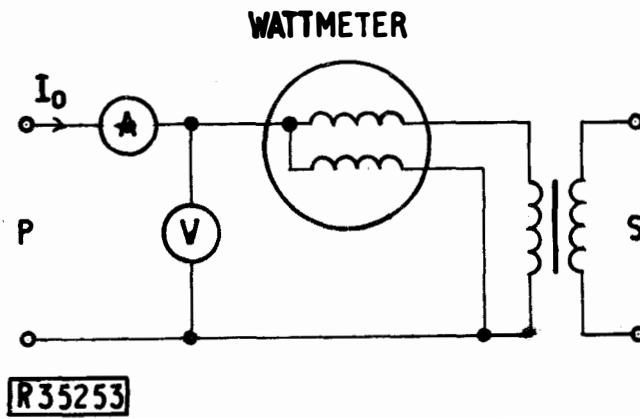


Fig. 2-14 Open circuit test to find core-losses

Core loss  $W_c = \text{wattmeter reading} -$

(Power loss in wattmeter +  
primary copper loss) watts

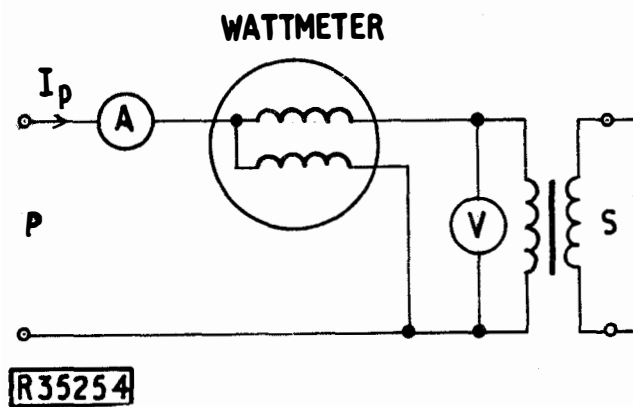
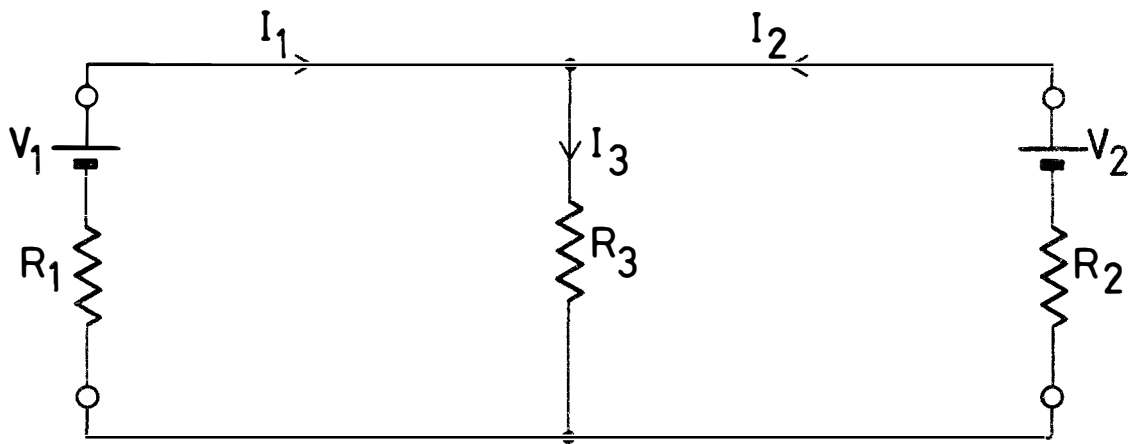


Fig. 2-15 Short circuit test to find copper losses

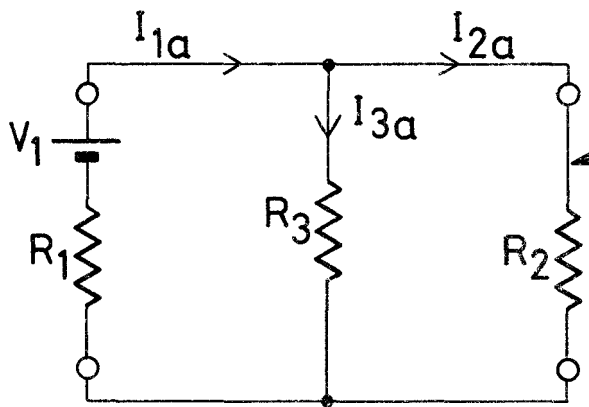
Copper losses  $W_w \approx \text{wattmeter reading} - \text{power}$

(loss in wattmeter watts,  
assuming the core losses are  
negligible)





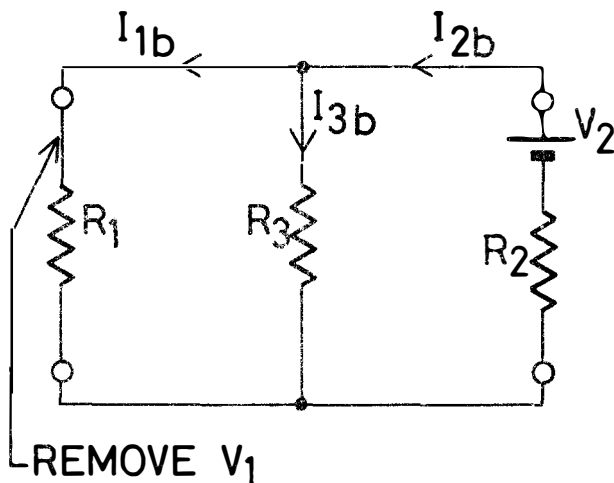
CIRCUIT CONTAINING LINEAR IMPEDANCES AND MORE THAN ONE E.M.F



REMOVE  $V_2$   
FROM THE SUPERPOSITION THEOREM

$$I_1 = I_{1a} + (-I_{1b})$$

$$\therefore I_1 = I_{1a} - I_{1b}$$



AND

$$I_2 = I_{2b} + (-I_{2a})$$

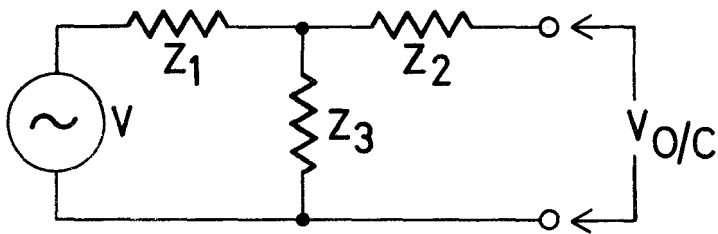
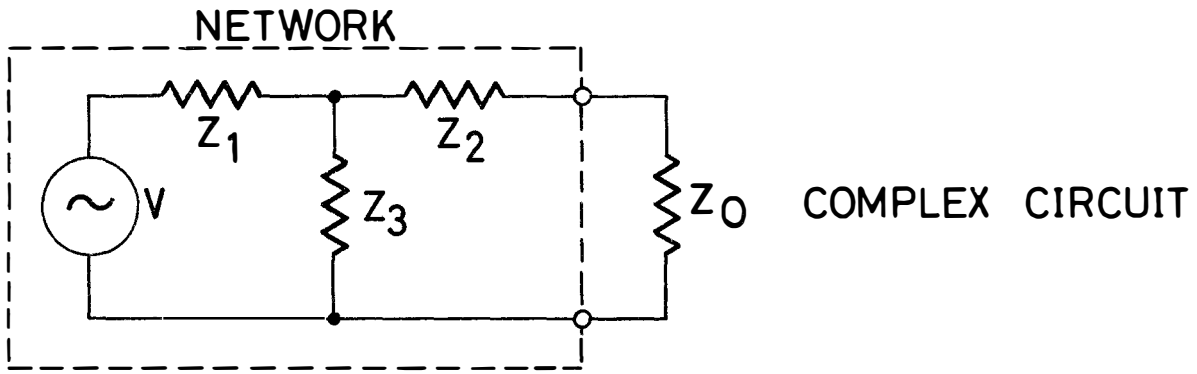
$$\therefore I_2 = I_{2b} - I_{2a}$$

AND

$$I_3 = I_{3a} + I_{3b}$$

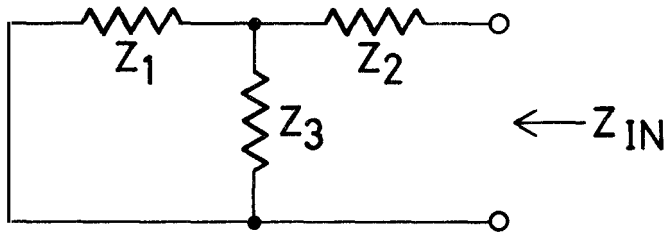
R36670

Fig. 3-1 The Superposition Theorem



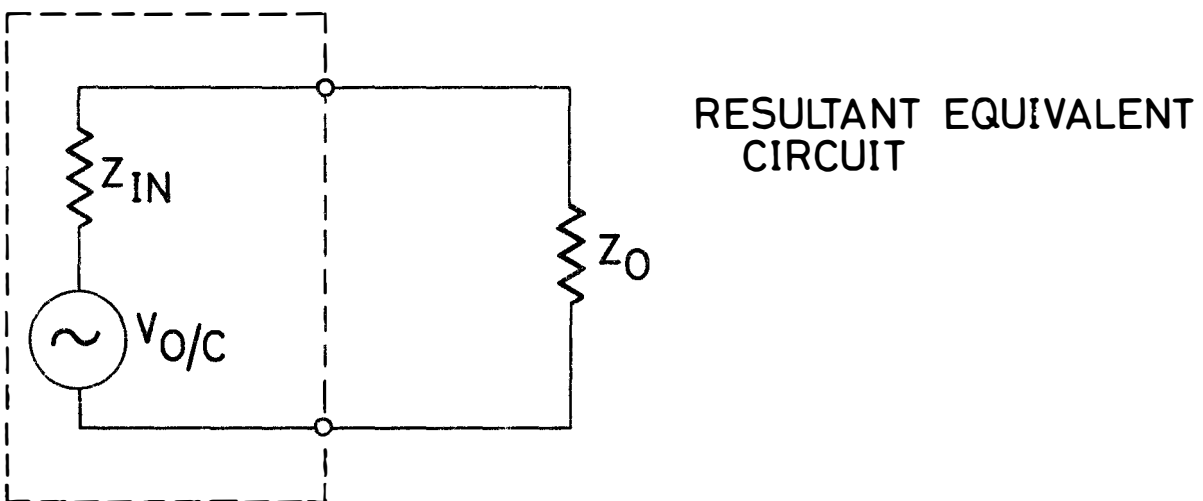
TERMINAL VOLTAGE

$$V_{0/C} = V \times \frac{Z_3}{Z_1 + Z_3}$$



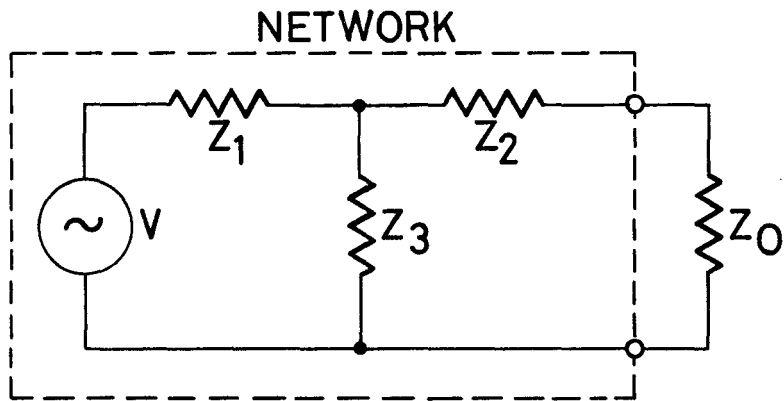
INTERNAL IMPEDANCE

$$Z_{IN} = Z_2 + \frac{Z_1 Z_3}{Z_1 + Z_3}$$

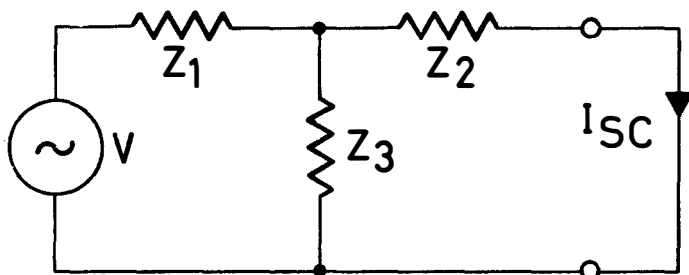


R 36671

Fig. 3-2 Thevenin's Theorem



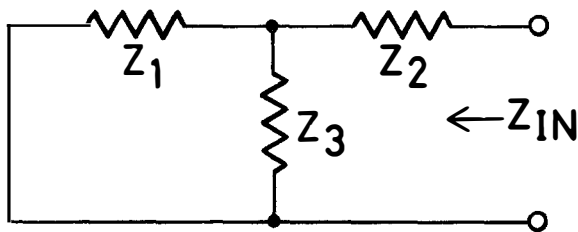
COMPLEX CIRCUIT



OUTPUT CURRENT

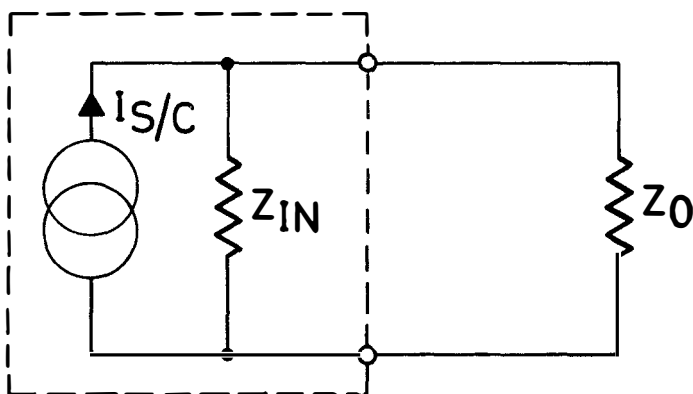
$$I_{SC} = \frac{V}{\frac{Z_1 + Z_2 Z_3}{Z_2 + Z_3}} \times \frac{Z_3}{Z_2 + Z_3}$$

$$= \frac{V Z_3}{Z_1 Z_2 + Z_1 Z_3 + Z_2 Z_3}$$



INTERNAL IMPEDANCE

$$Z_{IN} = Z_2 + \frac{Z_1 Z_3}{Z_1 + Z_3}$$

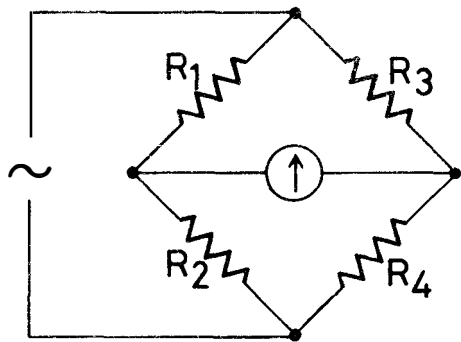


RESULTANT EQUIVALENT CIRCUIT

R36672

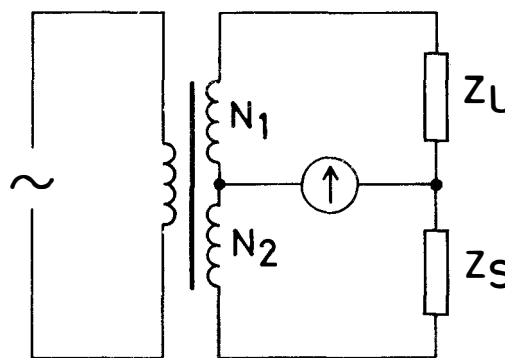
Fig. 3-3 Norton's Theorem

R36673



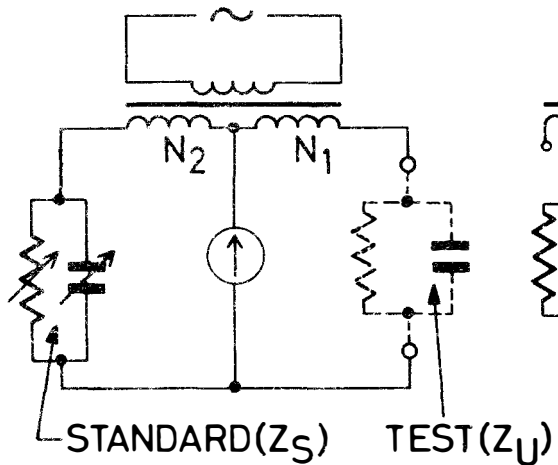
$$\frac{R_1}{R_2} = \frac{R_3}{R_4}$$

GENERAL CONDITIONS

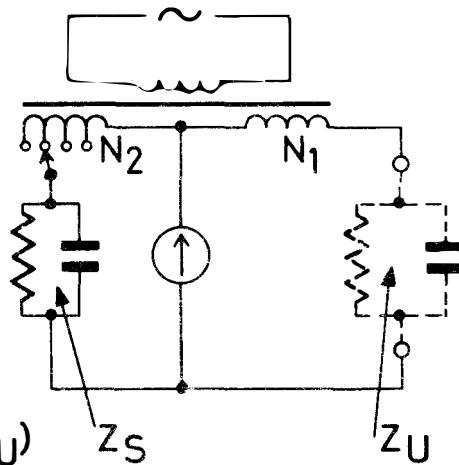


$$Z_U = \frac{N_1}{N_2} Z_S$$

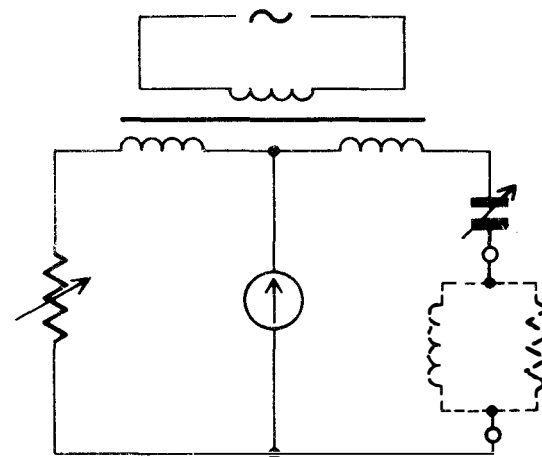
TRANSFORMER RATIO ARMS



VARYING THE STANDARD IMPEDANCE

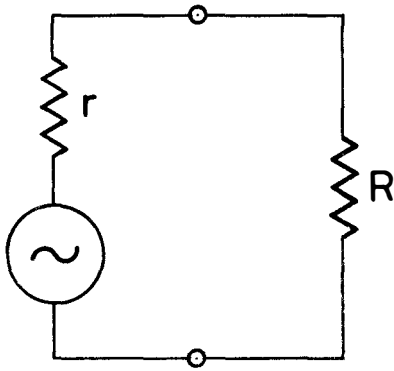


VARYING THE TURNS RATIO

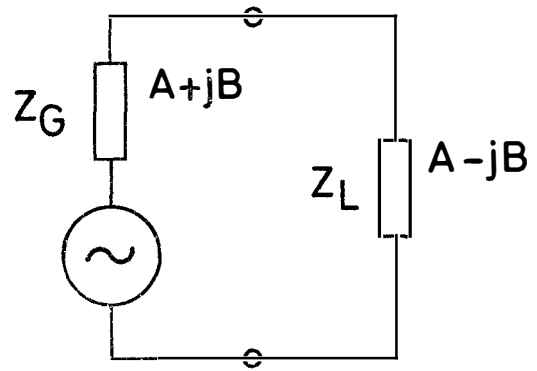


REARRANGEMENT OF COMPONENTS TO MEASURE INDUCTANCE

Fig. 3-4 The 3-Winding transformer bridge



MAX POWER WHEN  $R = r$



MAX POWER WHEN  $A + jB = A - jB$

R36674

Fig. 3-5 Conditions required for maximum power transfer

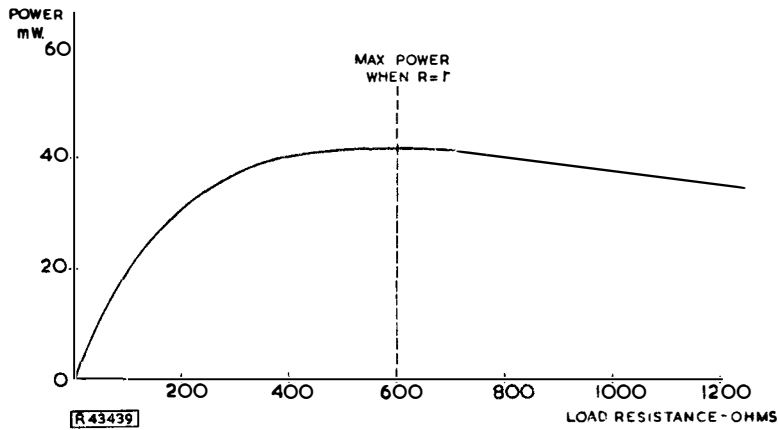
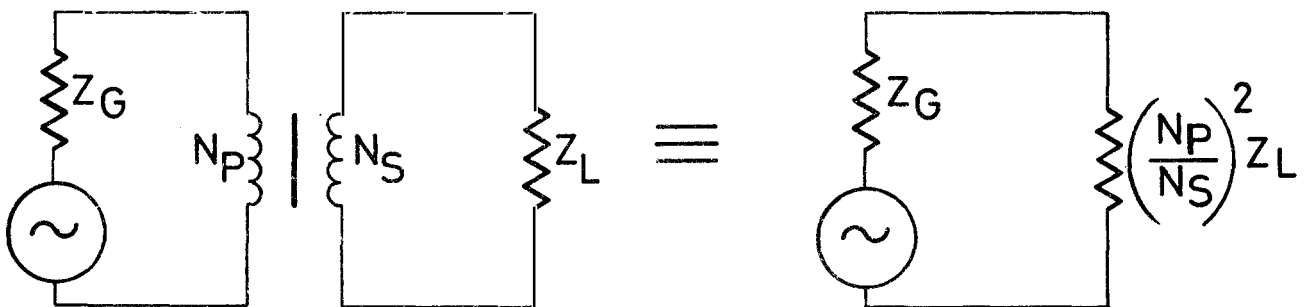


Fig. 3-6 Variation of load power against load resistance when the generator has an internal resistance of  $600\Omega$  and a terminal voltage of 10 volts.



R36675

Fig. 3-7 Impedance matching with the aid of a transformer

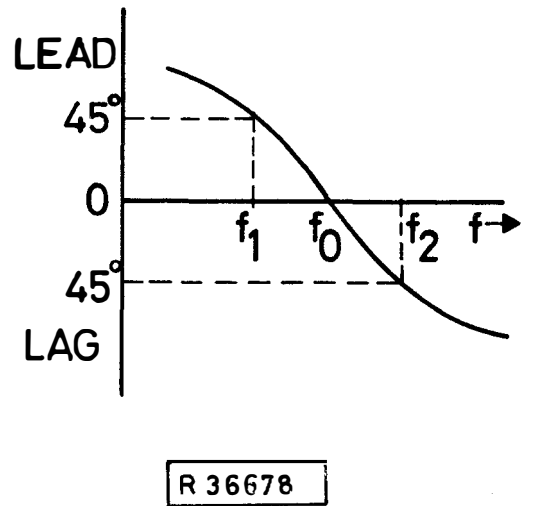
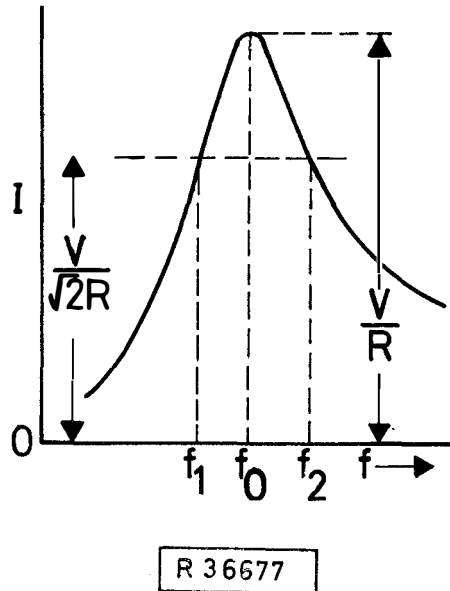
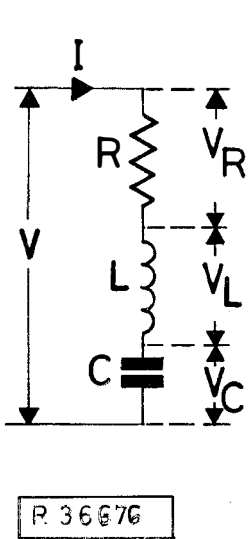


Fig. 4-1 Series circuit

Fig. 4-2 Current response and half power points

Fig. 4-3 Phase angle

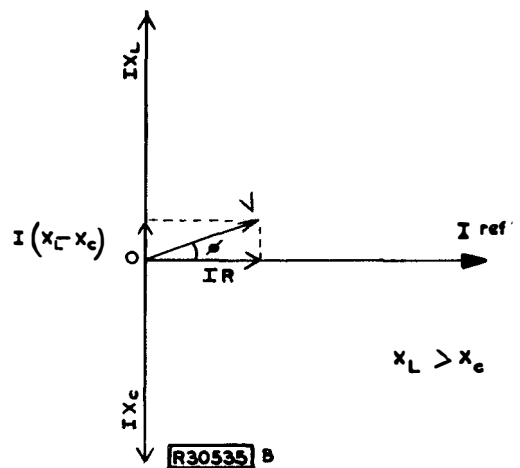
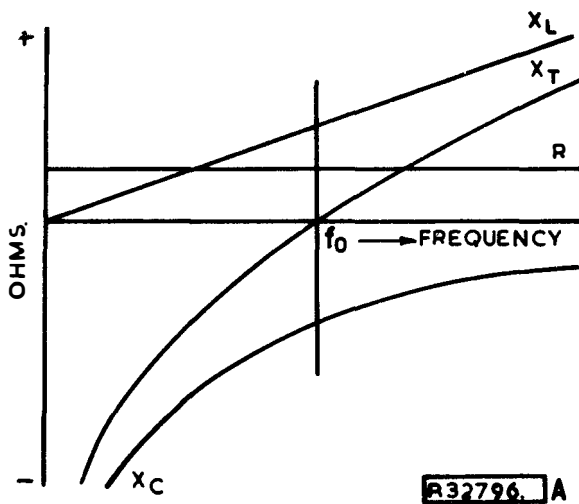


Fig. 4-4 Variation of resistance, capacitive reactance, inductive reactance and total reactance with frequency

Fig. 4-5 Series circuit phasor diagram

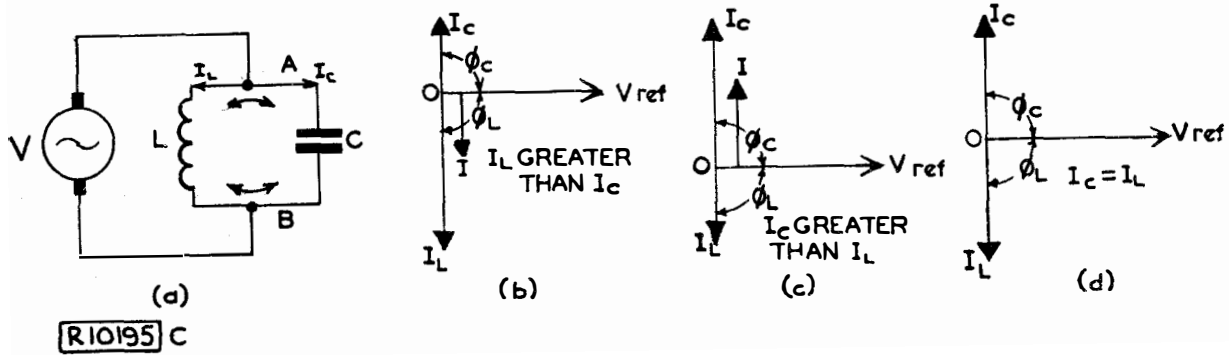


Fig. 4-6 Branch currents in a basic parallel circuit

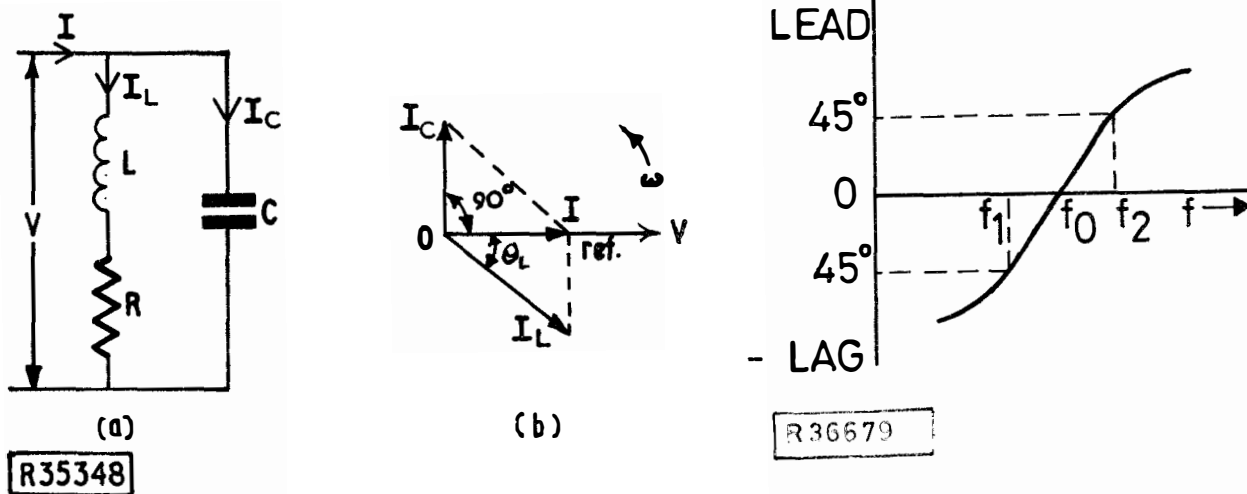
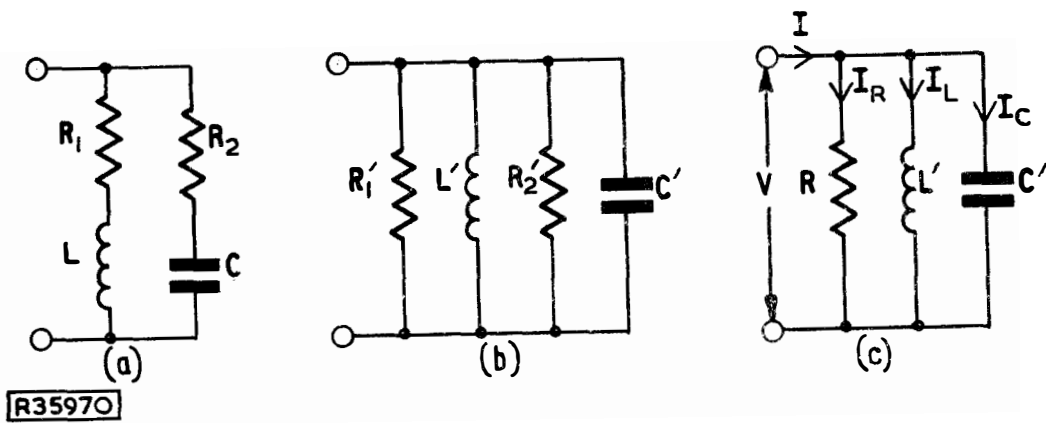


Fig. 4-8 Phase angle against frequency

Fig. 4-7 Parallel circuit and phasor diagram



where

$$R_1' = R_1(1 + Q_L^2)$$

$$R_2' = R_2(1 + Q_C^2)$$

and

$$R = \frac{R_1' R_2'}{R_1' + R_2'}$$

$$C' = \frac{C}{1 + \frac{1}{Q_C^2}}$$

and

$$L' = L \left( 1 + \frac{1}{Q_L^2} \right)$$

Fig. 4-9 Simplification of the general parallel tuned circuit

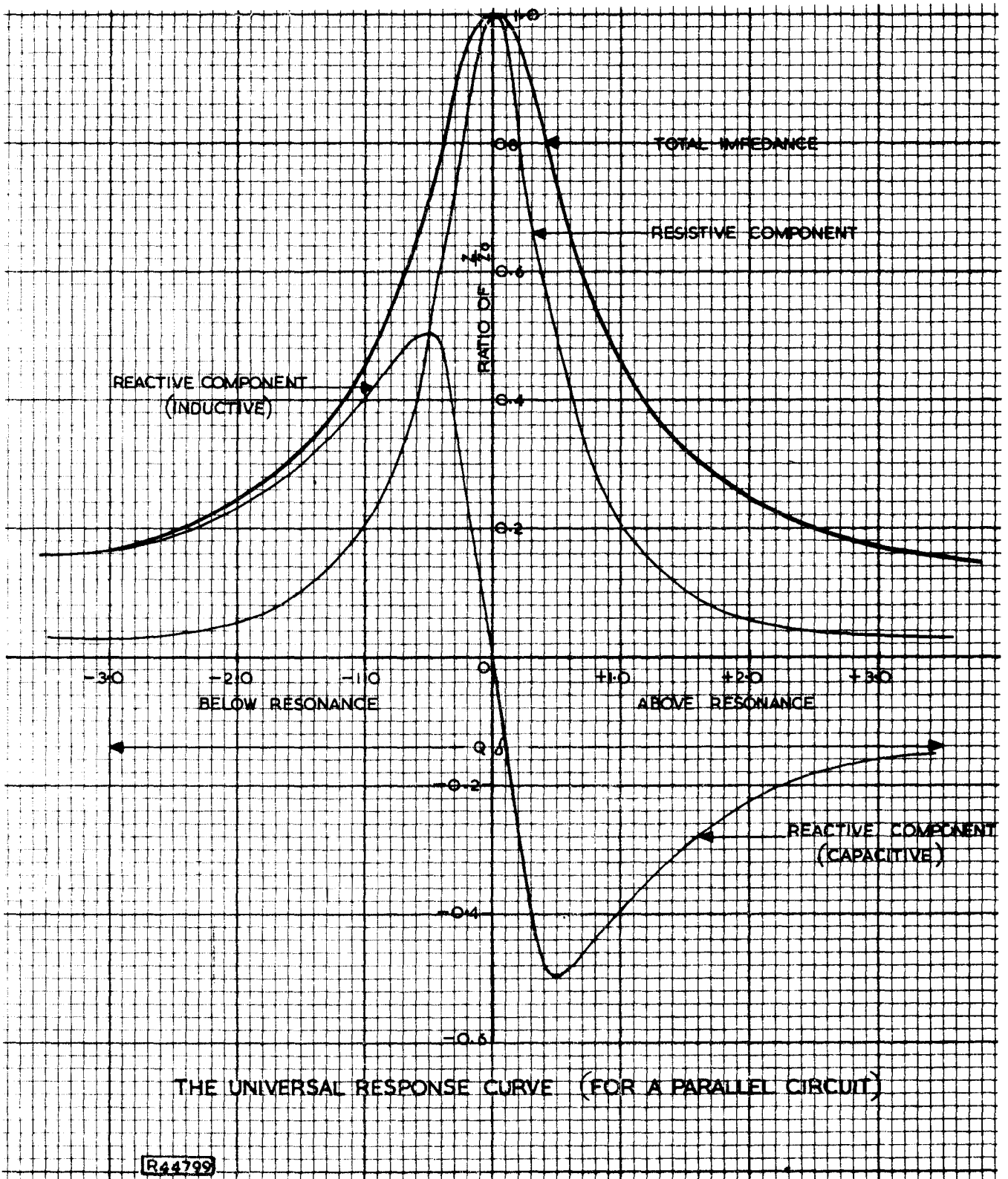
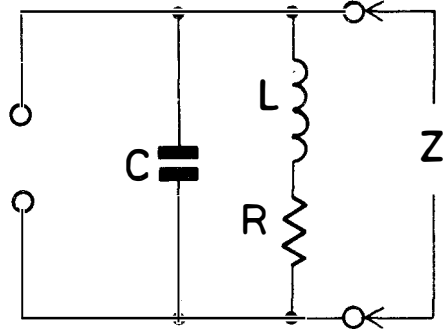
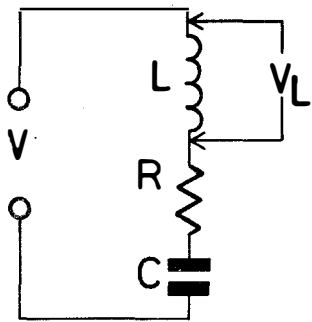
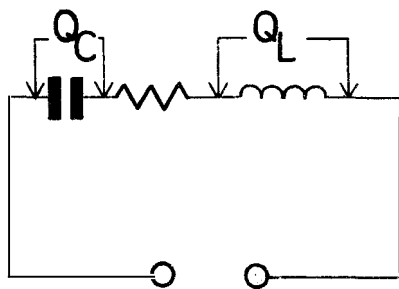
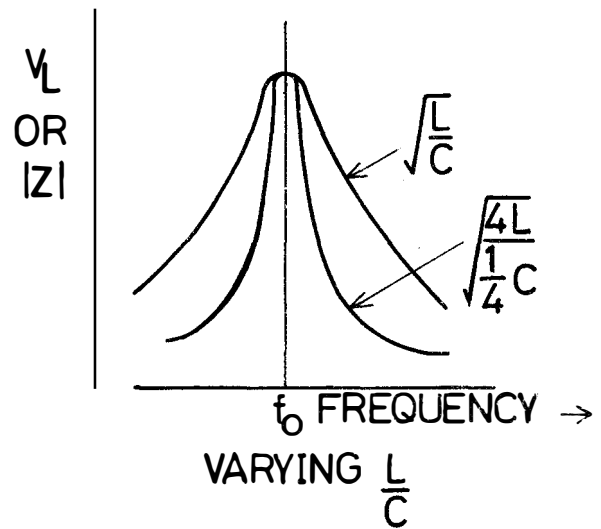
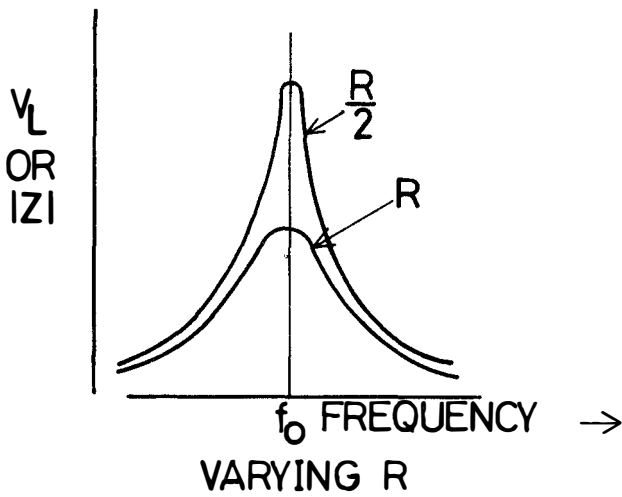


Fig. 4-10 The universal response curve for a parallel circuit showing its resistive and reactive components





$$Q = \frac{V_L}{V} = \frac{\omega_0 L}{R} = \frac{1}{R} \sqrt{\frac{L}{C}}$$



$$Q_T = \frac{1}{\frac{1}{Q_L} + \frac{1}{Q_C}}$$

R36680

Fig. 4-11 Q factor of series and parallel tuned circuits

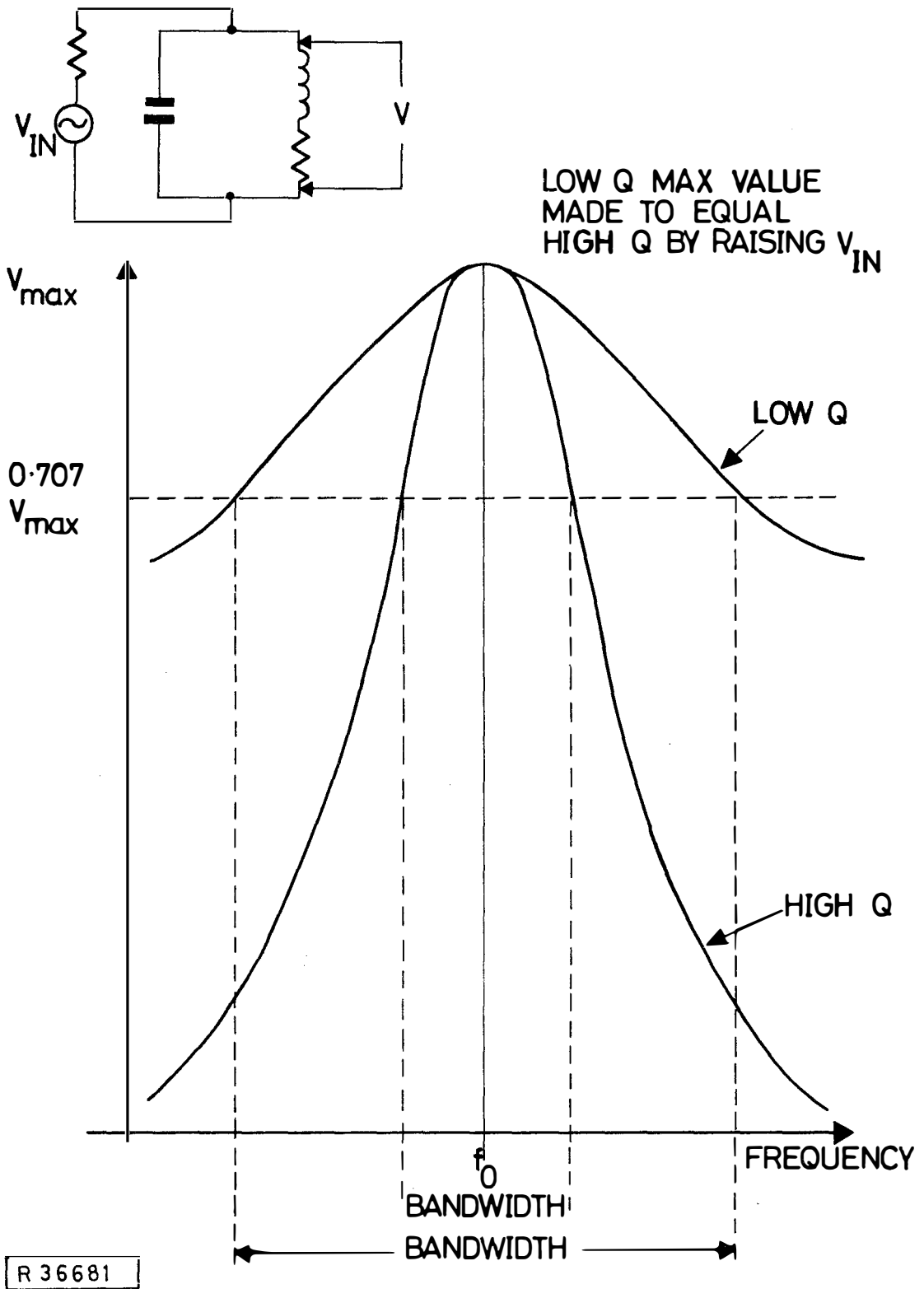
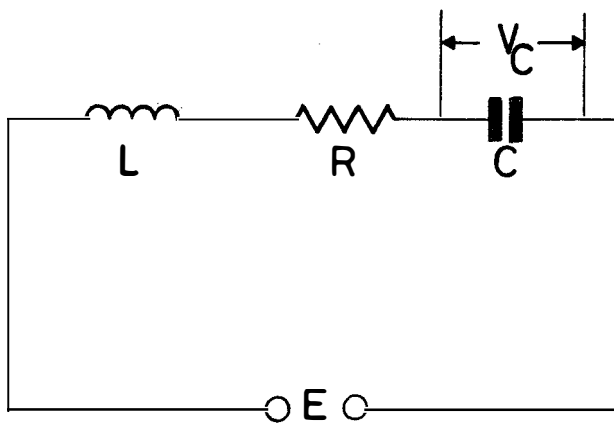
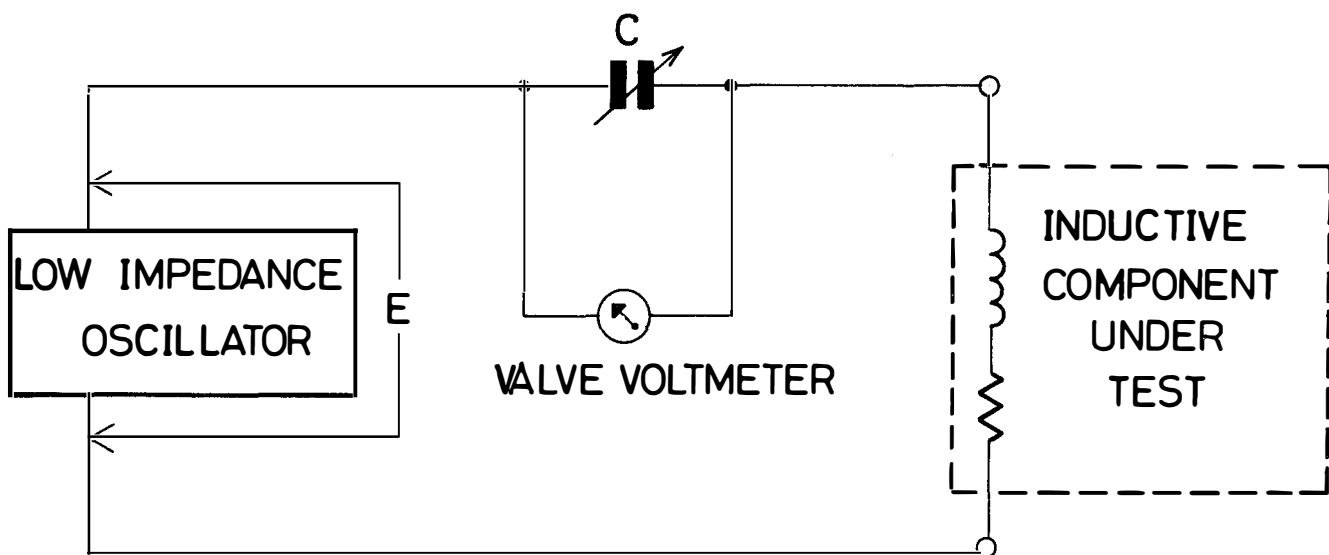


Fig. 4-12 Diagram showing the effect of Q factor on the selectivity of a circuit. The bandwidth is given as the range of frequencies between the half power points.



$$Q = \frac{V_C}{E} = \frac{V_L}{E}$$

### PRINCIPLE OF THE Q METER



THE LOW IMPEDANCE OSCILLATOR PROVIDES CONSTANT E.  
 THE VALVE VOLTMETER IS HIGH IMPEDANCE AND IS  
 CALIBRATED TO READ DIRECT VALUES OF Q.  
 IF C IS LOW LOSS THE CIRCUIT  $Q \approx$  INDUCTOR Q

R 36682

Fig. 4-13 Simple Q meter

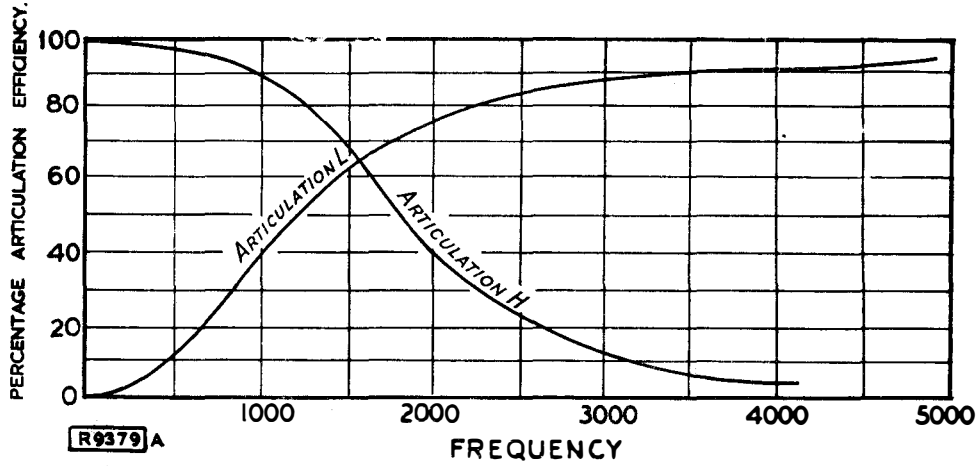


Fig. 5-1 How the articulation efficiency (intelligibility) is affected by the frequency range transmitted.

L = all frequencies transmitted below the frequency shown on the horizontal axis  
 H = " " " above " " " " " " " " "

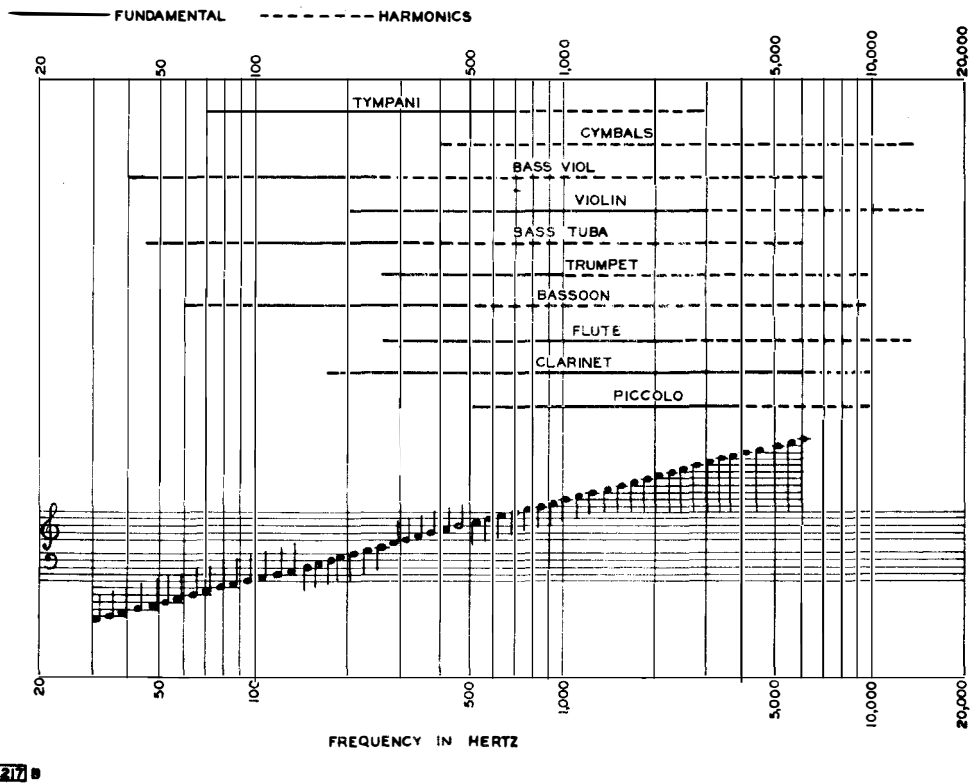
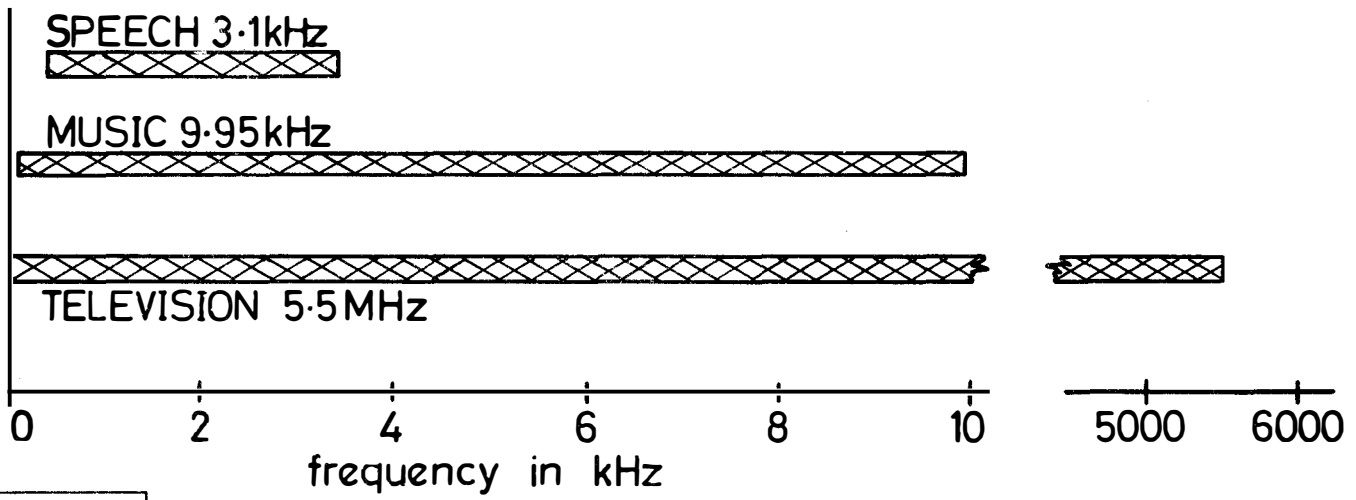
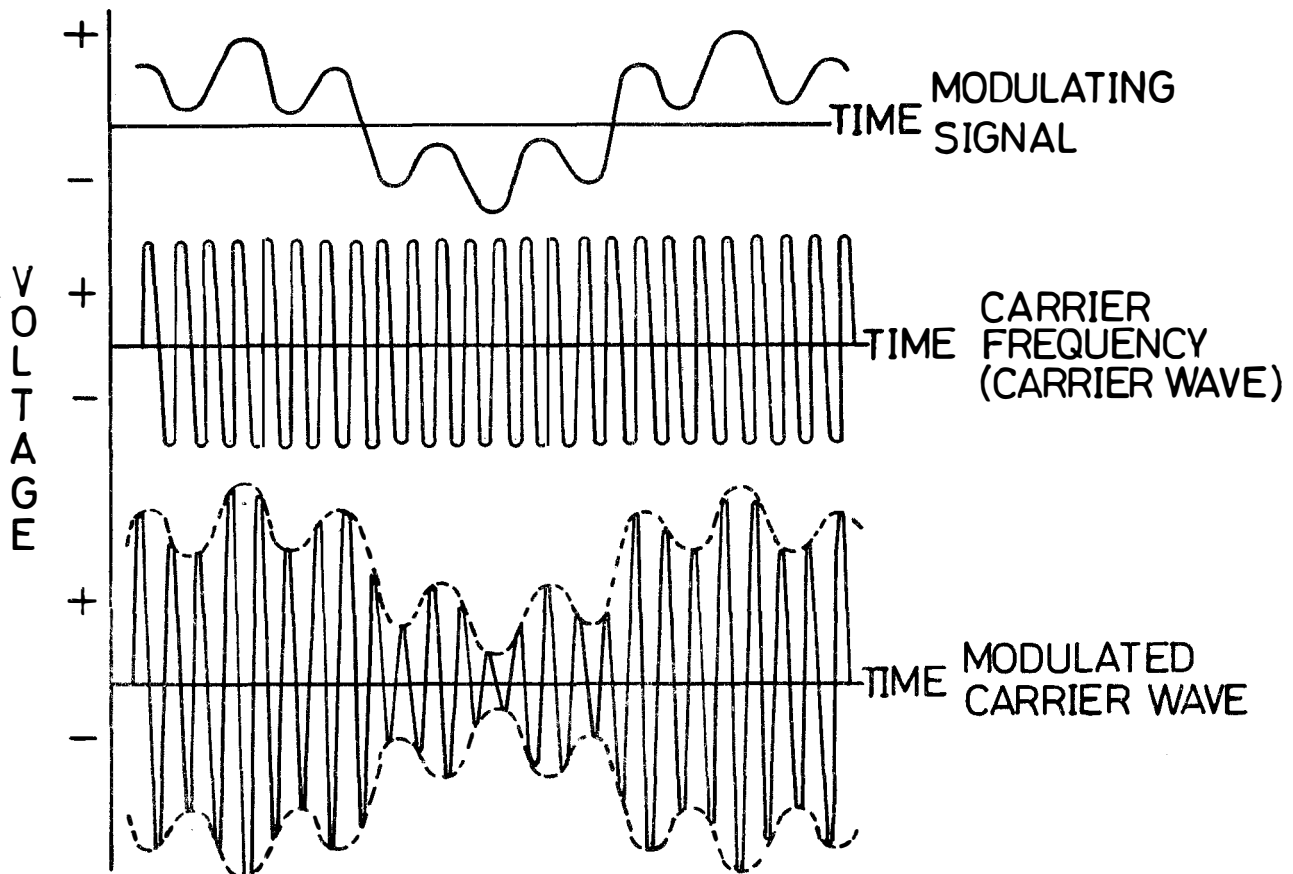


Fig. 5-2 Musical instrument fundamental and harmonic frequency ranges



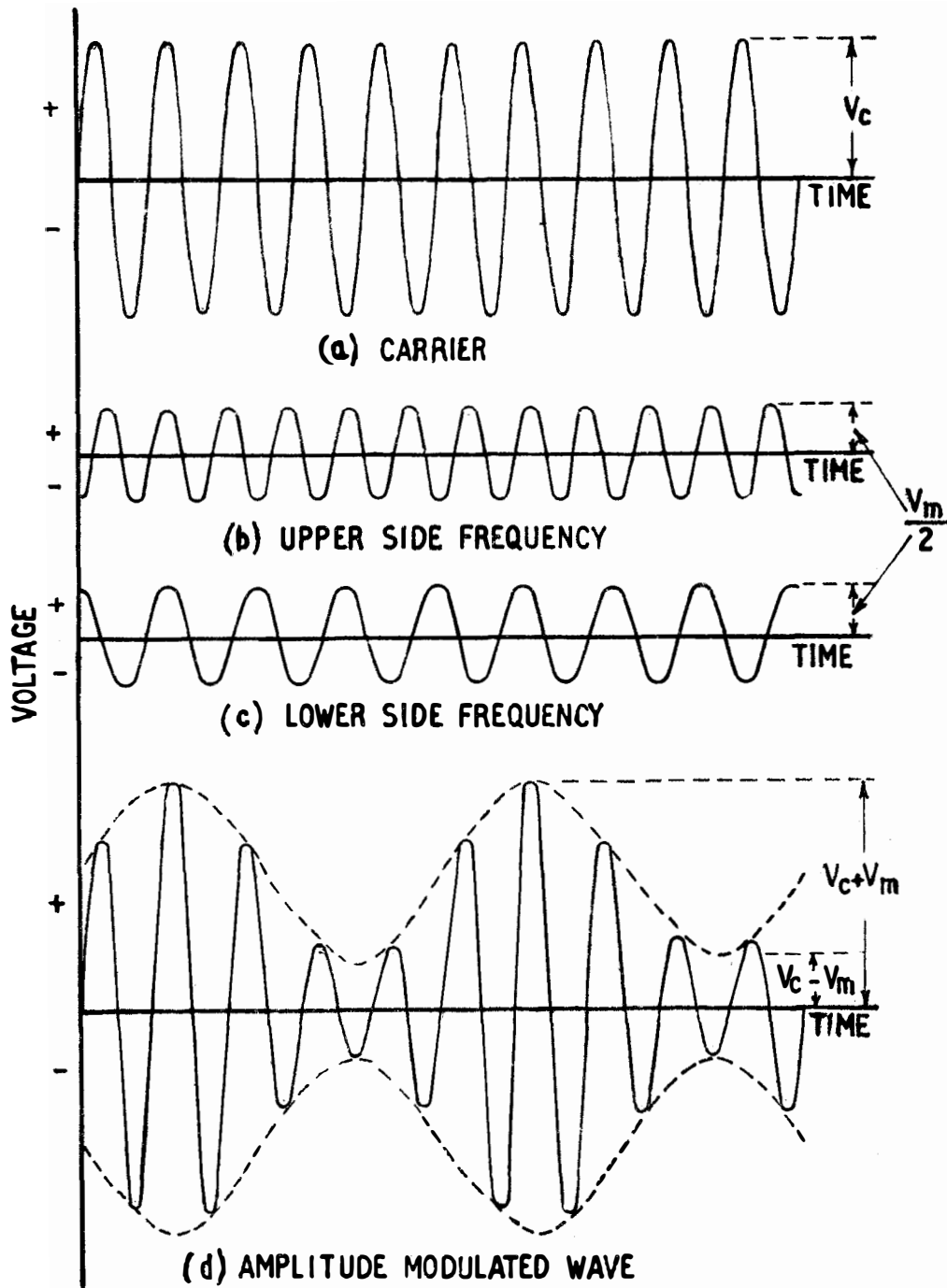
R 36683

Fig. 5-3 Commercial bandwidths for speech, music and television channels



R 36684

Fig. 5-4 The principle of amplitude modulation



**R33878**A

$$\begin{aligned}
 v_{mc} &= V_c \sin \omega t + \frac{V_m}{2} \left\{ \cos (\omega - \rho) t - \cos (\omega + \rho) t \right\} \\
 &= V_c \sin \omega t + \frac{V_m}{2} \sin \left\{ (\omega - \rho) t + \frac{\pi}{2} \right\} \\
 &\quad + \frac{V_m}{2} \sin \left\{ (\omega + \rho) t - \frac{\pi}{2} \right\}
 \end{aligned}$$

Fig. 5-5 Component frequencies of an amplitude modulated wave

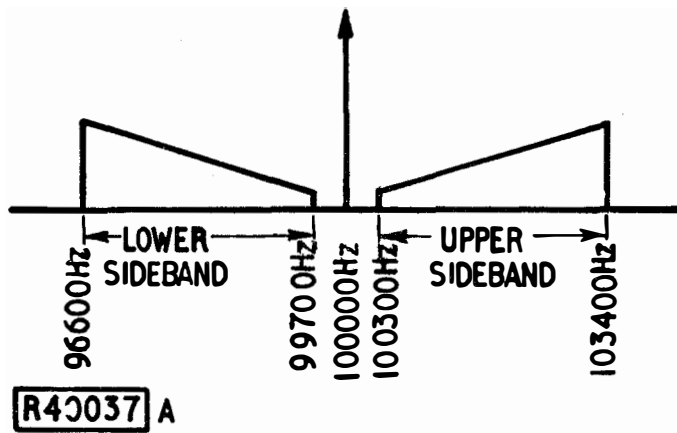
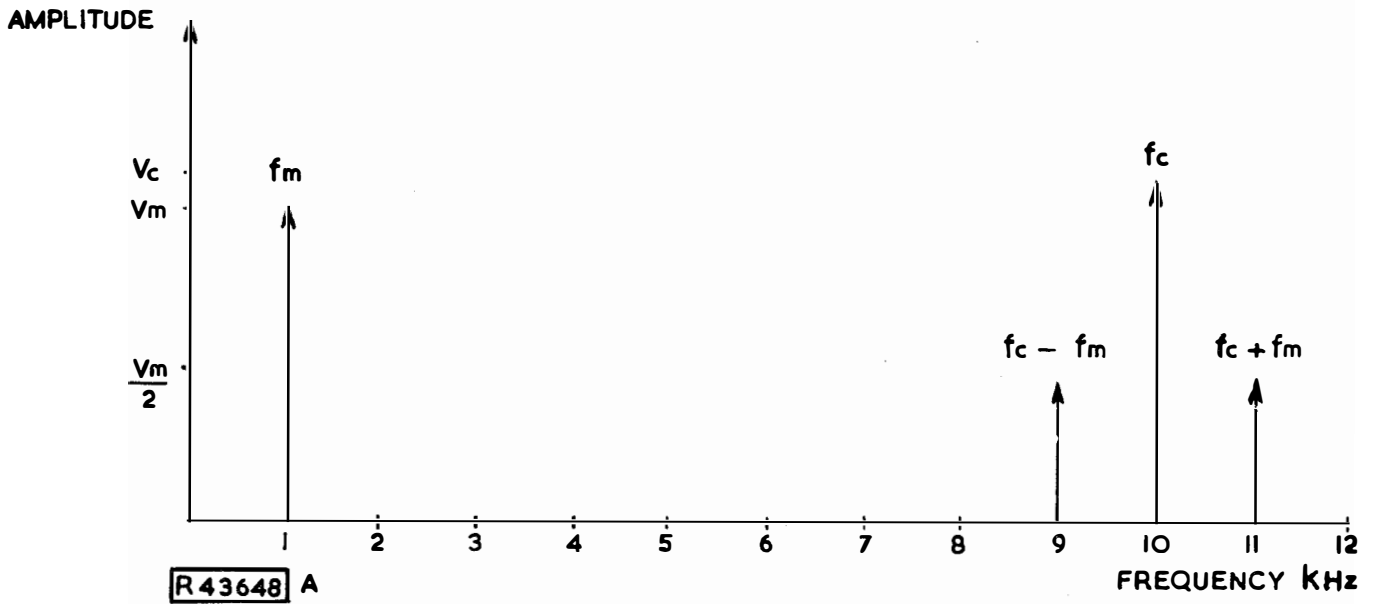
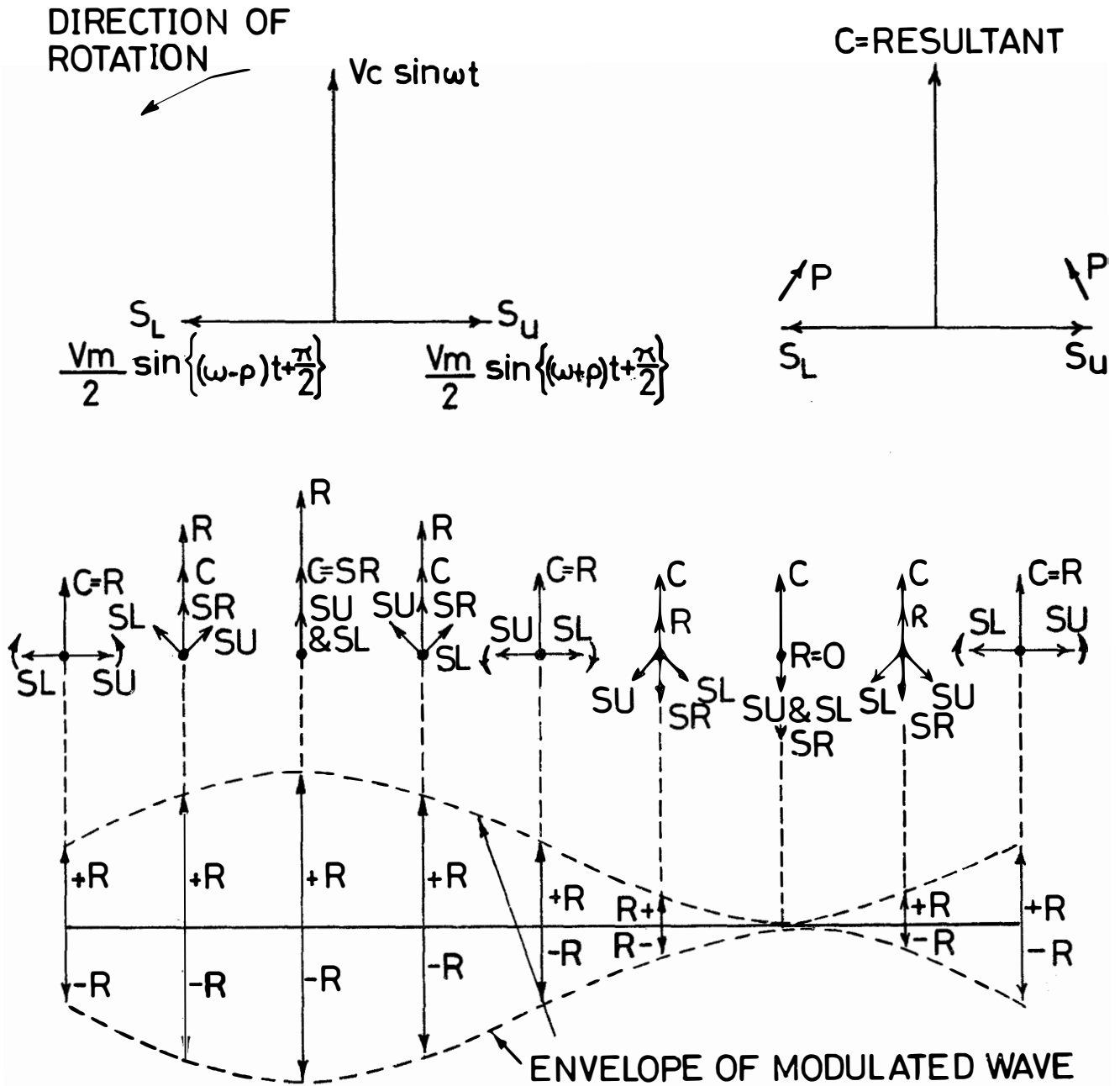


Fig. 5-6 Frequency spectrum diagrams

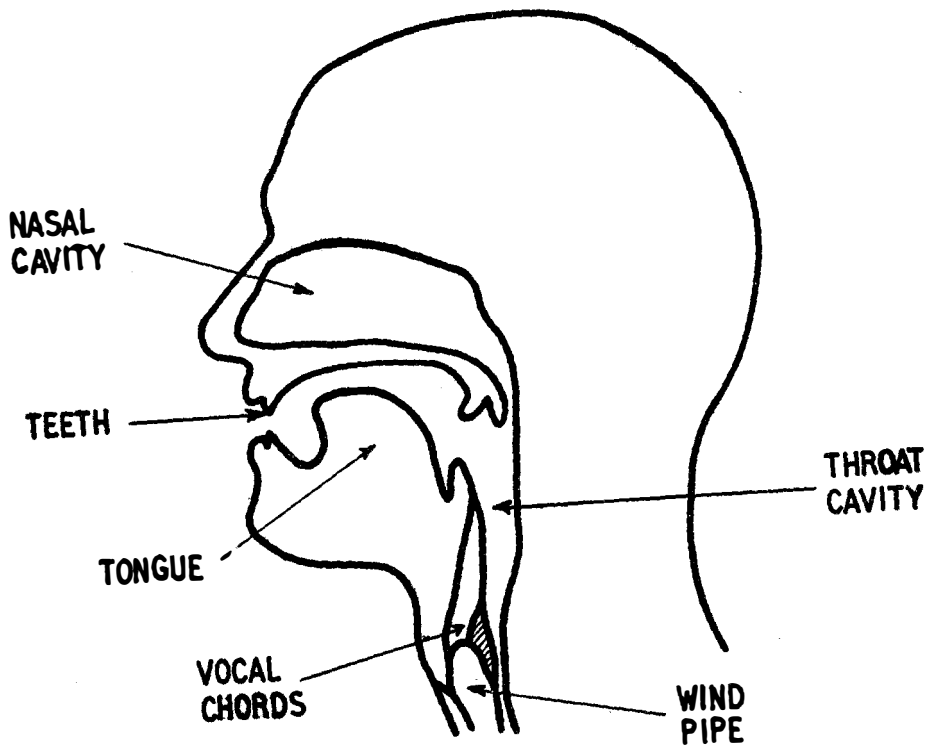
$$V_{mc} = V_c \sin \omega t + \frac{V_m}{2} \sin \left\{ (\omega - \rho) t + \frac{\pi}{2} \right\} - \frac{V_m}{2} \sin \left\{ (\omega + \rho) t + \frac{\pi}{2} \right\}$$



R 36685

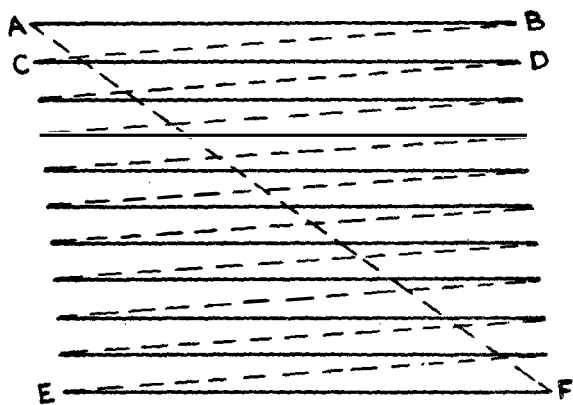
Fig. 5-7 Phasor representation of an amplitude modulated wave showing the revolving side frequency phasors modulating the carrier wave





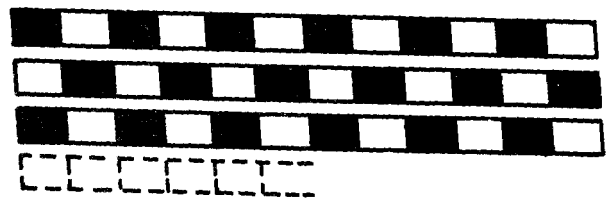
R34513

Fig. 5-8 Diagram showing the features of the head involved in producing sound



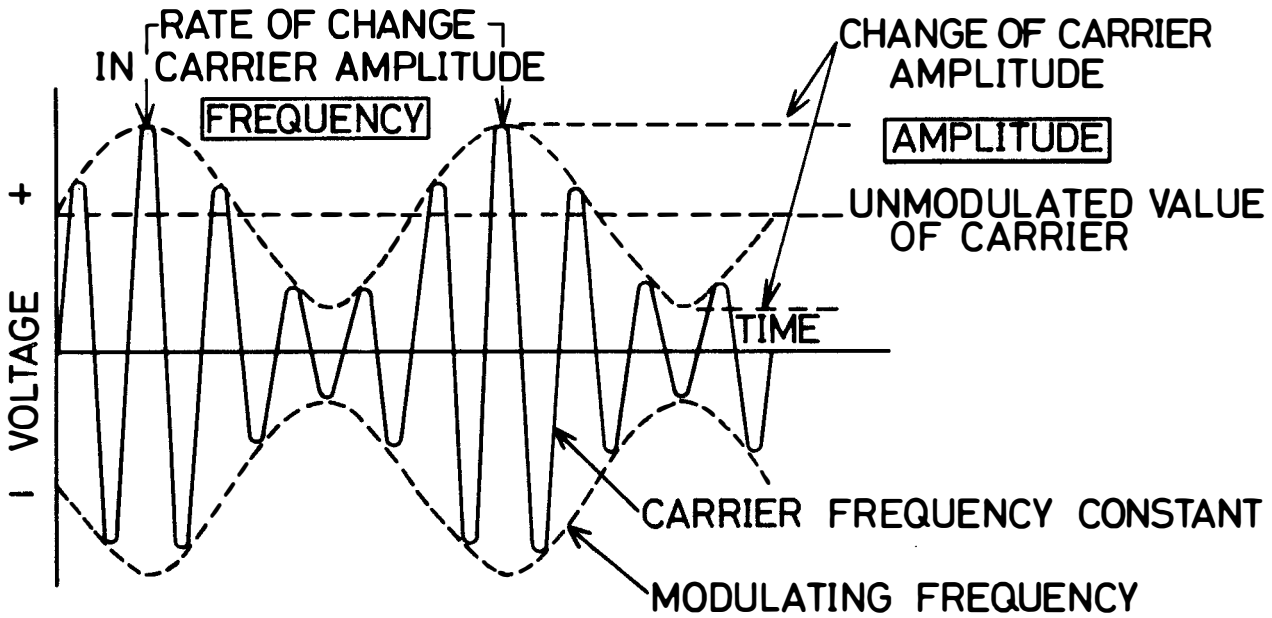
R11542

Fig. 5-9 Television picture scanning showing a line trace A-B, line fly-back B-C, and fly-back to begin a new frame F-A

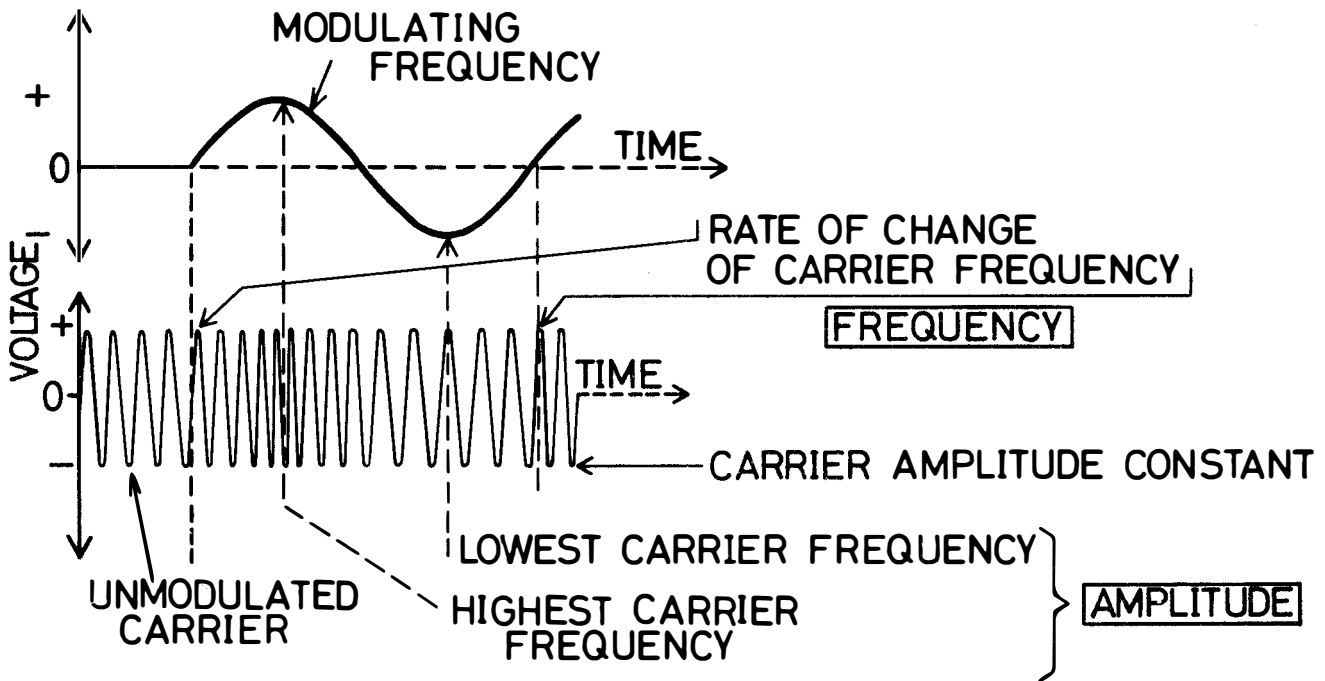


R42292

Fig. 5-10 Television picture lines showing how the lines are composed of elements



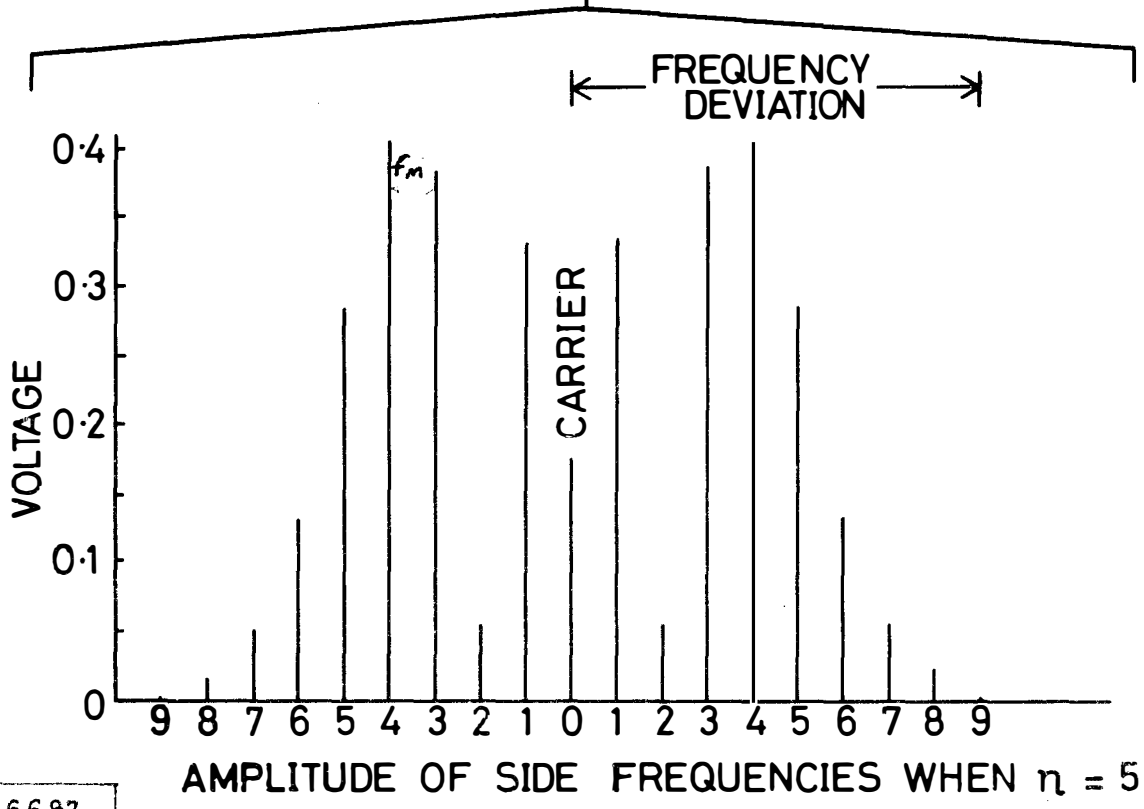
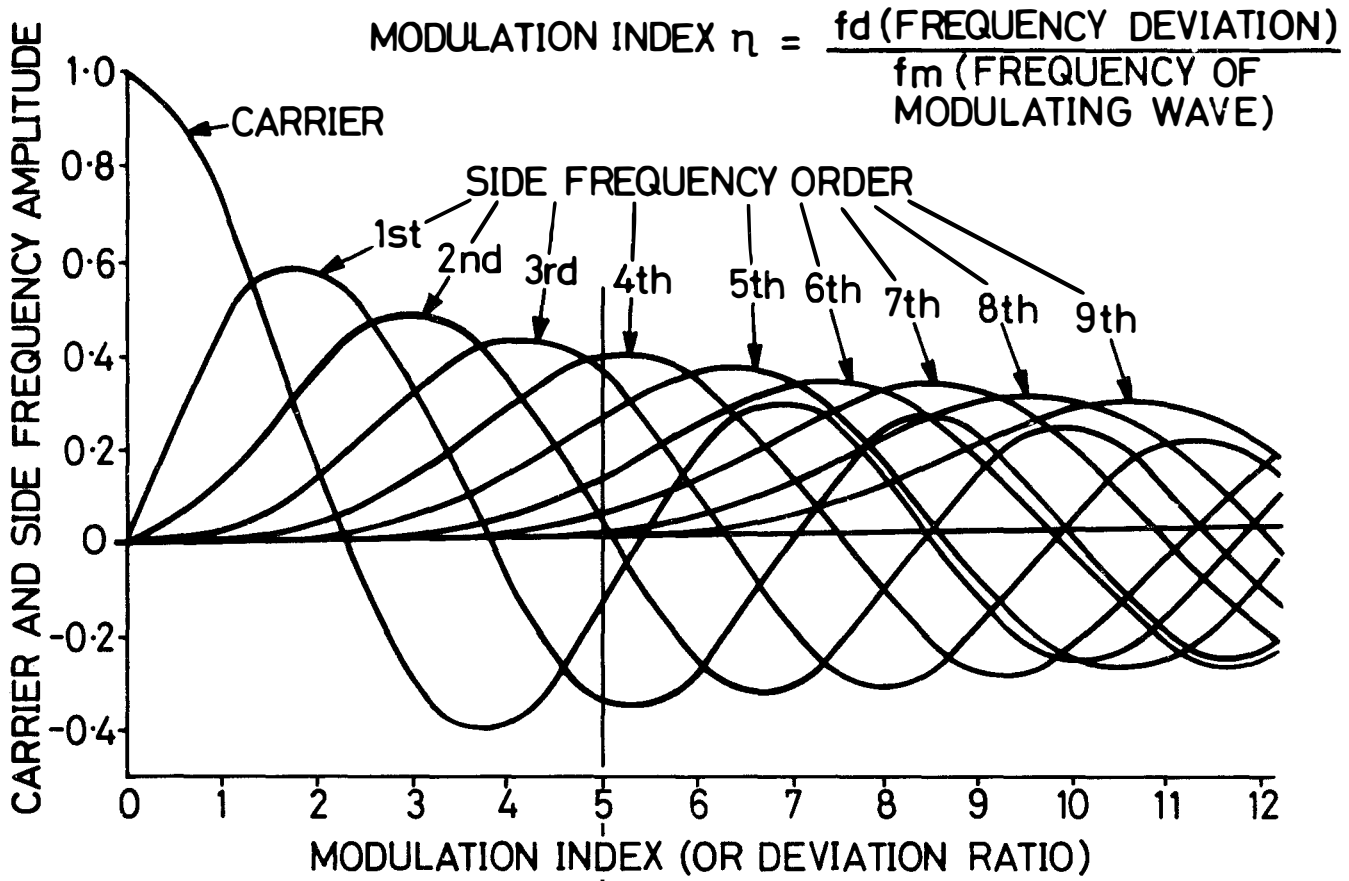
AMPLITUDE MODULATION



FREQUENCY MODULATION

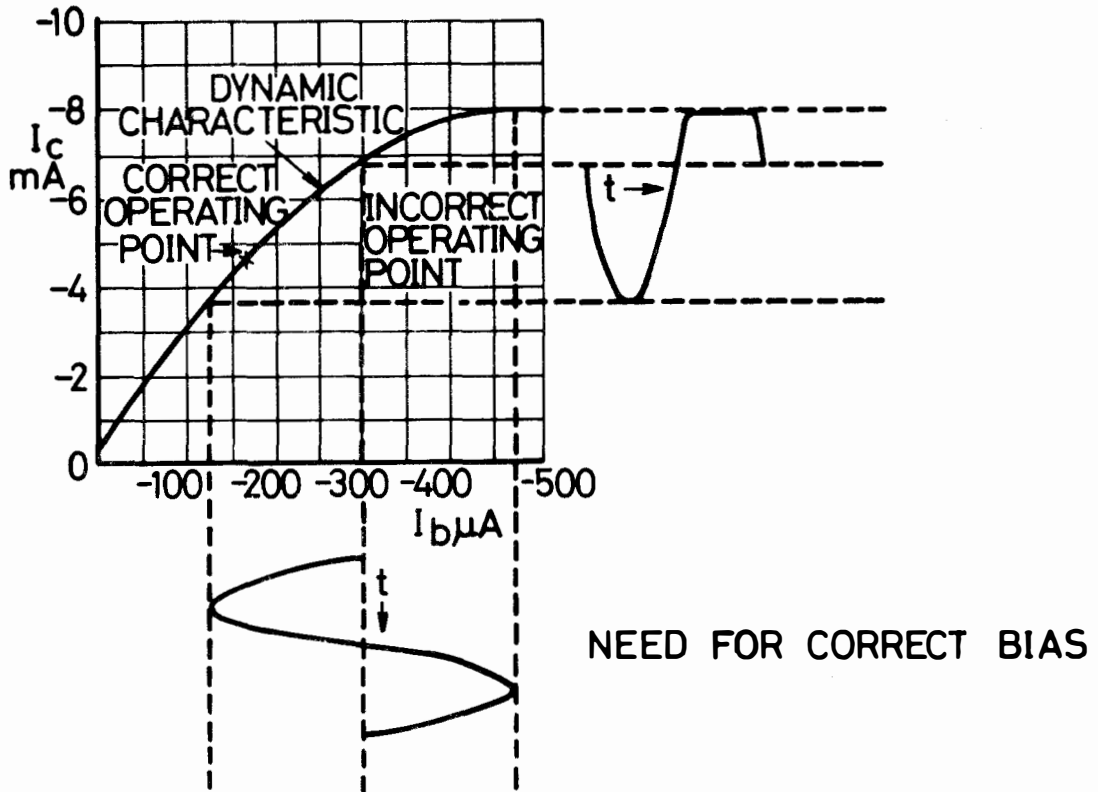
R 36686

Fig. 6-1 Comparison of A.M. and F.M.

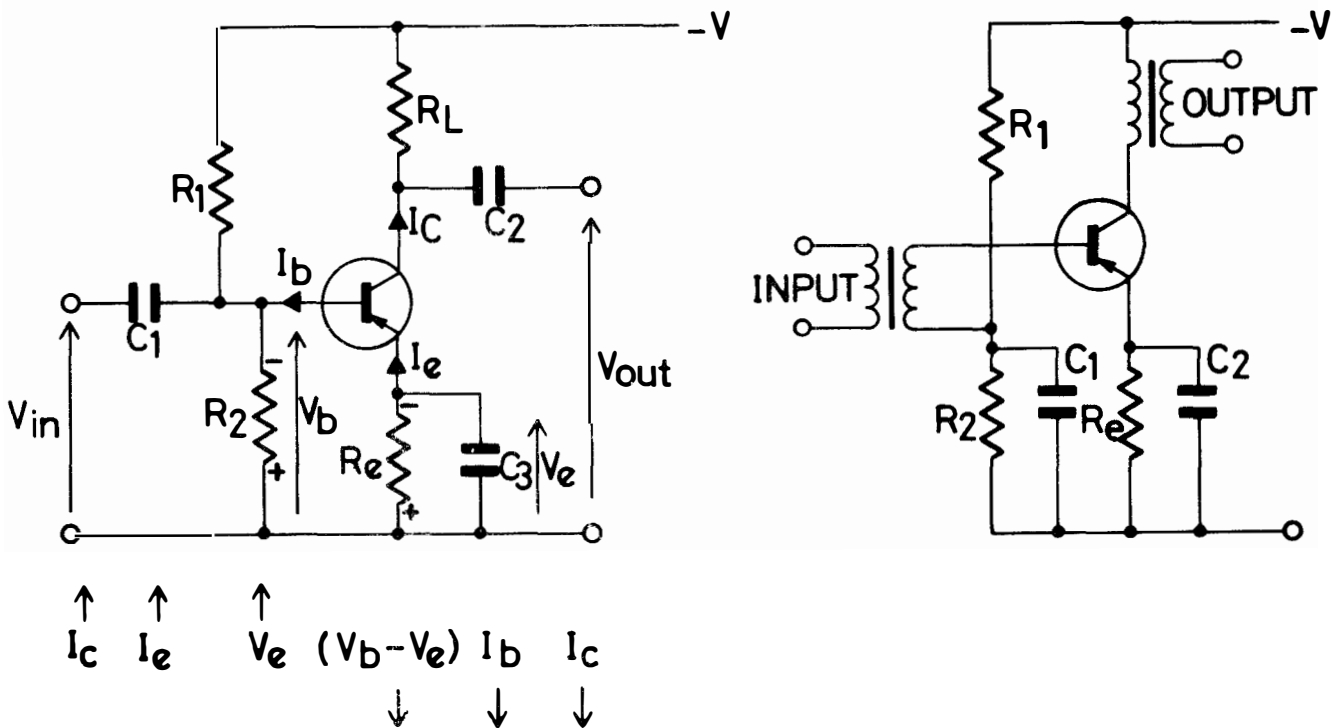


R 36687

Fig. 6-2 Spectrum diagram showing the amplitude of the side frequencies when the modulation index is 5

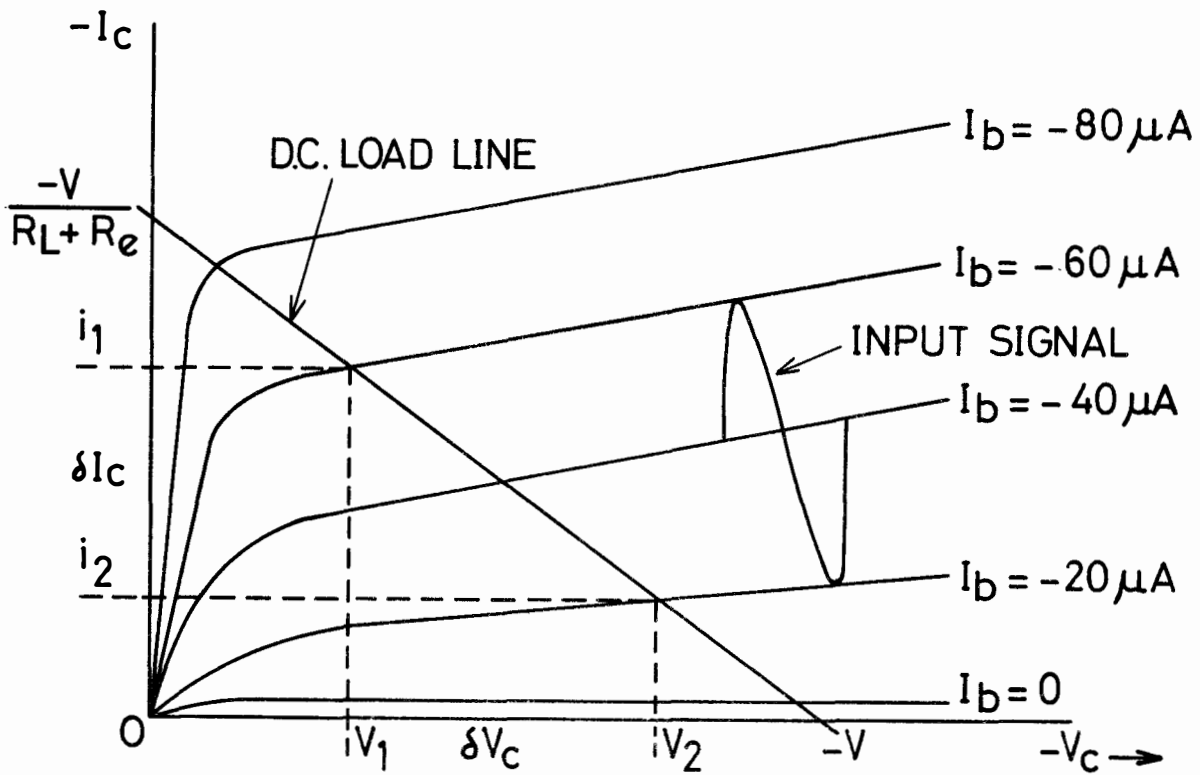
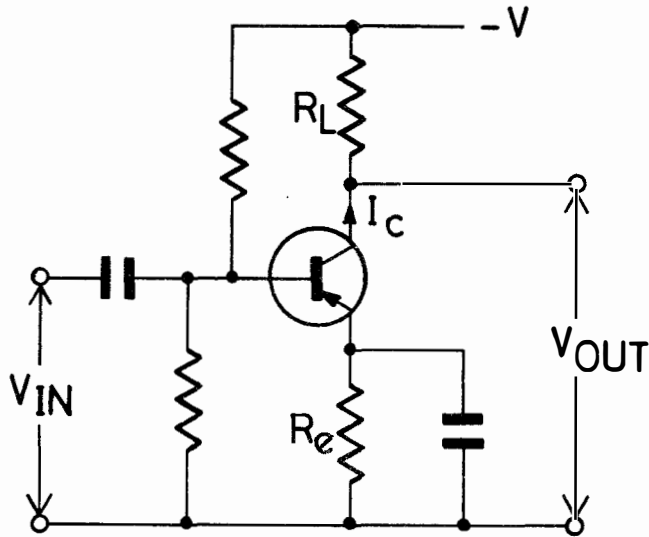


NEED FOR CORRECT BIAS



R 36688

Fig. 7-1 The need for correct bias and the potential divider method of achieving bias stabilization



$$I_{OUT} = \frac{(i_1 - i_2)}{\sqrt{2.2}}$$

$$V_{OUT} = \frac{(V_2 - V_1)}{\sqrt{2.2}}$$

$$P_{OUT} = I_{OUT} \times V_{OUT} = \frac{(i_1 - i_2)(V_2 - V_1)}{8}$$

R 366 89

Fig. 7-2 Common emitter amplifier. Obtaining output from the load line

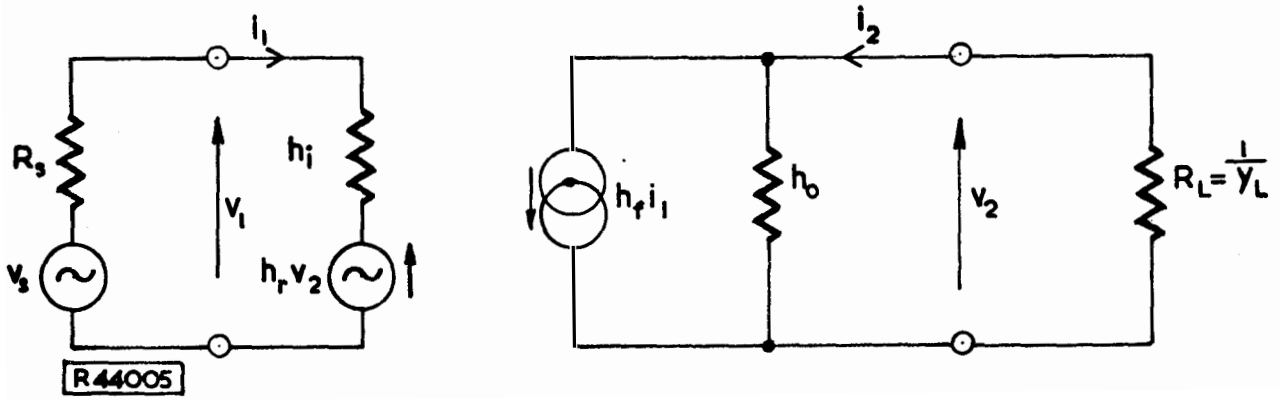


Fig. 7-3 h parameter complete equivalent circuit

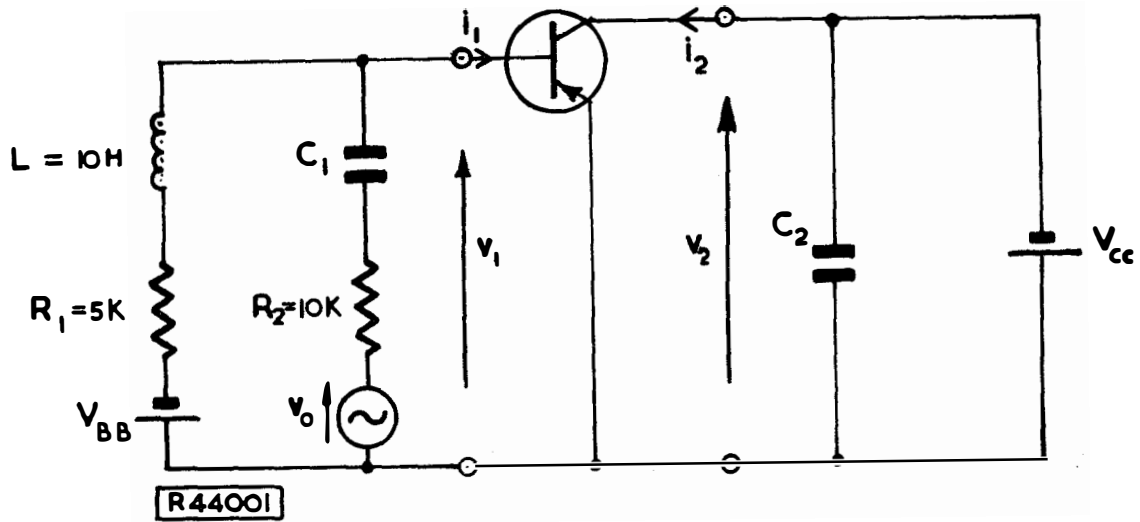
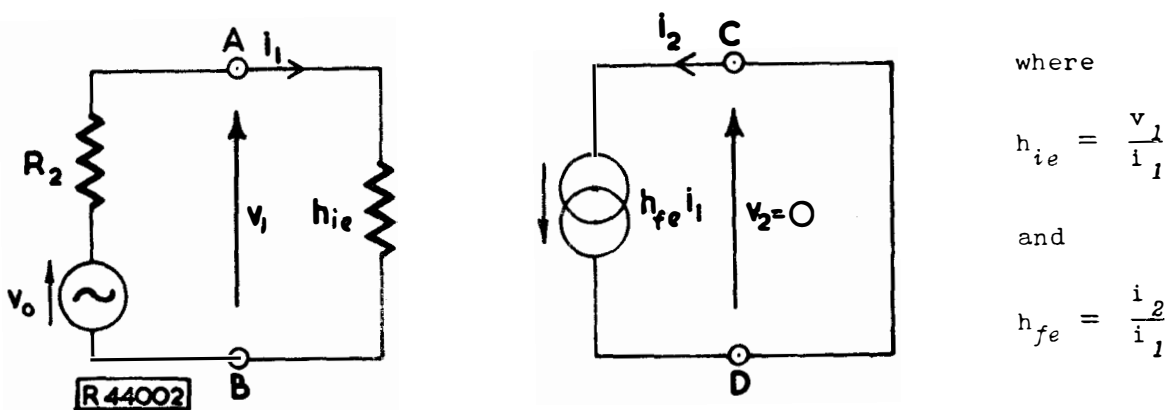


Fig. 7-4 Measuring the input impedance parameter  $h_{ie}$  and the forward current transfer parameter  $h_{fe}$



where

$$h_{ie} = \frac{v_1}{i_1}$$

and

$$h_{fe} = \frac{i_2}{i_1}$$

Fig. 7-5 Equivalent circuit

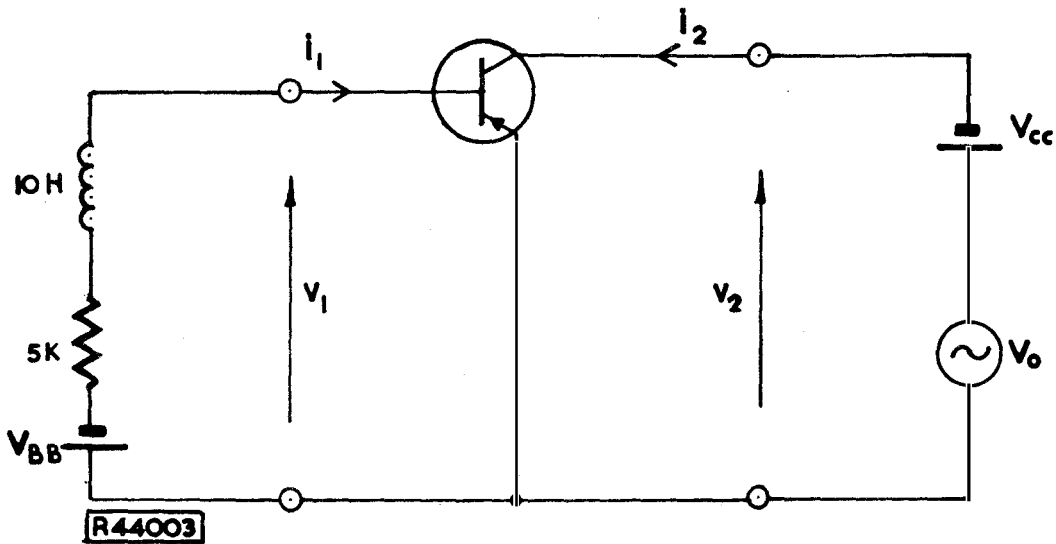
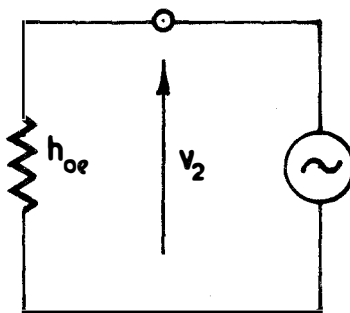
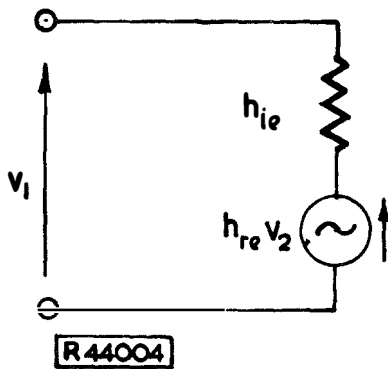


Fig. 7-6 Measuring the reverse voltage transfer ratio parameter  $h_{re}$  and the output admittance parameter  $h_{oe}$



where

$$h_{re} = \frac{v_1}{v_2}$$

and

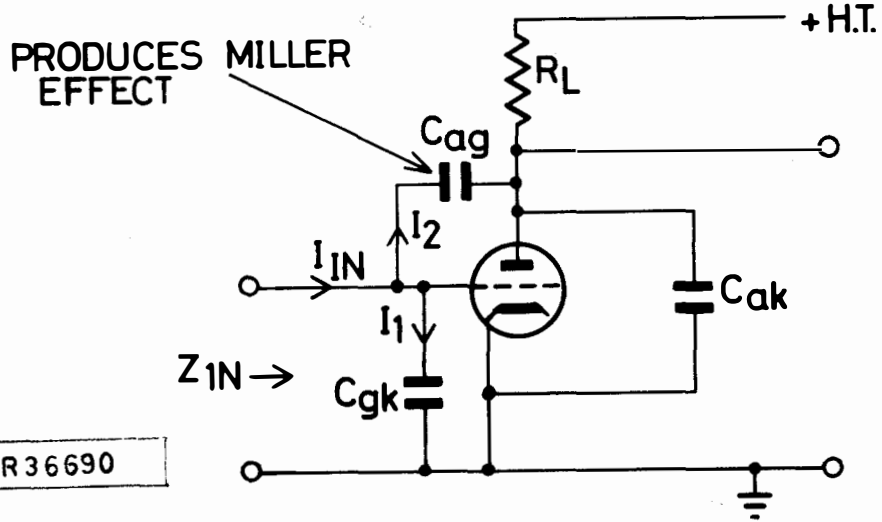
$$h_{oe} = \frac{i_2}{v_2}$$

Fig. 7-7 Equivalent circuit

COMMON BASE	COMMON EMITTER	COMMON COLLECTOR
$(h_{11}) h_{ib} = 35 \text{ ohms}$	$(h'_{11}) h_{ie} = 1450 \text{ ohms}$	$(h''_{11}) h_{ic} = 1500 \text{ ohms}$
$(h_{22}) h_{ob} = 10^{-6} \text{ siemen}$	$(h'_{22}) h_{oe} = 42 \times 10^{-6} \text{ siemen}$	$(h''_{22}) h_{oc} = 42 \times 10^{-6} \text{ siemen}$
$(h_{12}) h_{rb} = 7 \times 10^{-4}$	$(h'_{12}) h_{re} = 7.6 \times 10^{-4}$	$(h'_{12}) h_{rc} = 1$
$(h_{21}) h_{fb} = -0.976$	$(h'_{21}) h_{fe} = 41$	$(h''_{21}) h_{fc} = -42$

Note that the Forward Current Transfer Ratio ( $h_f$ ) for both common base and common collector configurations is negative. The previous symbols used for the parameters are shown in brackets as they are still encountered in some text books.

Fig. 7-8 Typical values of h parameters for an audio frequency transistor



$$Z_{IN} \equiv C_{gk} + (1+A)C_{ag}$$

WHERE A = STAGE GAIN

Fig. 8-1 Anode to grid feedback via  $C_{ag}$  producing Miller Effect

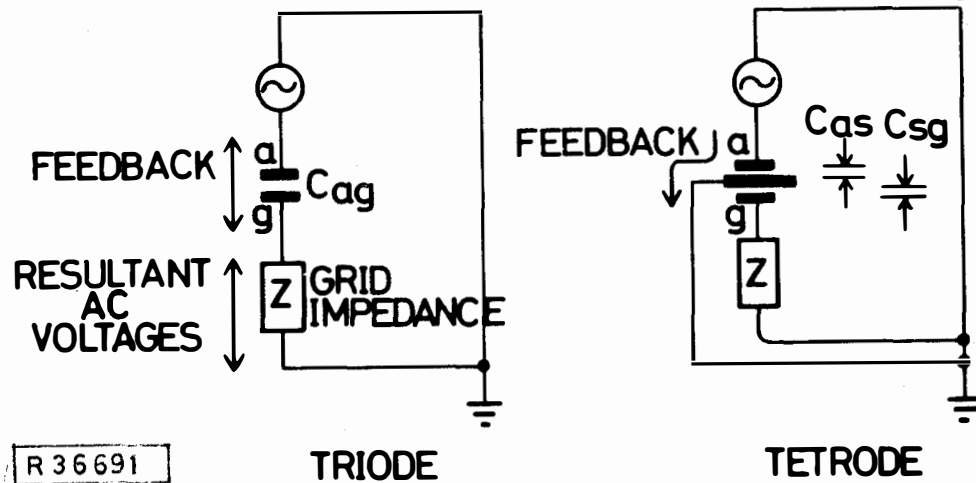


Fig. 8-2 Theory of screening

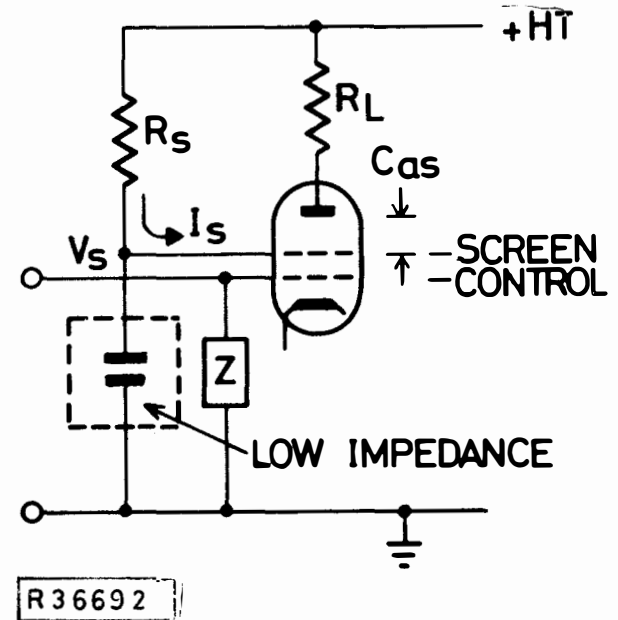
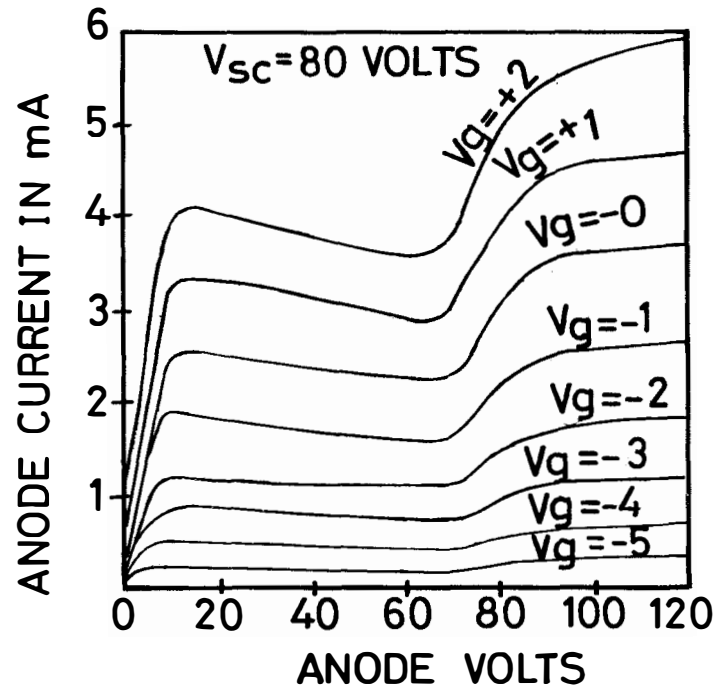
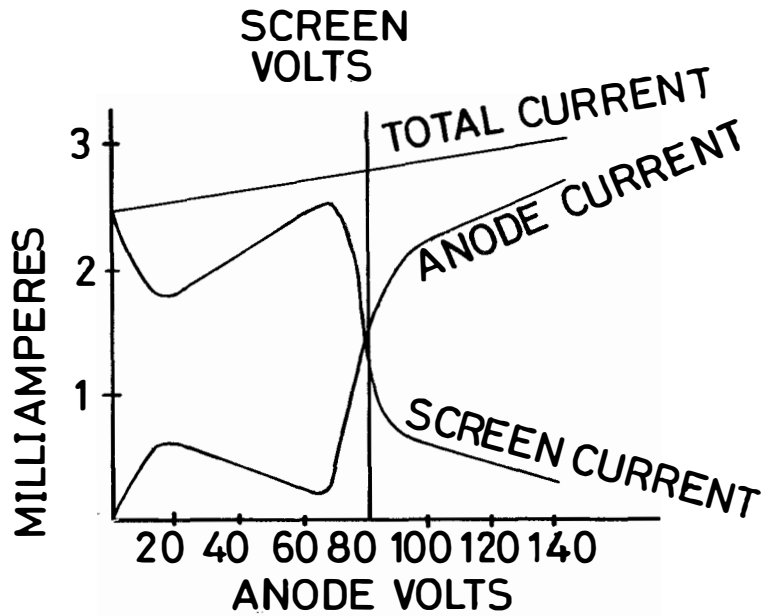
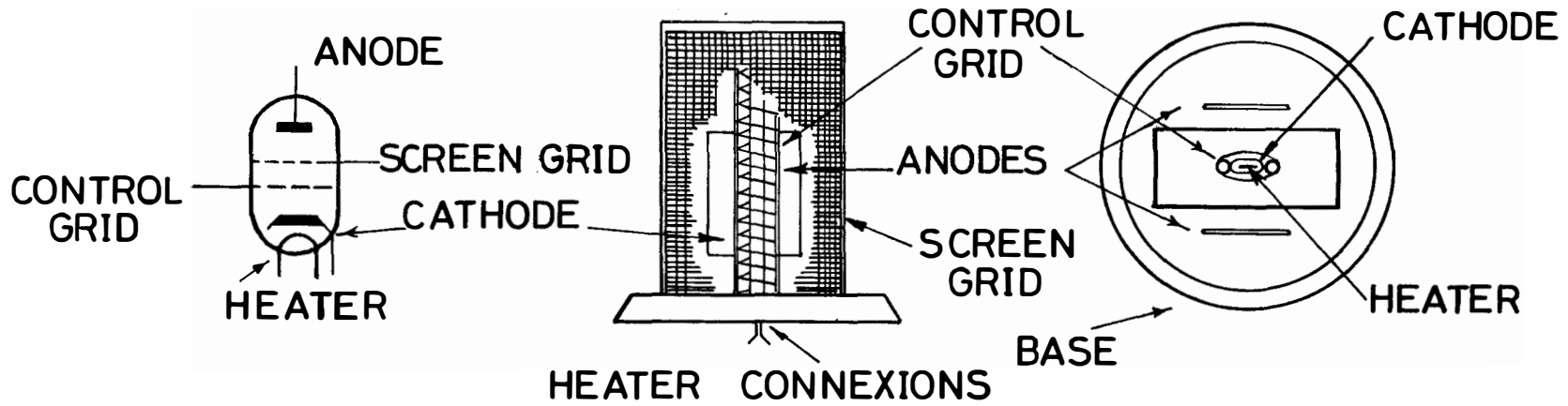


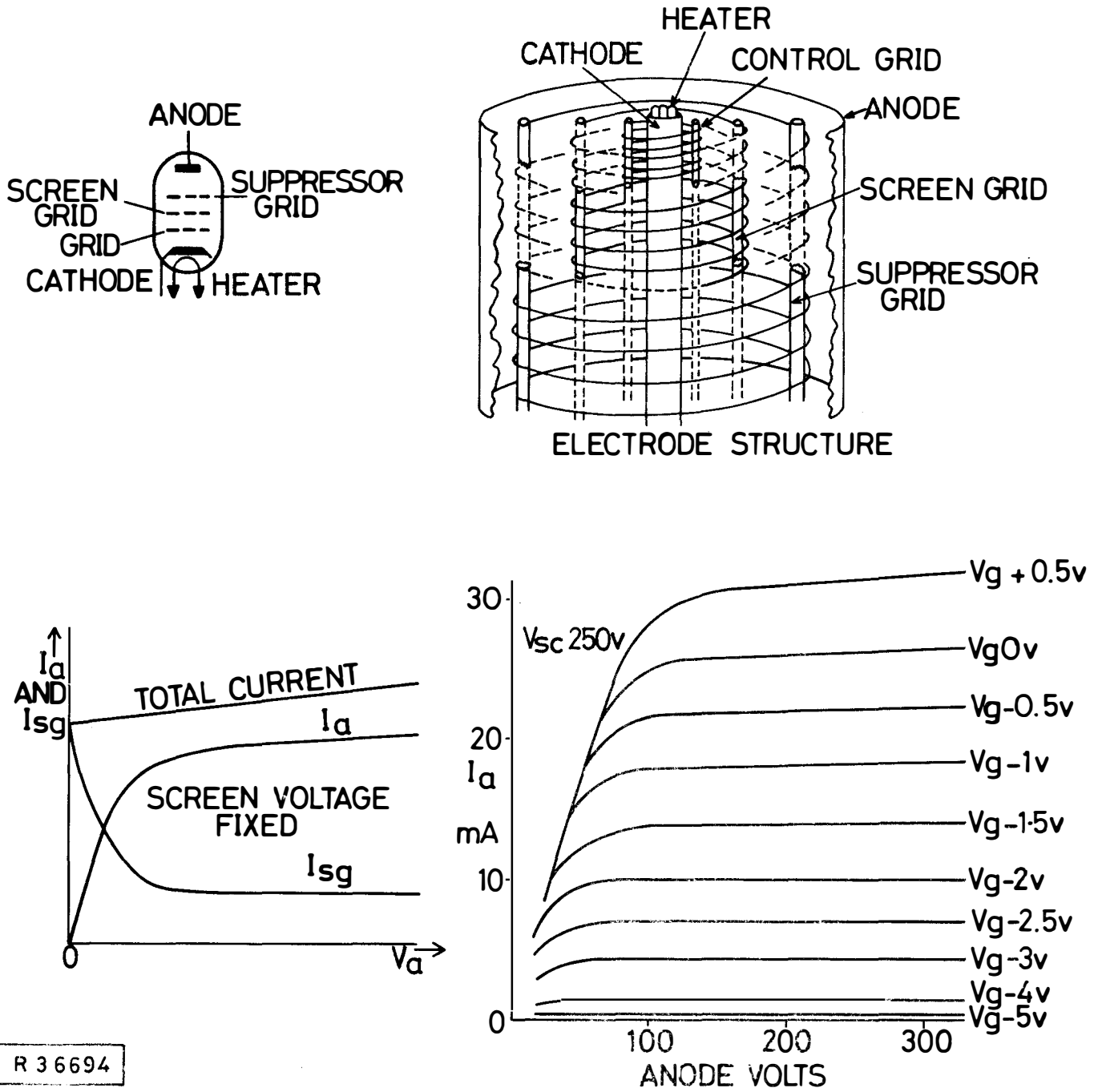
Fig. 8-3 The Tetrode circuit. Note that the screen is at a +ve potential, hence the need for the capacitor connected to the earth line





R 3 6 6 9 3

Fig. 8-4 The tetrode valve



R 3 6694

Fig. 8-5 The pentode valve

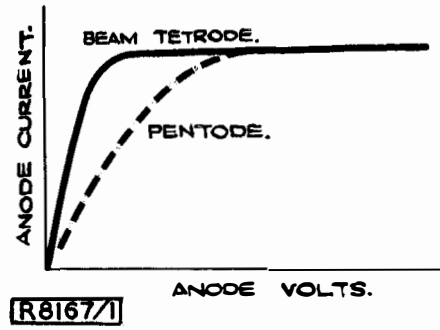
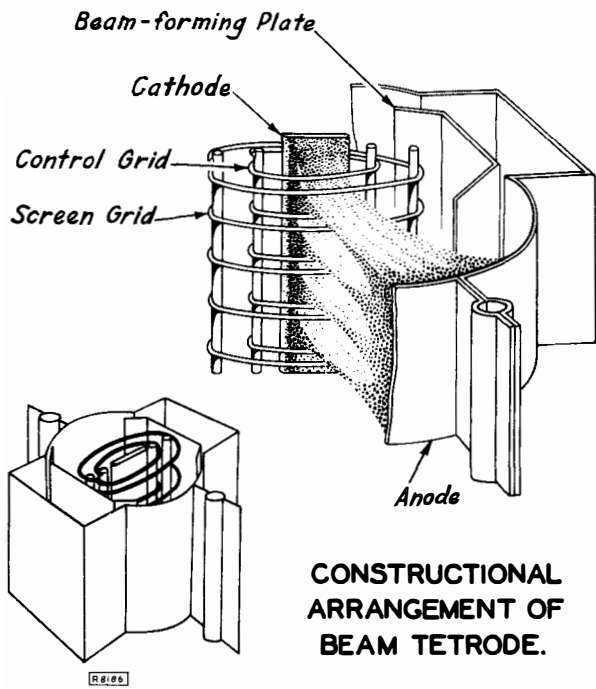


Fig. 8-7 Comparison of Beam Tetrode and Pentode Characteristics

Fig. 8-6 Beam forming plates in the Beam Tetrode

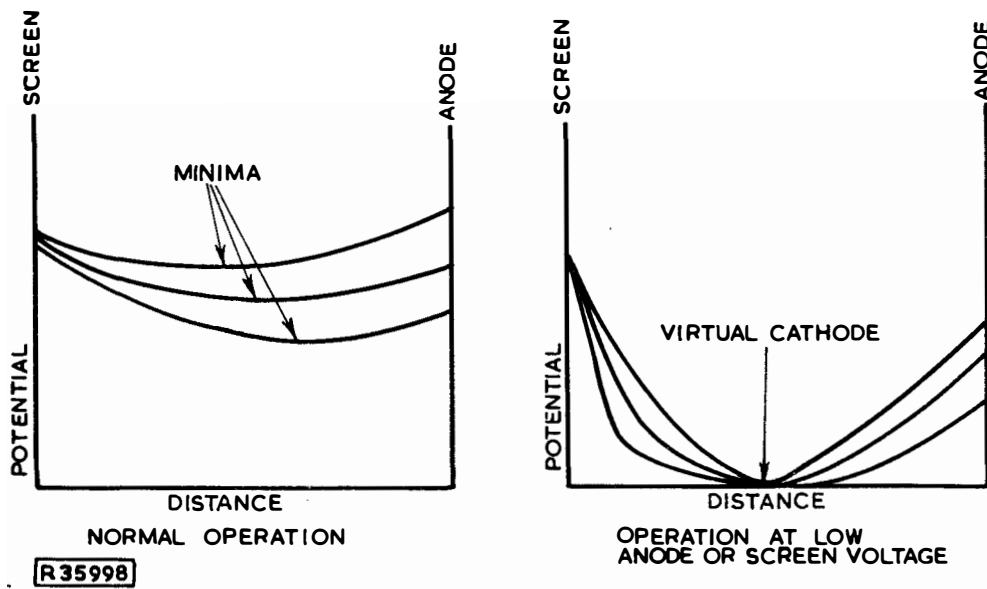
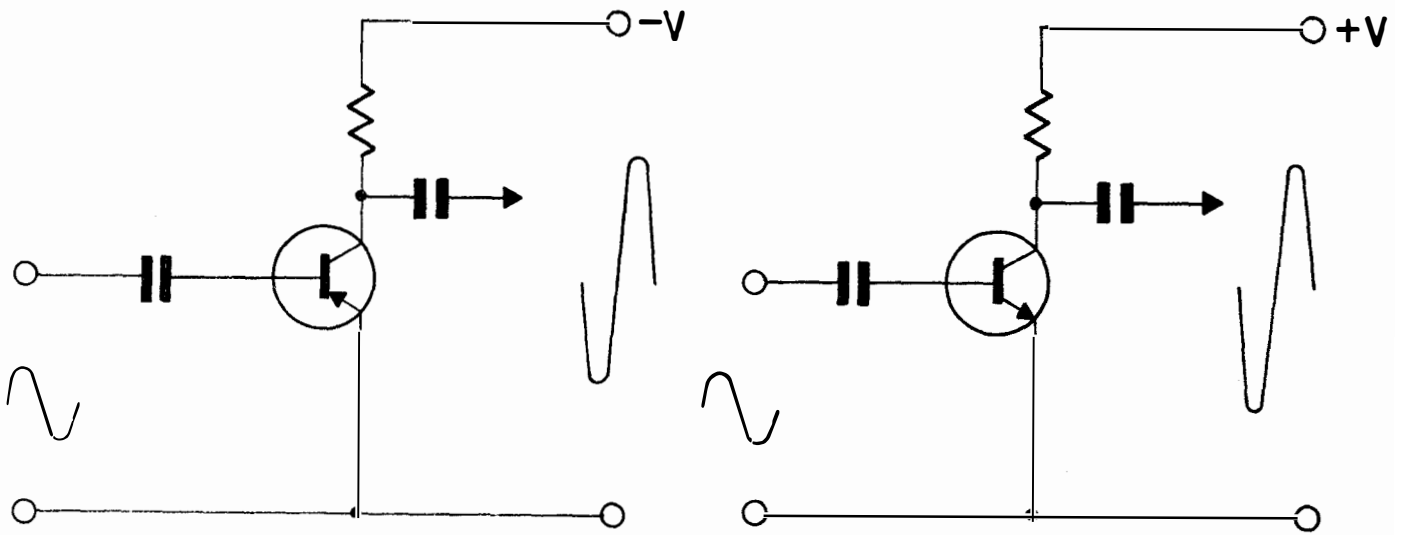
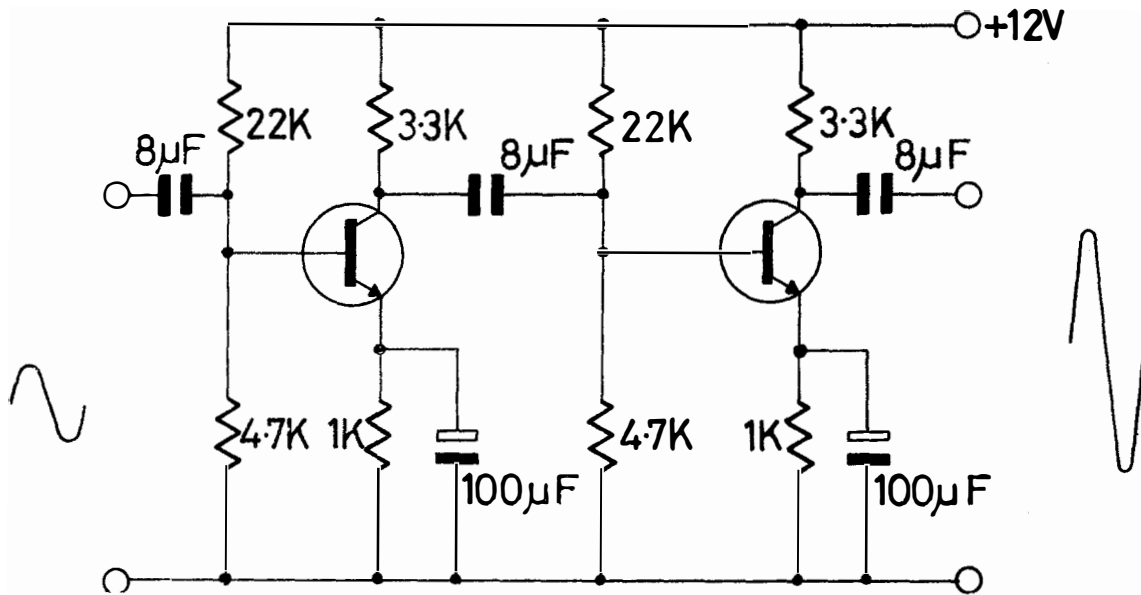


Fig. 8-8 Potential distribution between the screen and anode in a Beam Tetrode



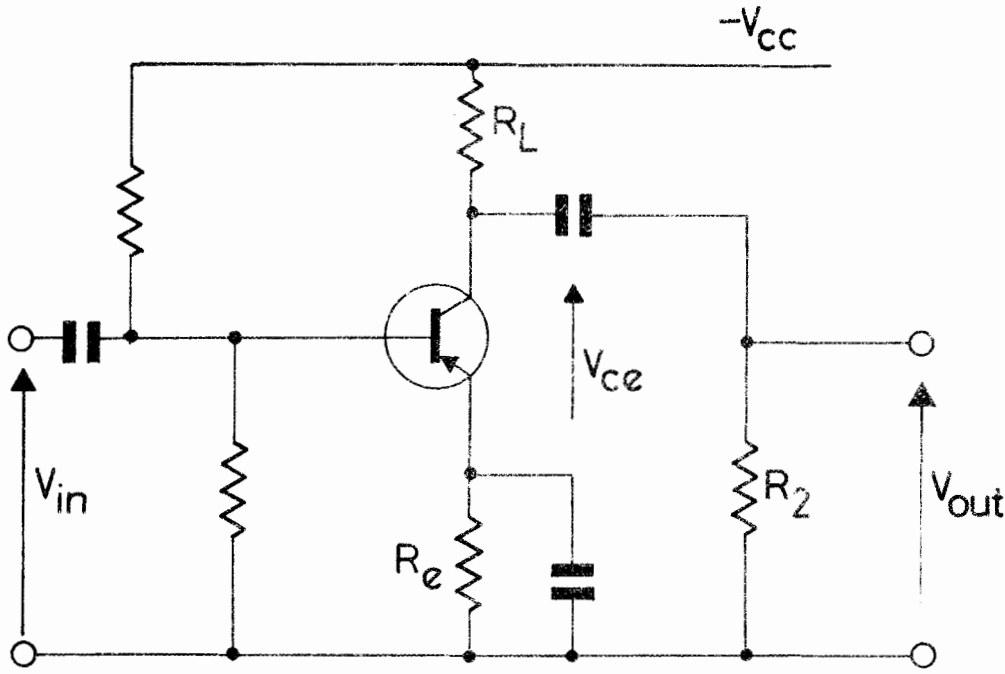
R 36695

Fig. 9-1 Representation of PNP and NPN transistors. Note that the polarity is reversed



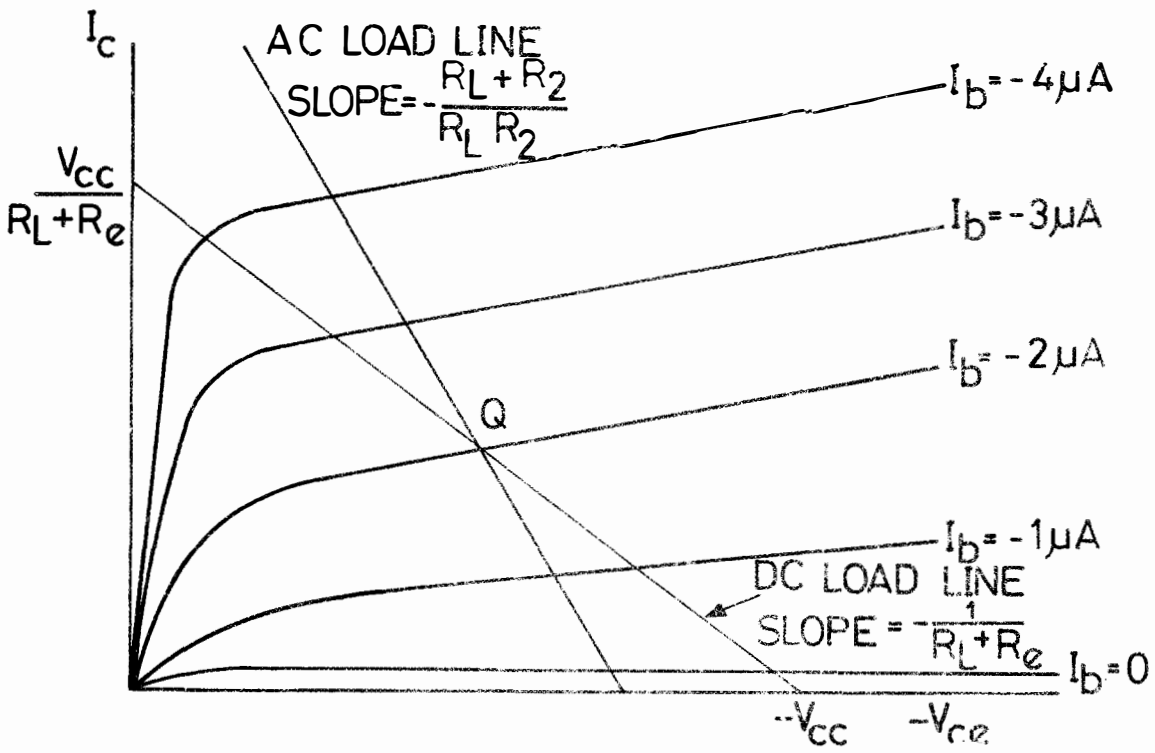
R 36696

Fig. 9-2 R.C. coupled 2 stage NPN transistor amplifier showing typical component values



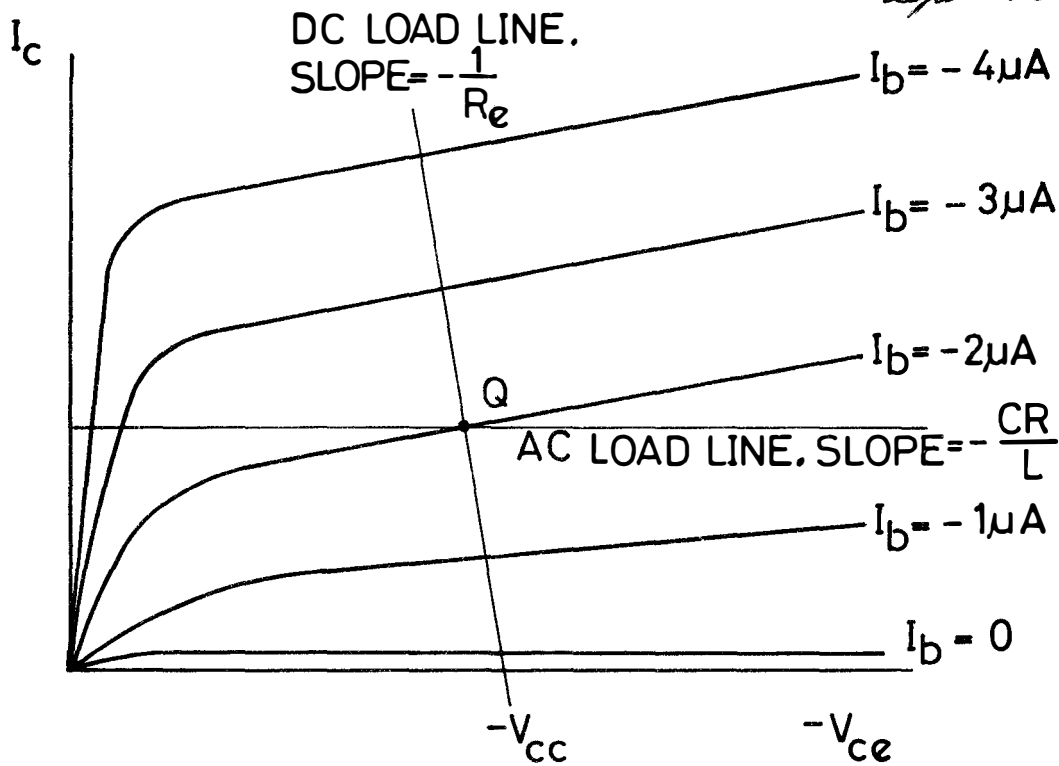
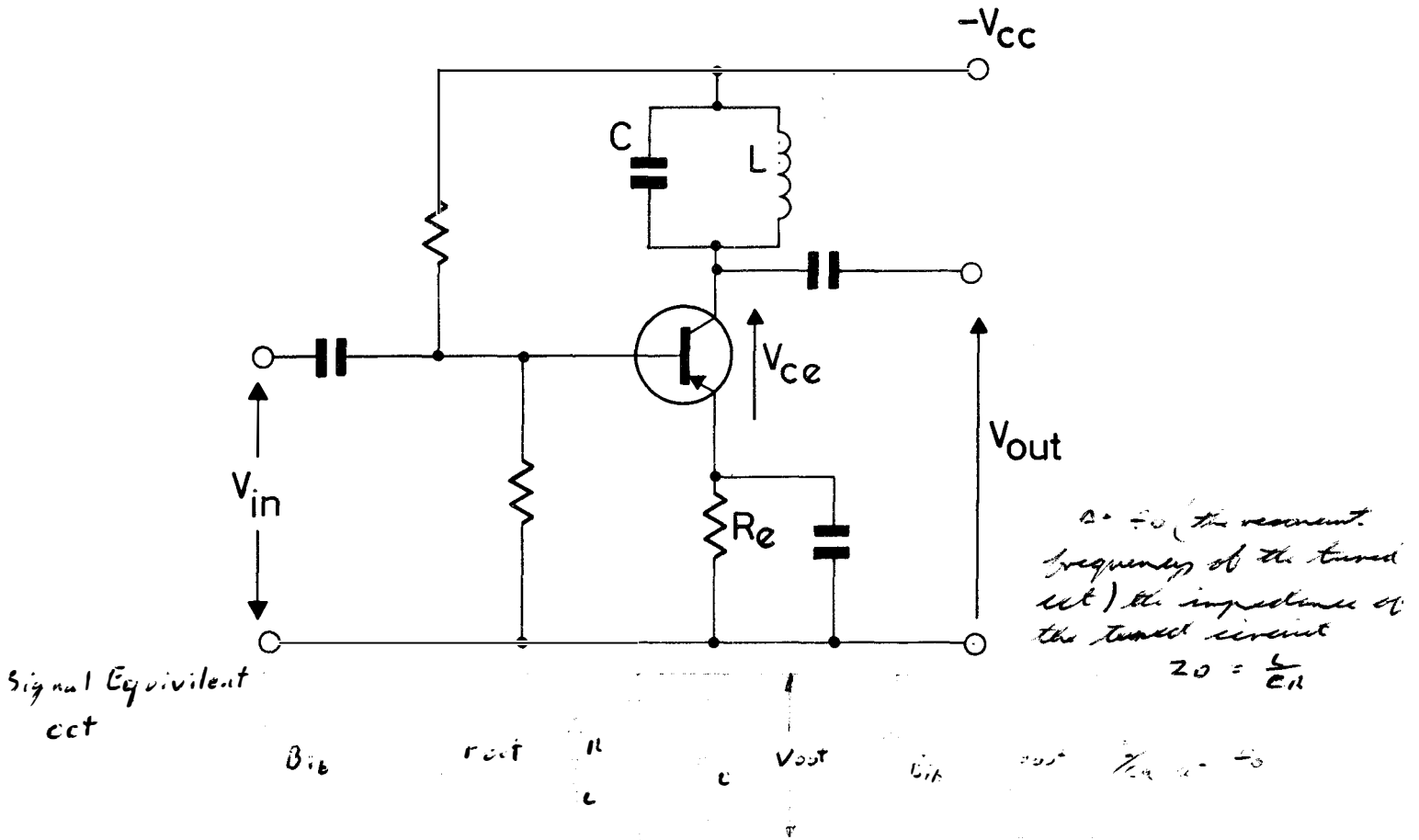
Signal Equivalent circuit for output stage of amplifier

If  $V_{out}$  is very much greater than  $R_1$  &  $R_2$  (as is usually the case)  $R_1$  &  $R_2$  can be neglected. Hence the effective load on the transistor is  $R_L$  in parallel with  $R_2$ .



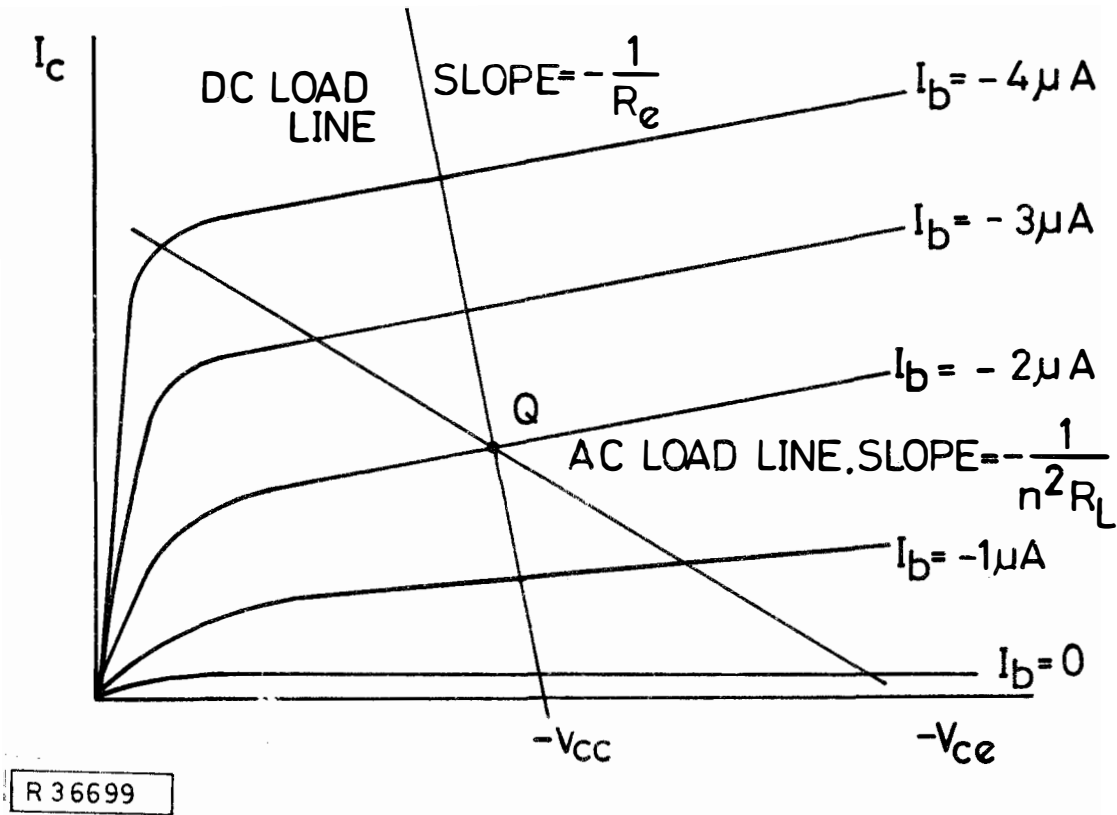
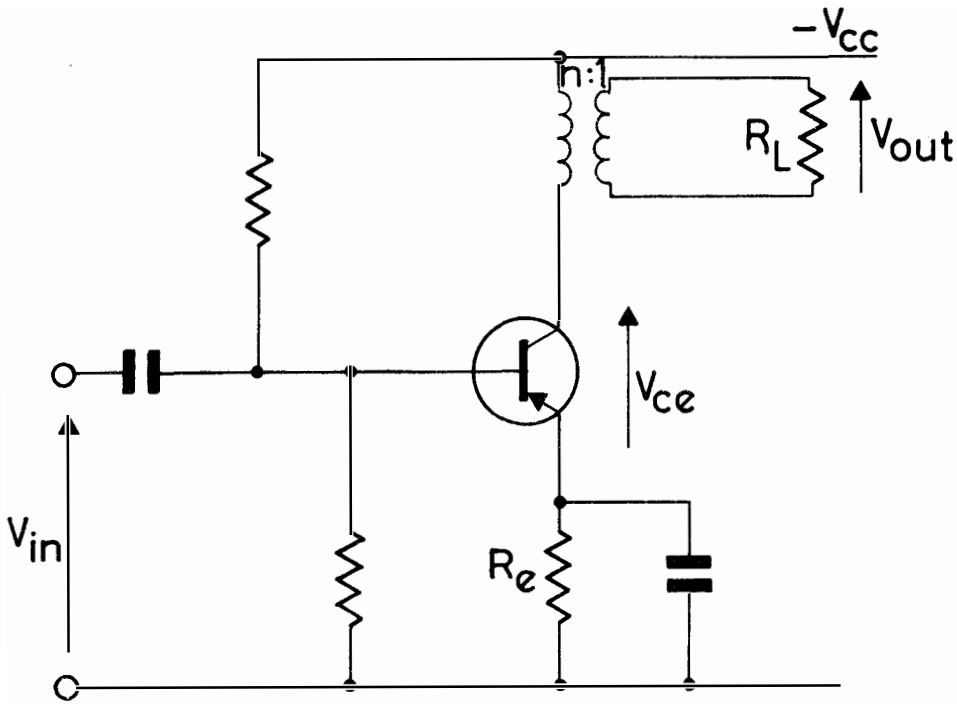
R 36697

Fig. 9-3 Resistance loaded transistor amplifier and load line



R 36698

Fig. 9-4 Tuned anode transistor amplifier



R 36699

Fig. 9-5 Transformer coupled transistor amplifier

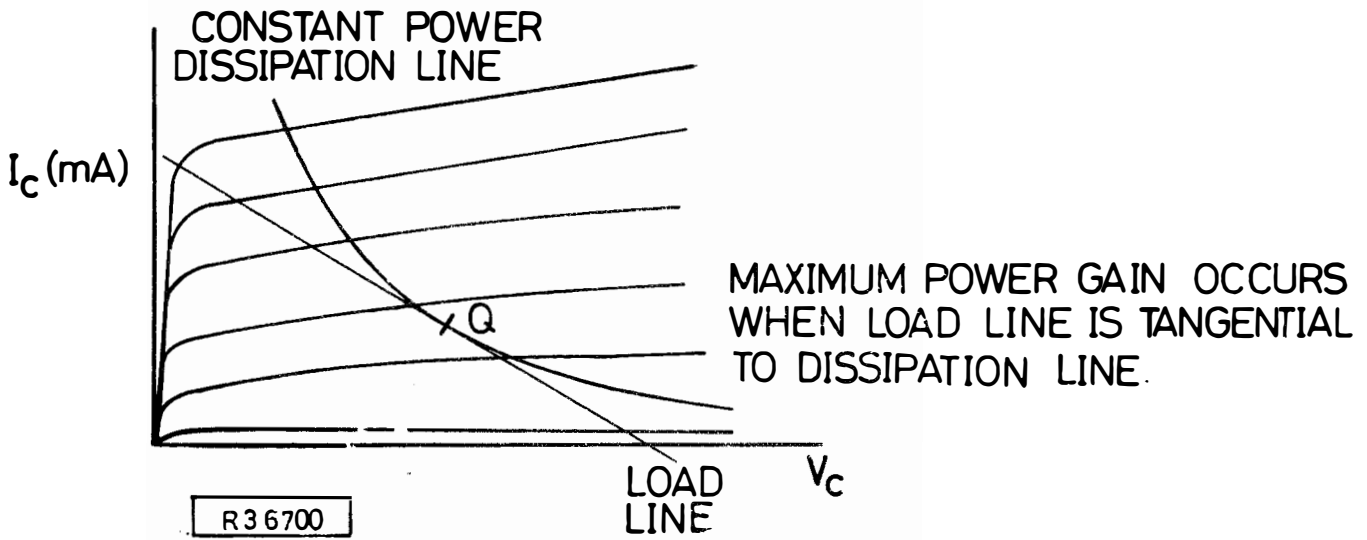


Fig. 9-6 Power dissipation line. The operating point  $Q$  must not be above the power line

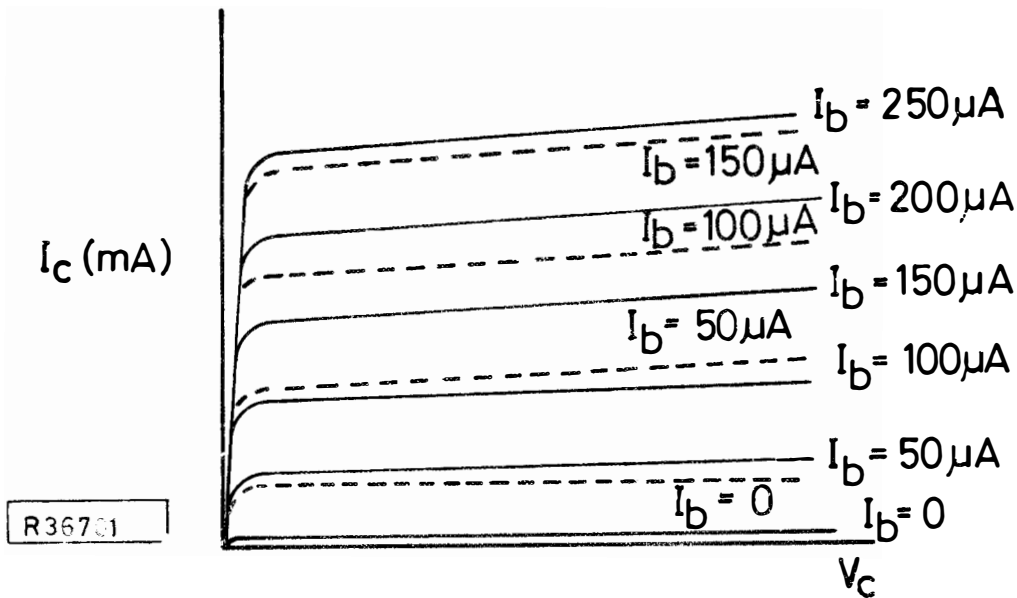


Fig. 9-7 The whole family of curves is raised when the room temperature is increased to  $70^\circ C$

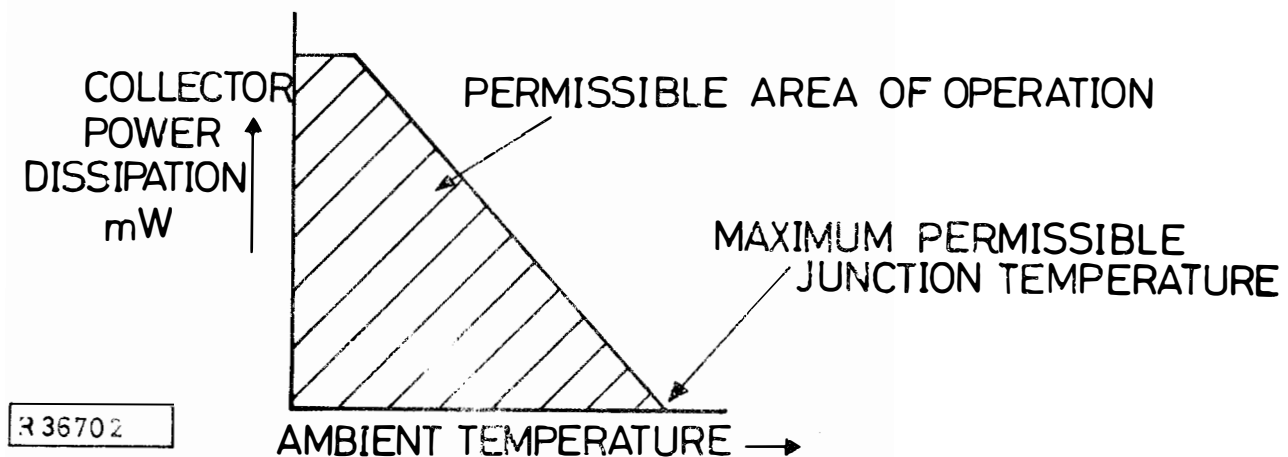
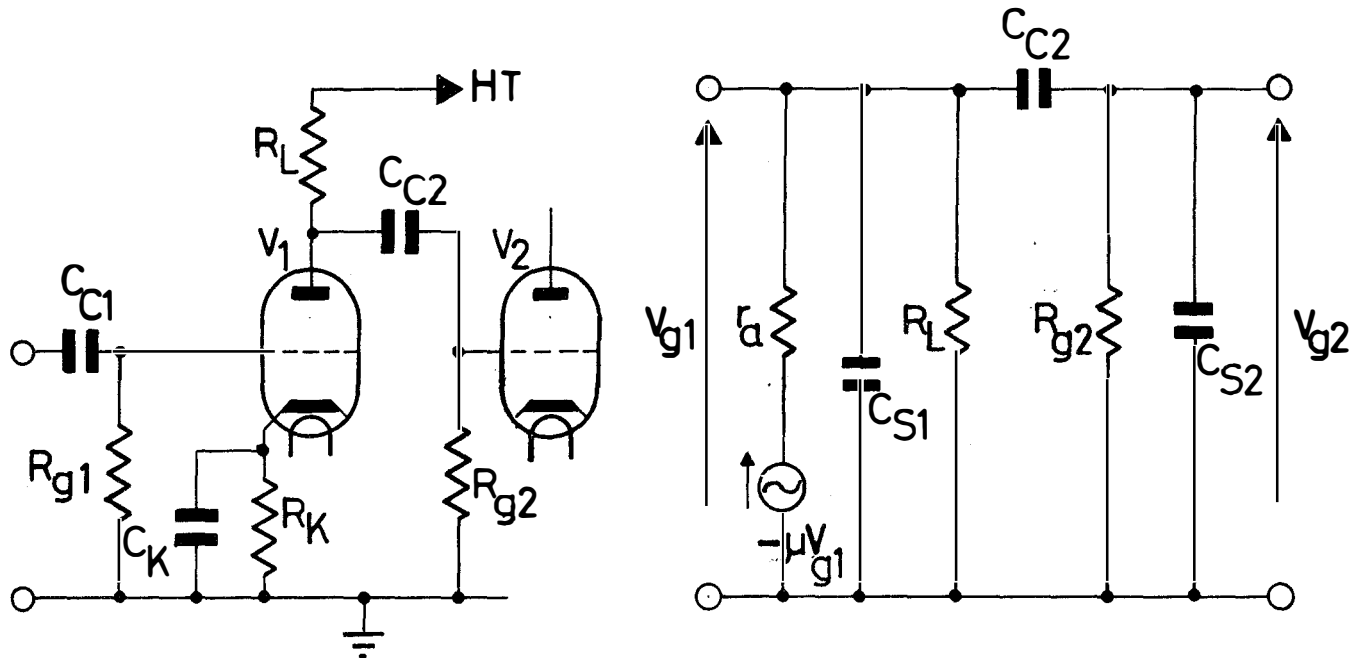


Fig. 9-8 Relationship between allowable collector power dissipation and ambient temperature





THE FUNCTIONS OF THE COMPONENTS ARE AS FOLLOWS.

$C_{C1}$  INPUT COUPLING CAPACITOR

$R_{g1}$  GRID RESISTOR

$R_L$  ANODE LOAD RESISTOR

$R_K$  CATHODE BIAS RESISTOR

$C_K$  CATHODE DECOUPLING CAPACITOR

$C_{C2}$  INTERSTAGE COUPLING CAPACITOR

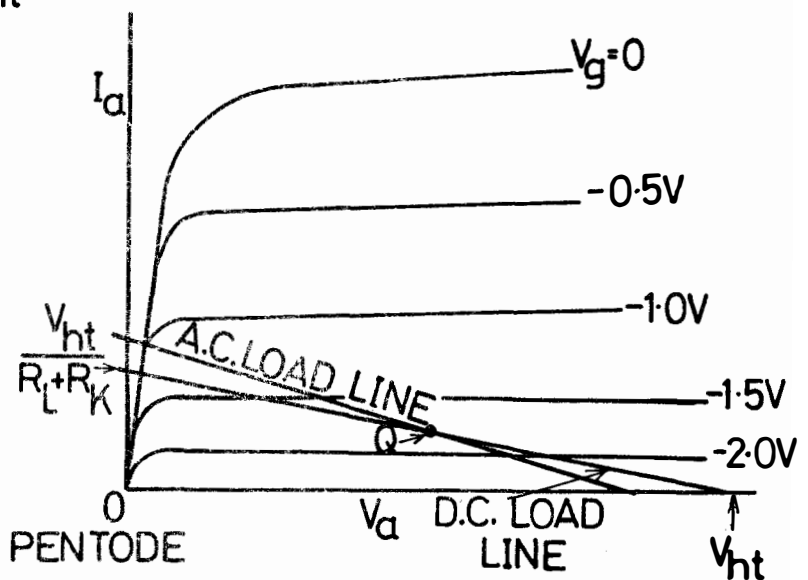
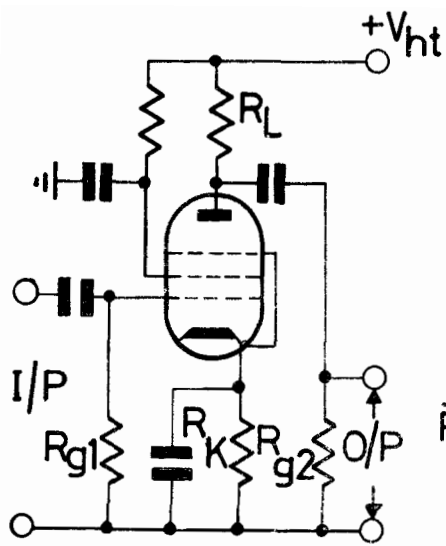
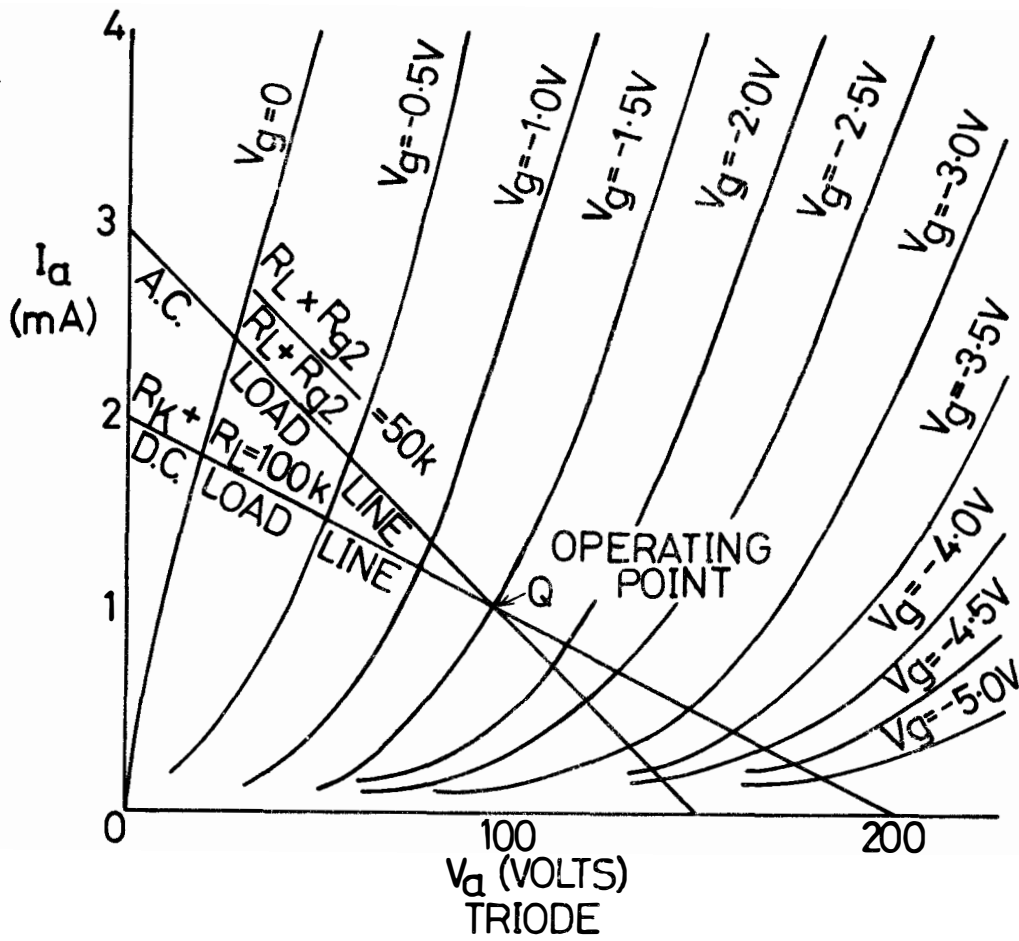
$R_{g2}$  GRID RESISTOR

$C_{S1}$  CIRCUIT WIRING CAPACITY AND OUTPUT CAPACITY OF  $V_1$

$C_{S2}$  CIRCUIT WIRING CAPACITY AND INPUT CAPACITY OF  $V_2$

R 36703

Fig. 9-9 R.C. coupled valve amplifier and its equivalent circuit



R367 04

Fig. 9-10 Triode and Pentode load lines

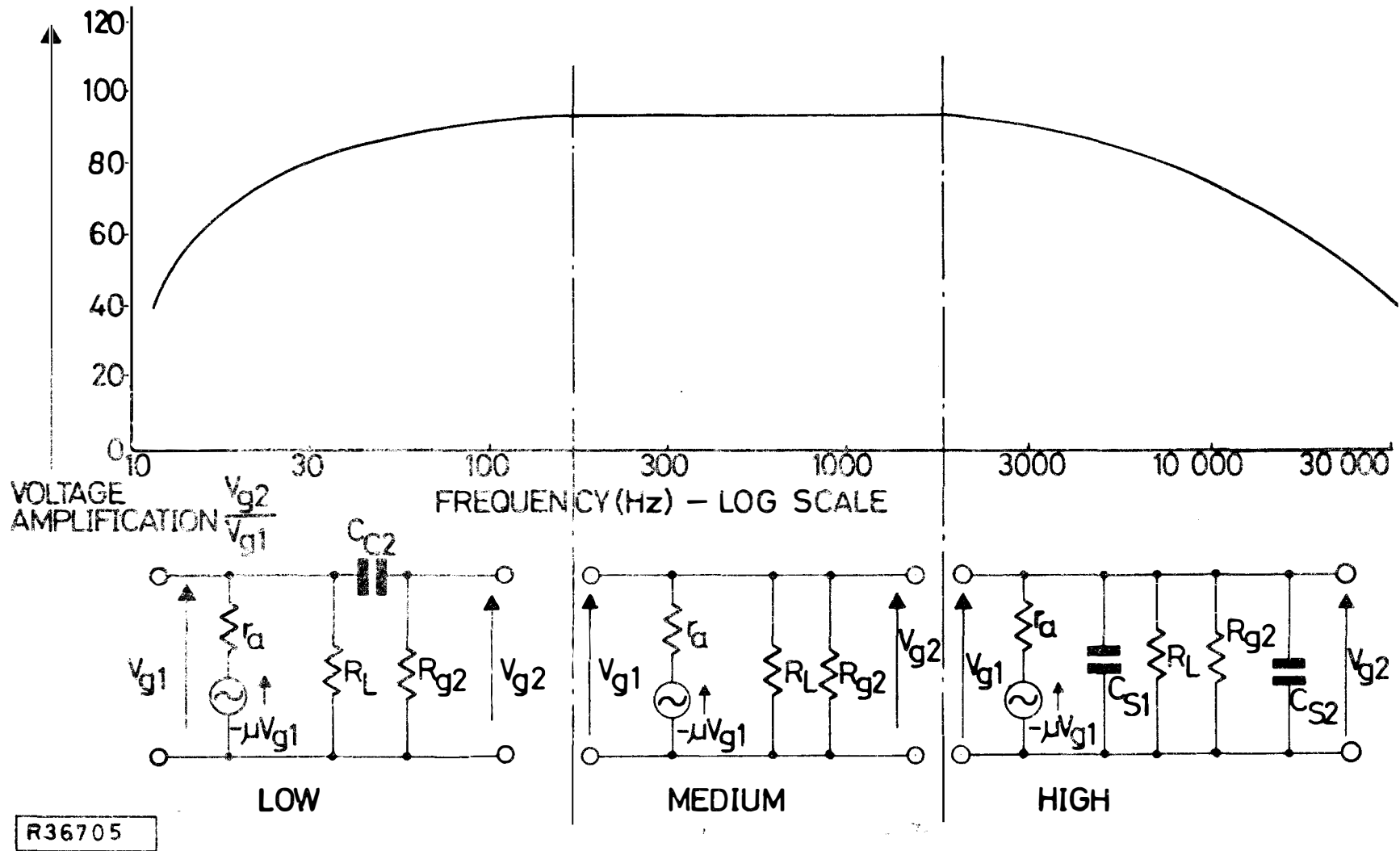
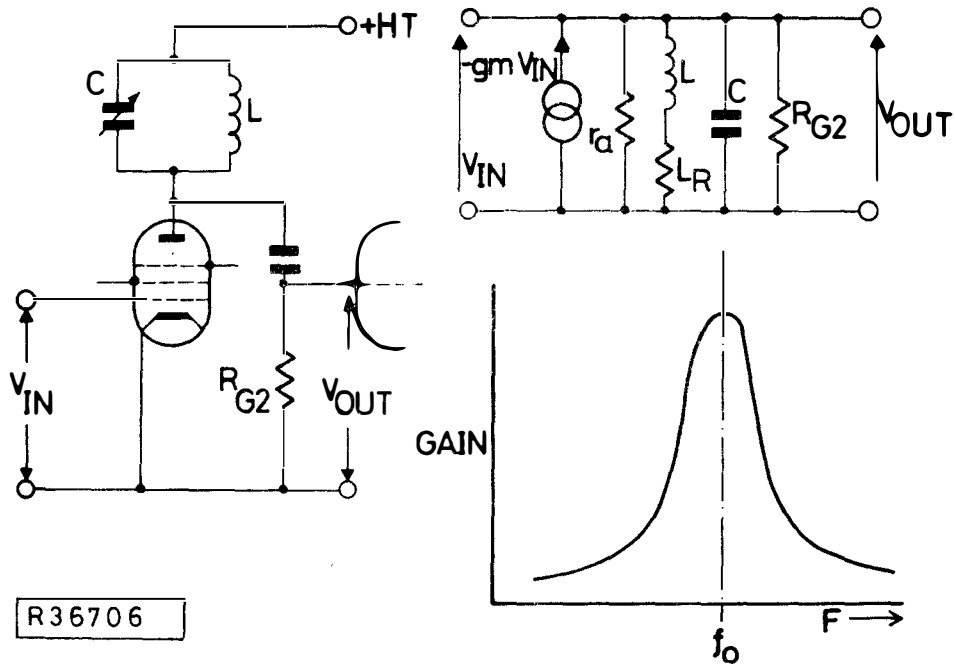
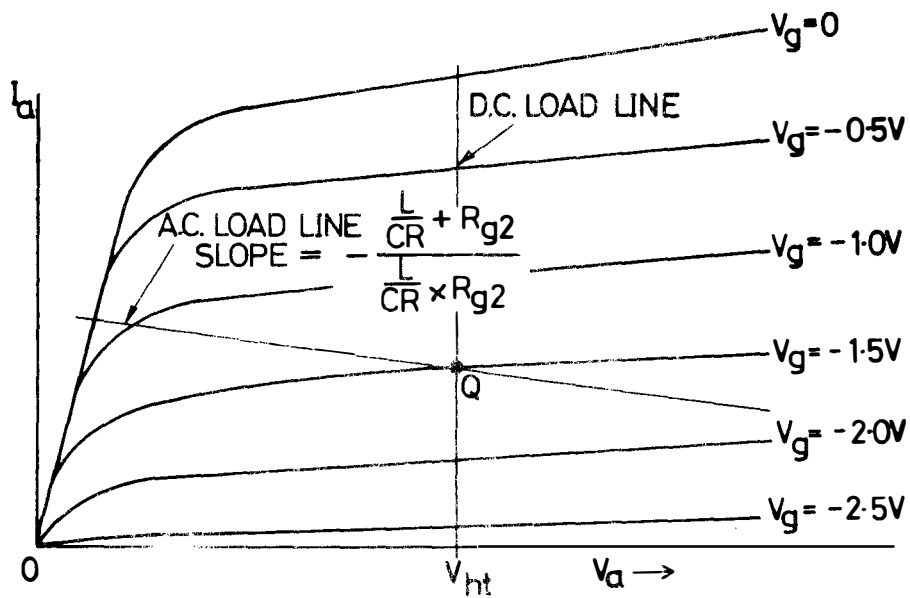


Fig. 9-11 B.C. coupled valve amplifier frequency response and equivalent circuits for low, medium and high frequencies



R36706

Fig. 9-12 Tuned anode valve amplifier, equivalent circuit and response curve



R36707

Fig. 9-13 Tuned anode load lines

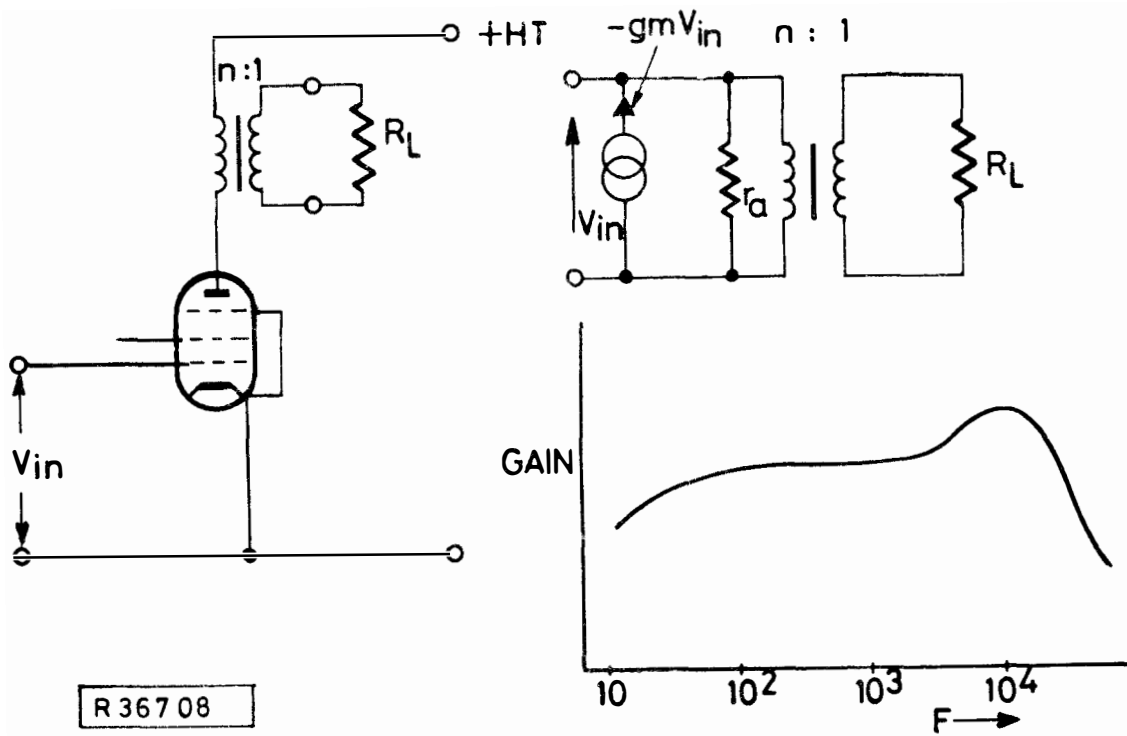
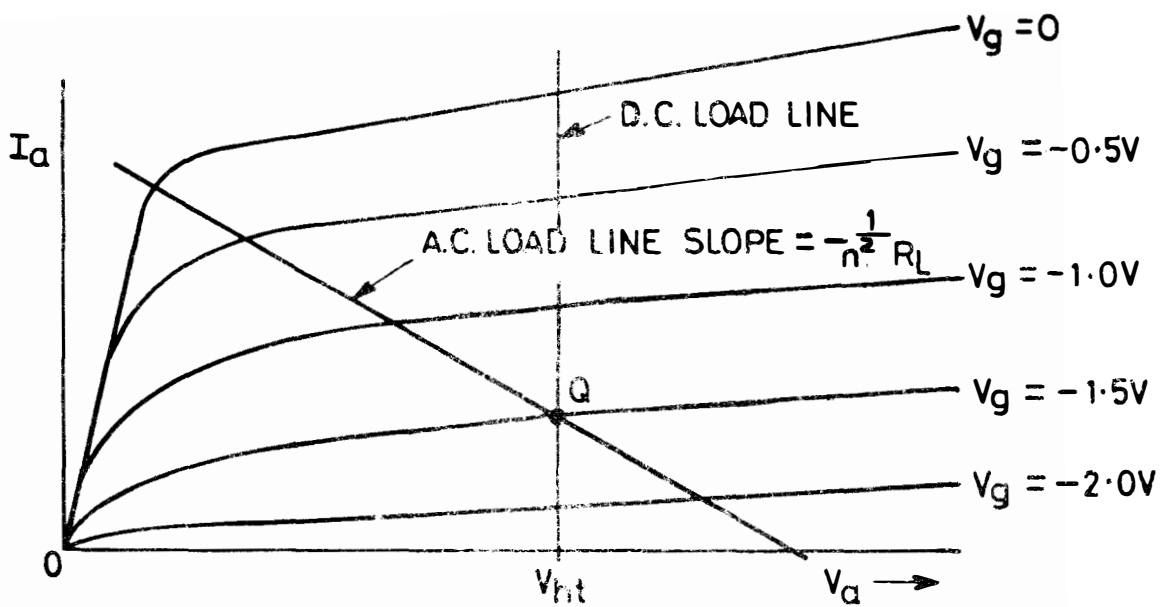
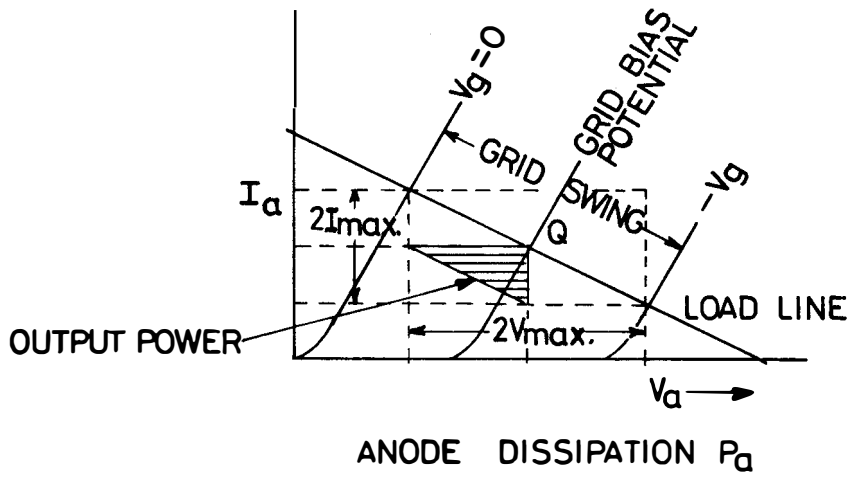


Fig. 9-14 Transformer coupled amplifier, equivalent circuit and frequency response



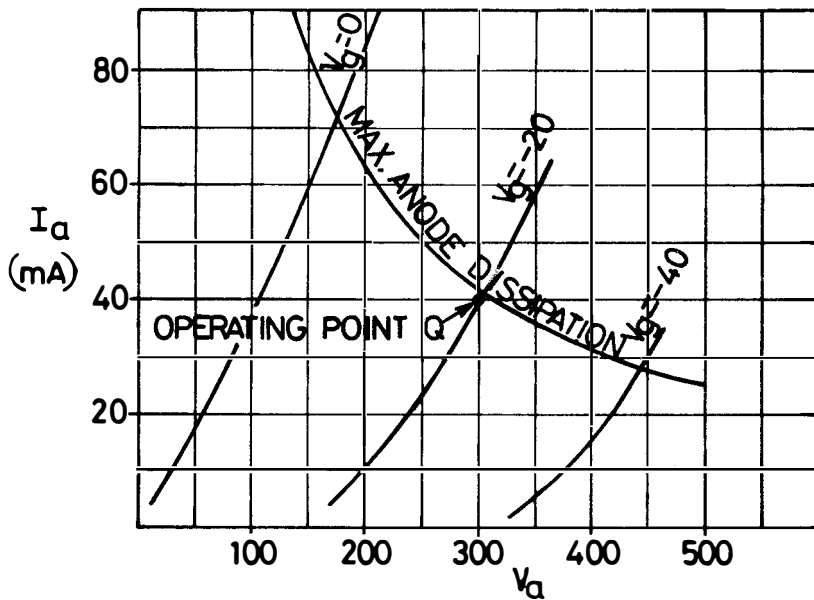
R36709

Fig. 9-15 Transformer coupled amplifier load lines



$P_a$  WITHOUT SIGNAL =  $V_a \times I_a$

$P_a$  WITH SIGNAL =  $[V_a \times I_a] - \frac{[V_a(max) - V_a(min)] [I_a(max) - I_a(min)]}{8}$



R36710

Fig. 9-16 Maximum anode dissipation

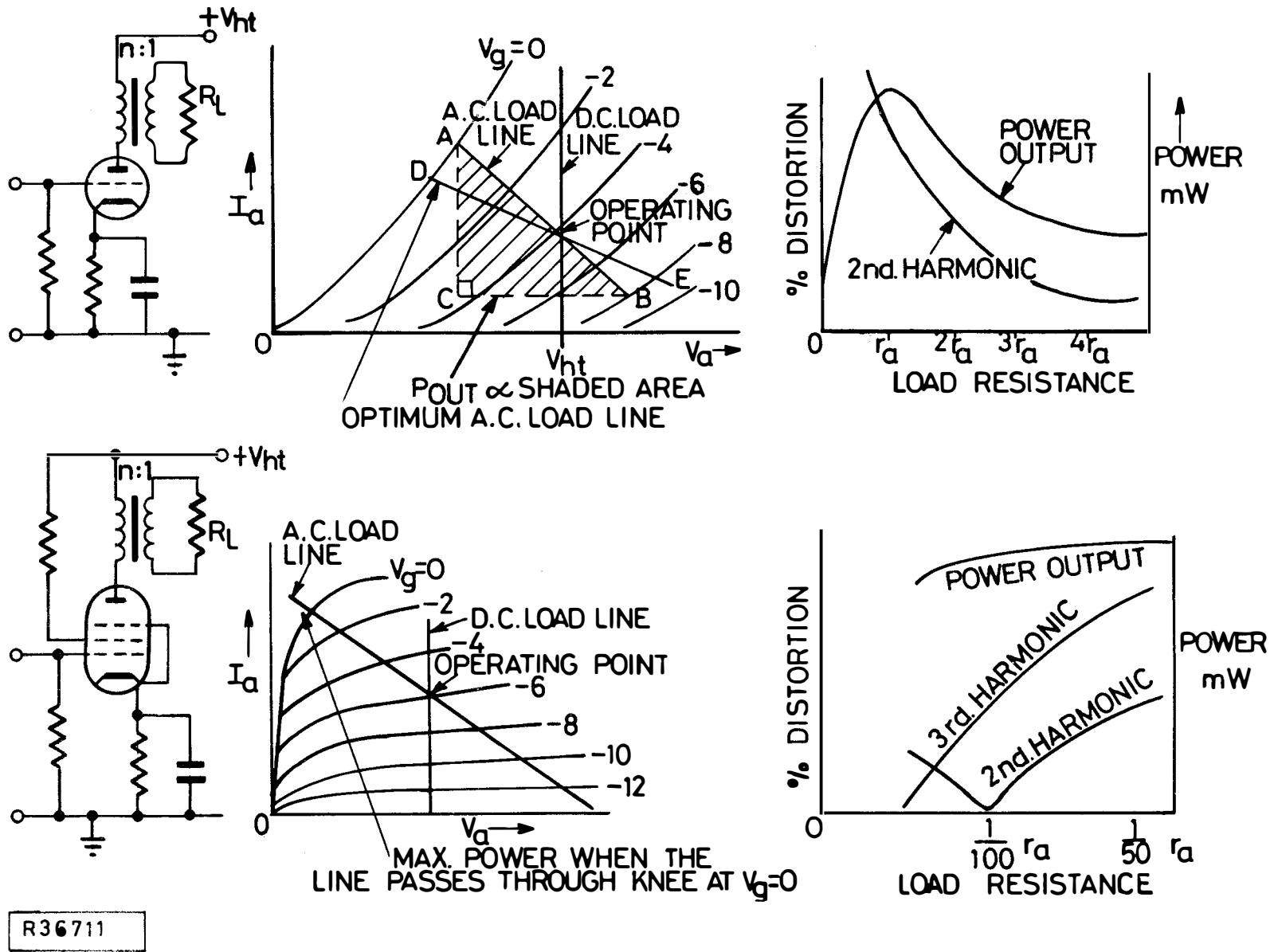


Fig. 9-17 Triode and Pentode anode power dissipation and the relationship between load resistance and harmonic distortion

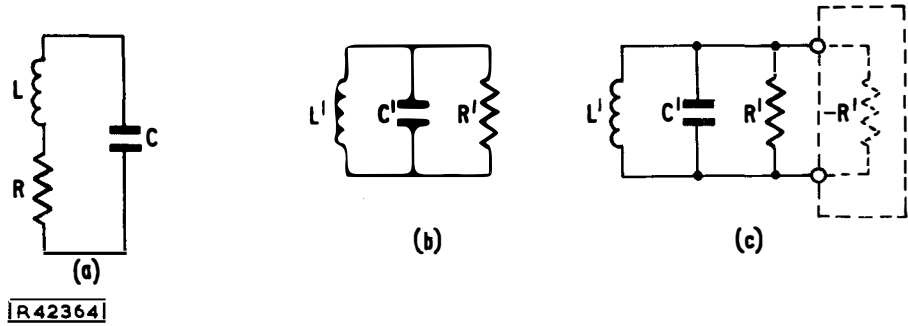


Fig. 10-1 Neutralizing the loss  $R^l$  by connecting a parallel negative resistance ( $-R^l$ )

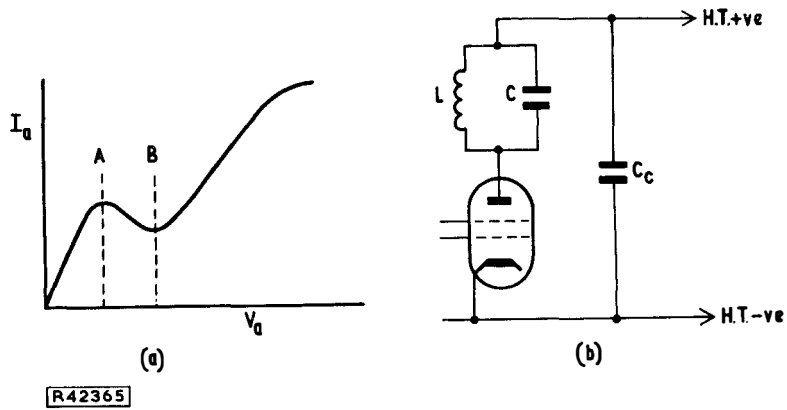
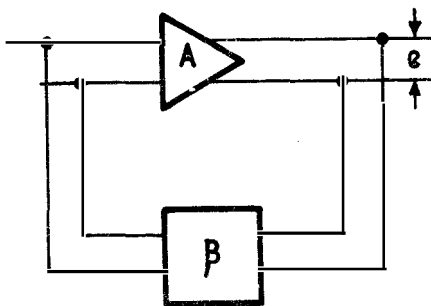


Fig. 10-2 Using the tetrode valve to provide  $-R^l$



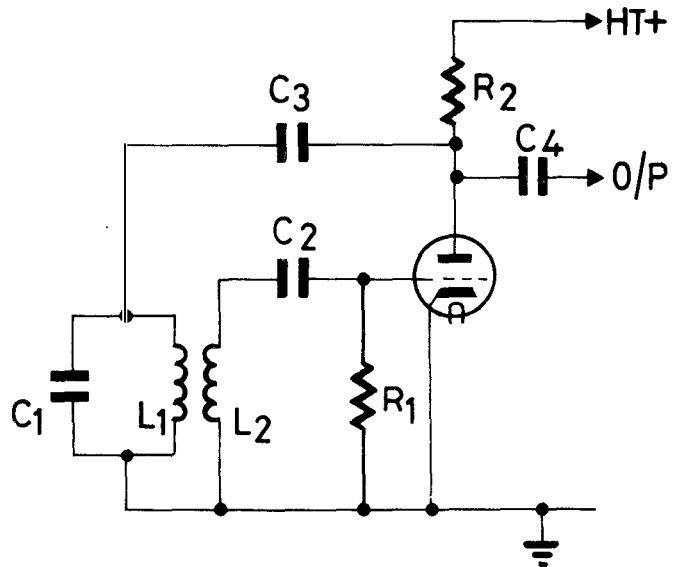
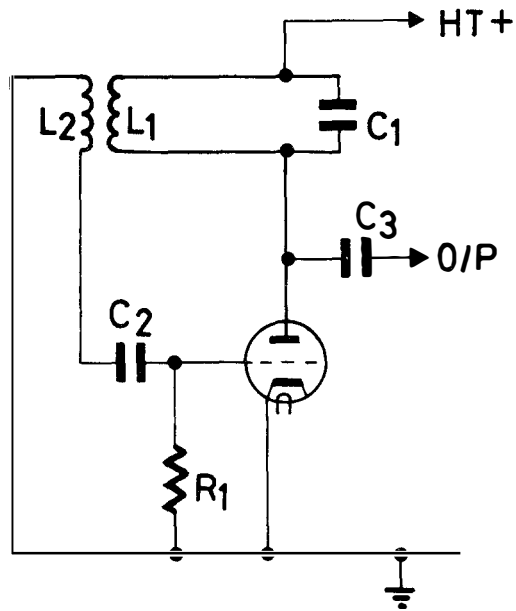
R42368

Condition for oscillation is when

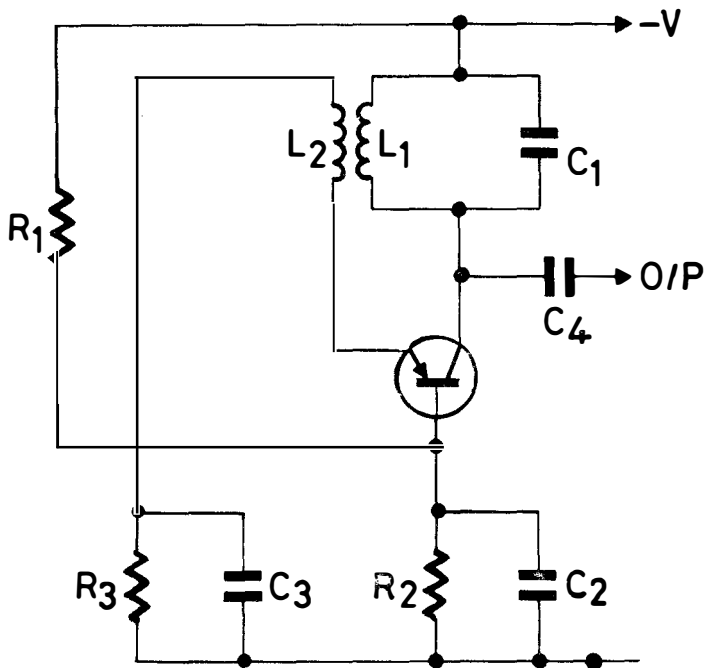
$$A\beta = 1/0 \text{ or } 1 + j0$$

Fig. 10-3 Principle of feedback oscillators

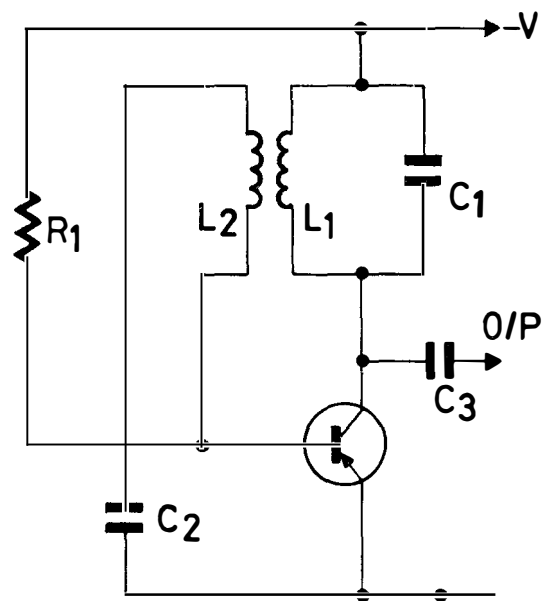




TUNED ANODE OSCILLATORS



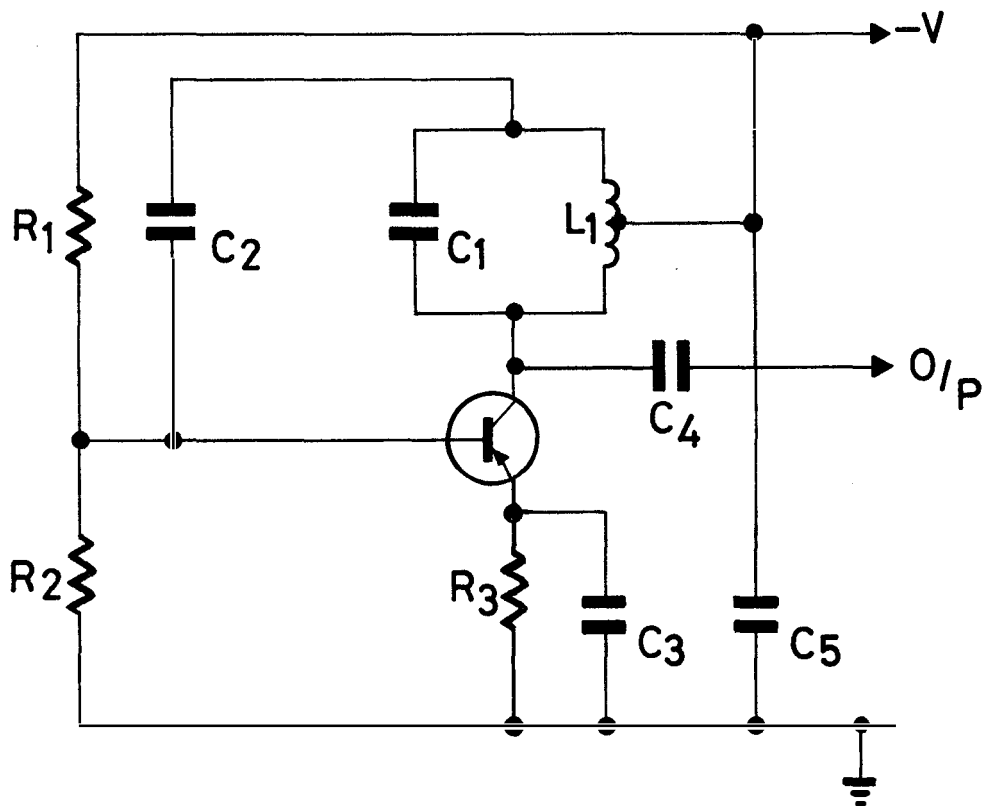
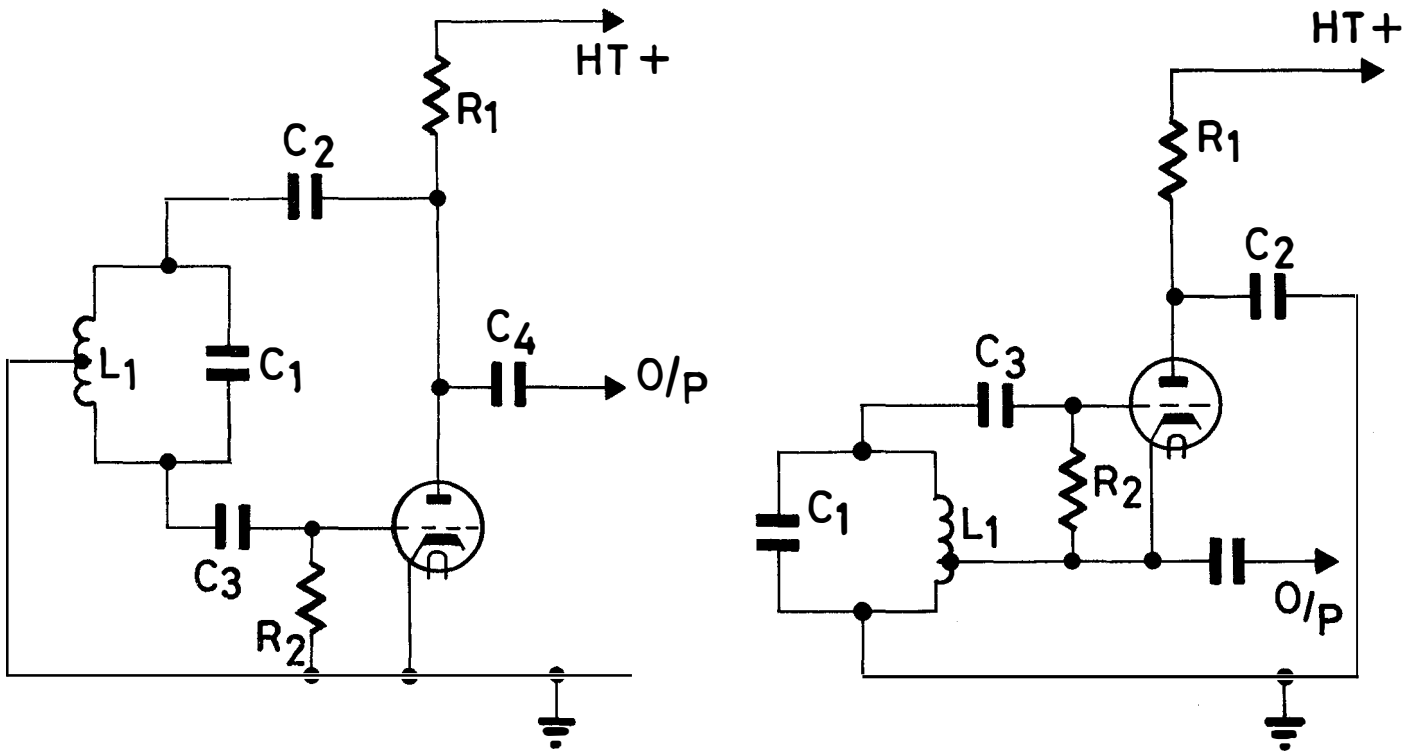
COMMON BASE TUNED COLLECTOR OSCILLATOR



COMMON EMITTER TUNED COLLECTOR OSCILLATOR

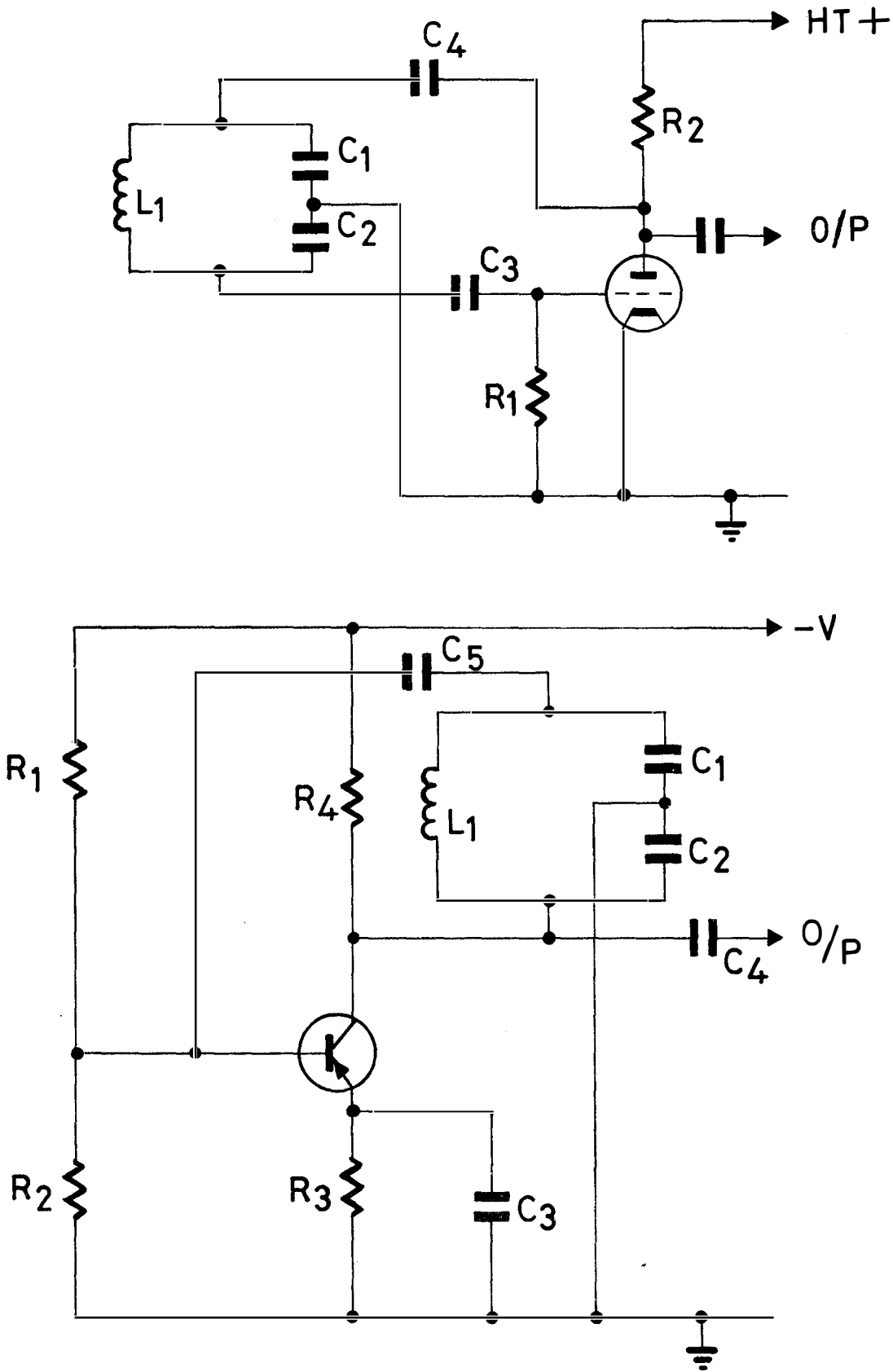
R 36712

Fig. 10-4 Tuned anode valve and transistor oscillators



R3 6713

Fig. 10-5 Hartley valve and transistor oscillators



R36714

Fig. 10-6 Colpitts valve and transistor oscillators

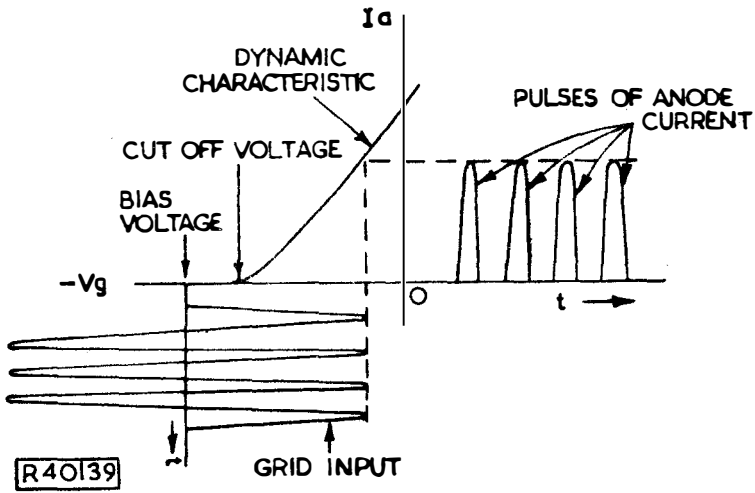


Fig. 10-7 Class C bias

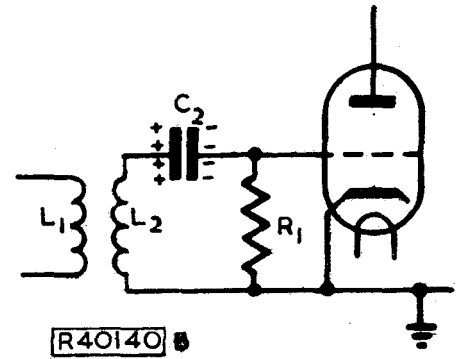


Fig. 10-8 Grid leak bias component arrangement

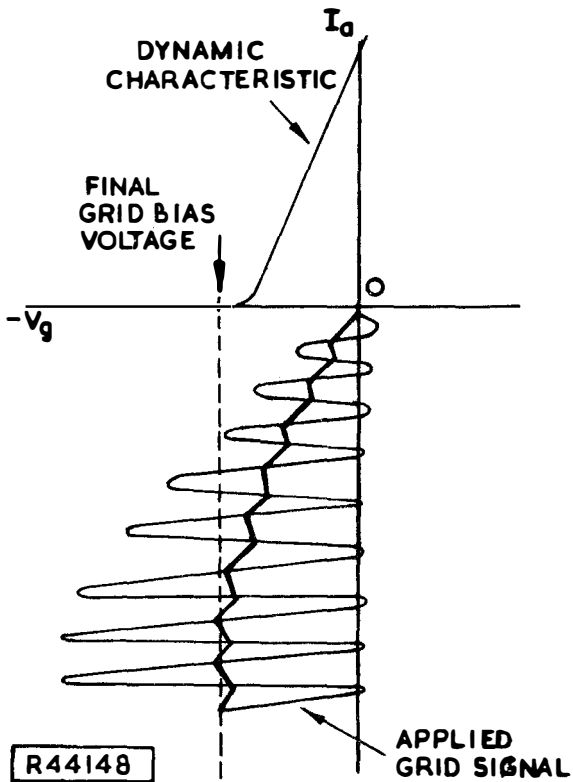


Fig. 10-10 Build up of bias voltage in the grid leak circuit

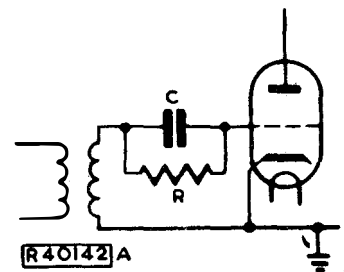
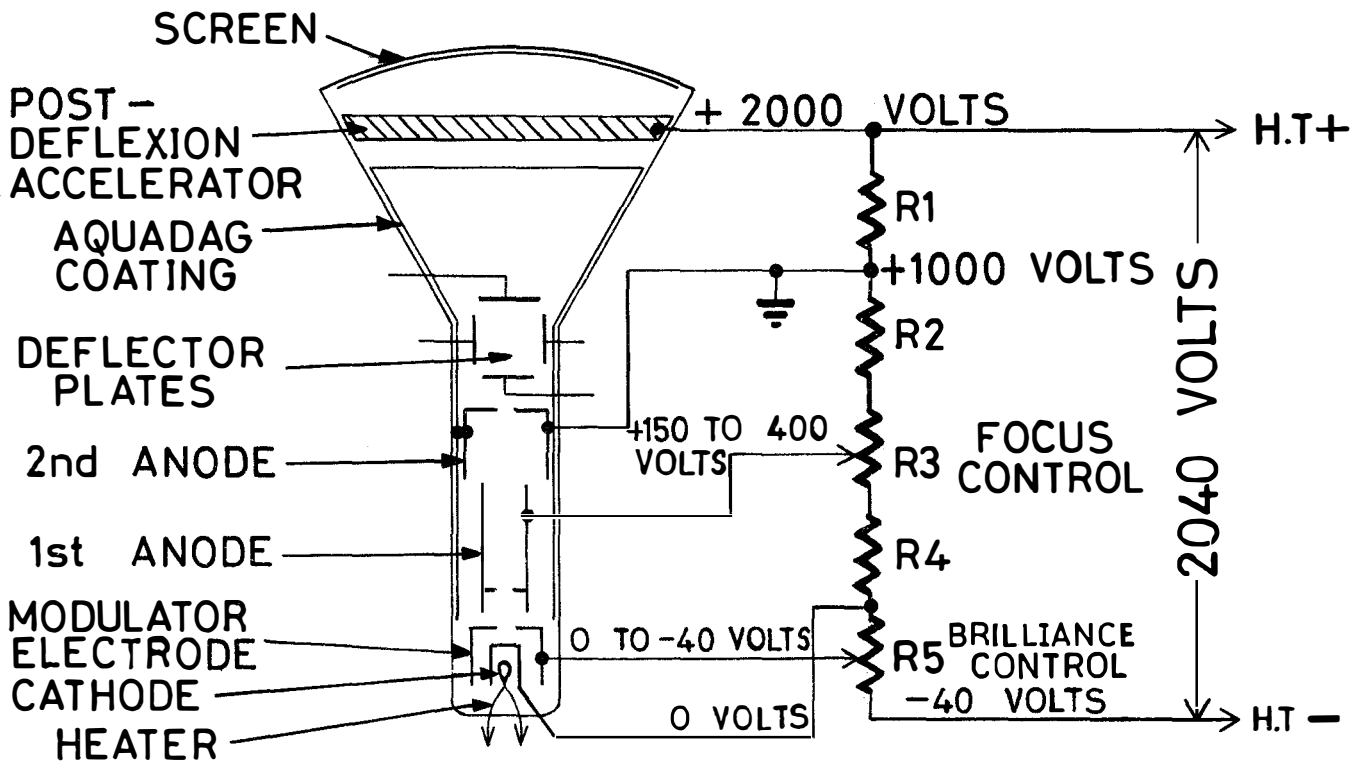
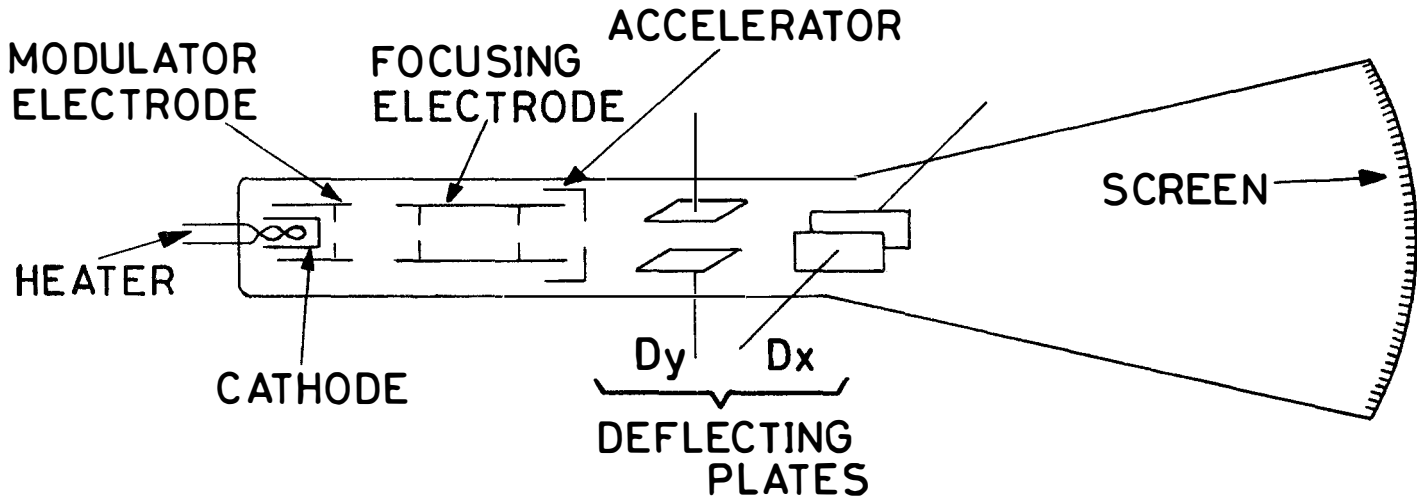
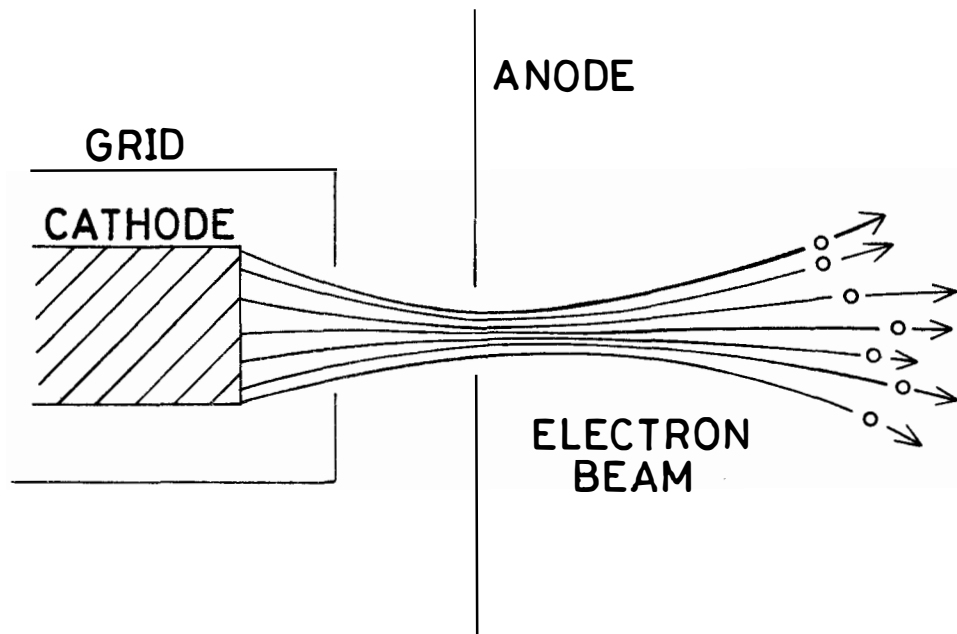
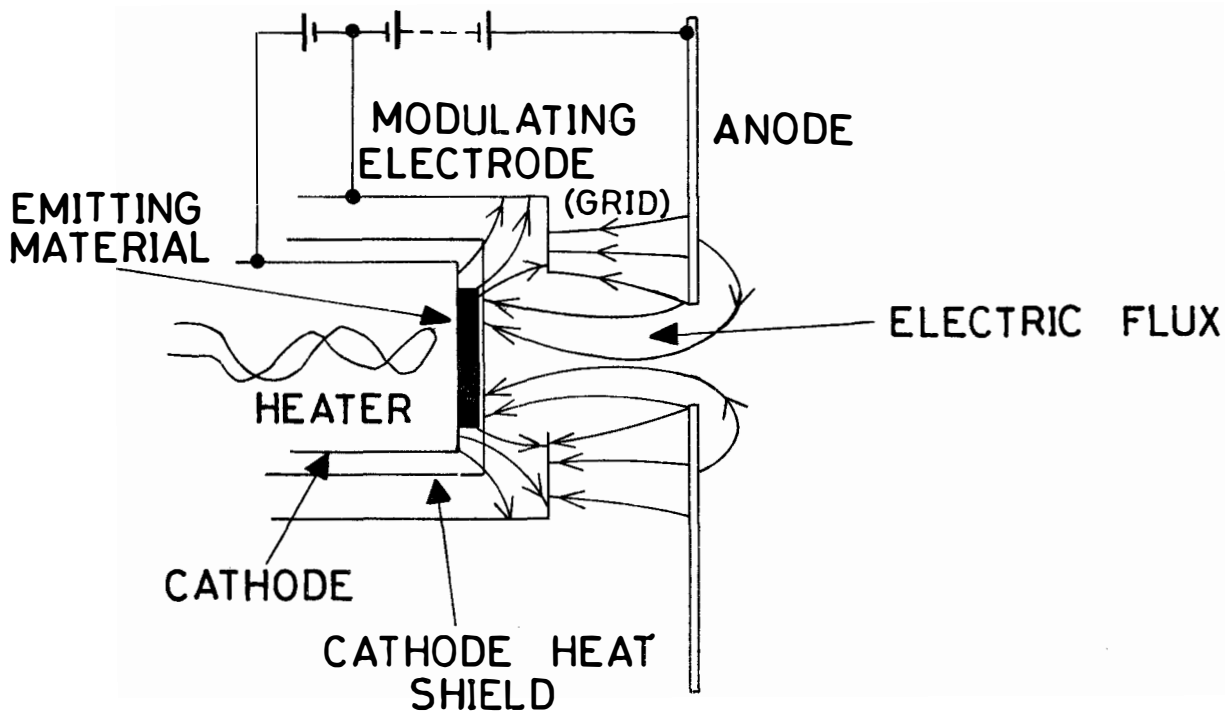


Fig. 10-9 Component variation



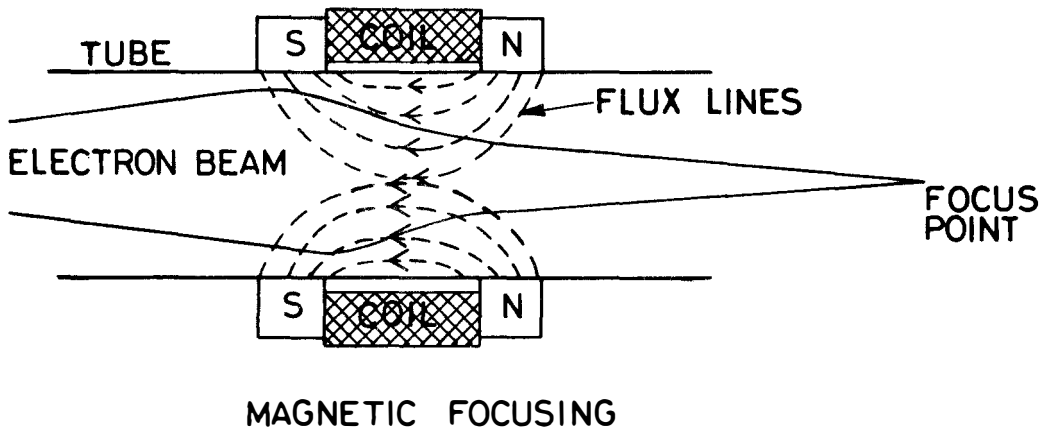
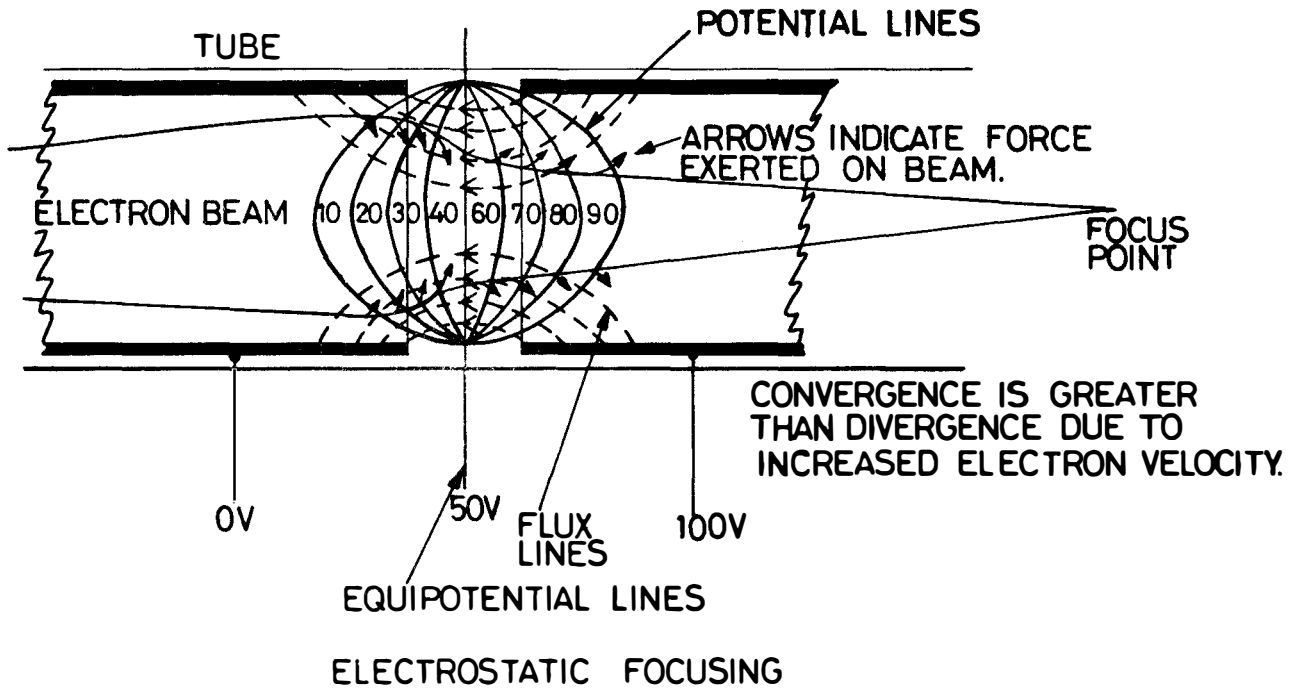
R 3 6 7 1 5

Fig. 11-1 Typical Cathode Ray Tube showing the arrangement of the electrodes and voltage supplies



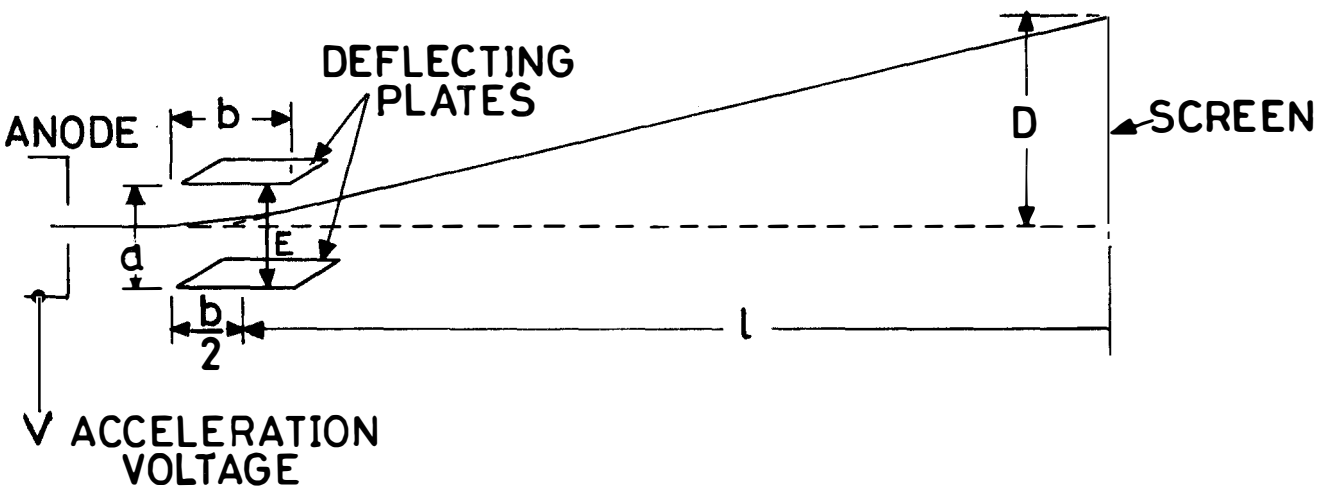
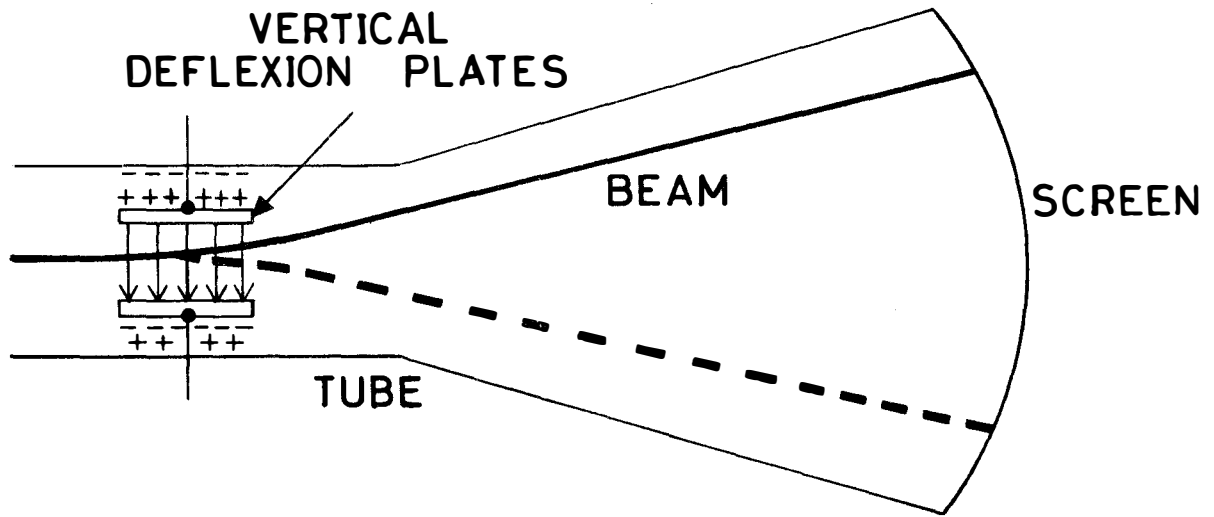
R 36 716

Fig. 11-2 Distribution of electric flux and the effect on an electron beam



R 36 717

Fig. 11-3 Comparison between electrostatic and magnetic focussing

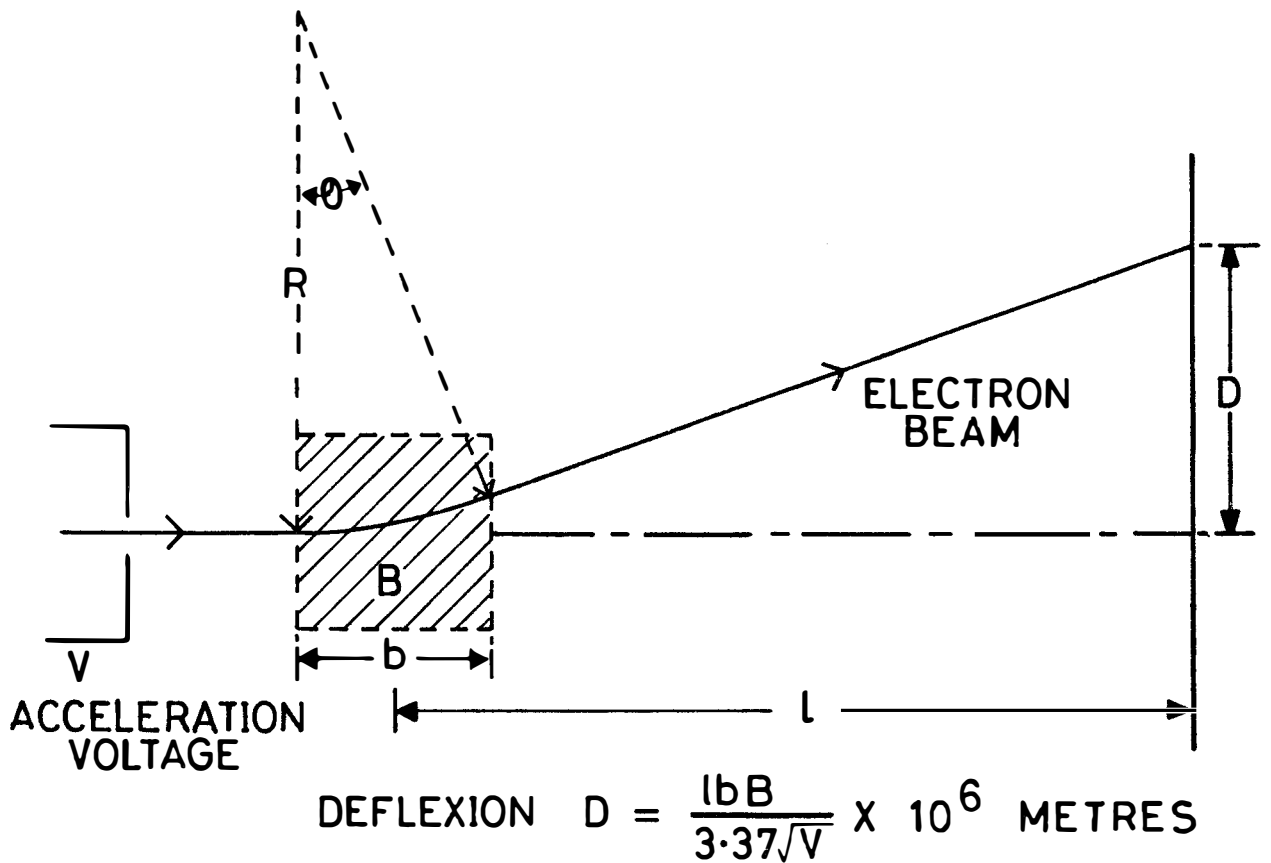
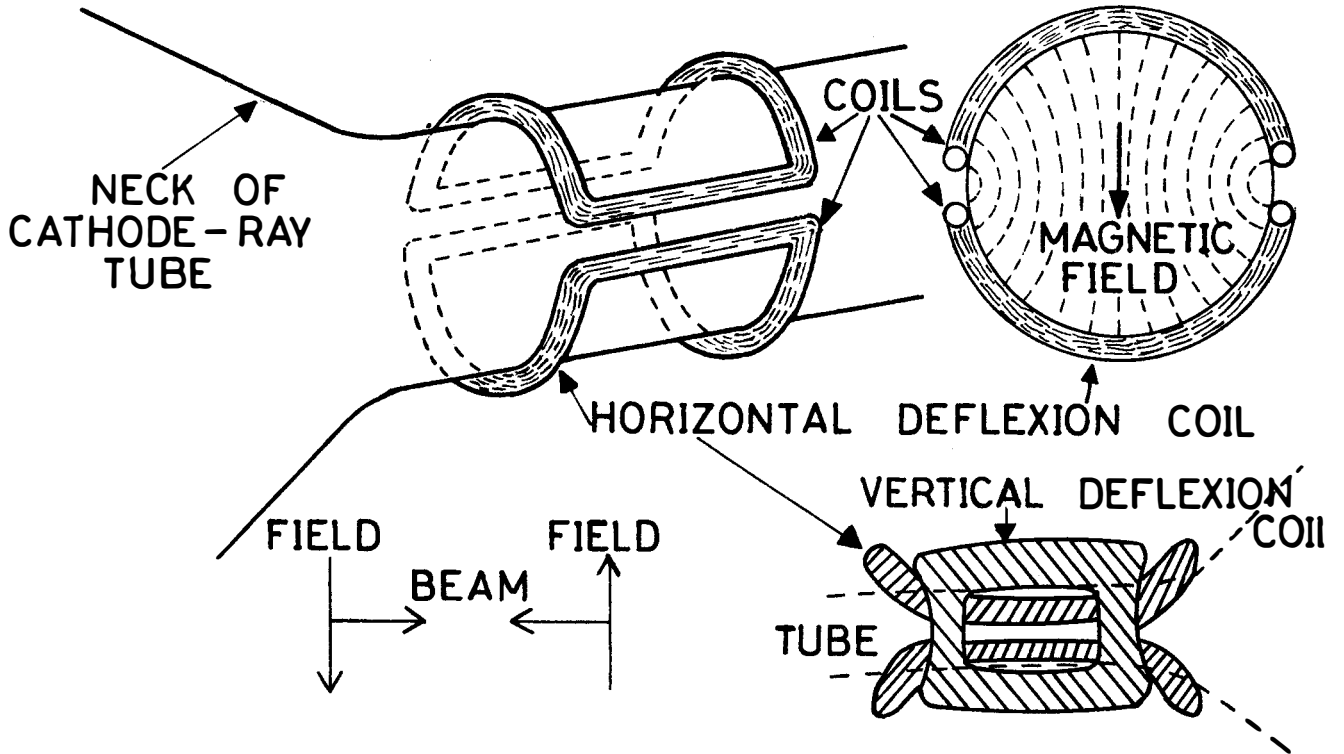


DEFLEXION  $D = \frac{Ebl}{2aV}$

R 3 6 7 1 8

Fig. 11-4 Electrostatic deflexion





R 36 719

Fig. 11-5 Electromagnetic deflexion

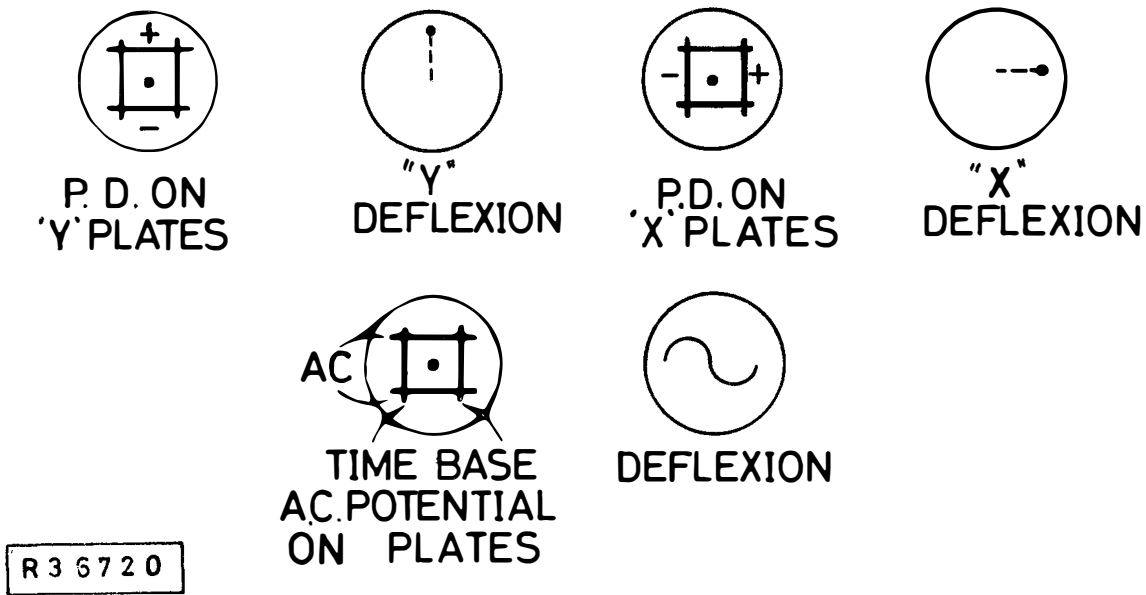


Fig. 11-6 Diagrams illustrating the effect of the deflexing plates on the electron beam

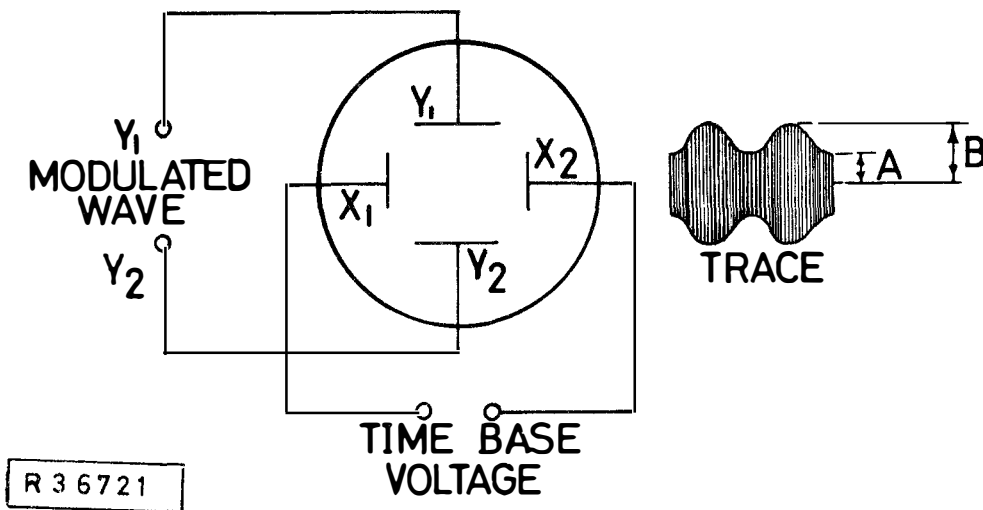


Fig. 11-7 C.R.T. display when the time base has twice the frequency of the modulating signal

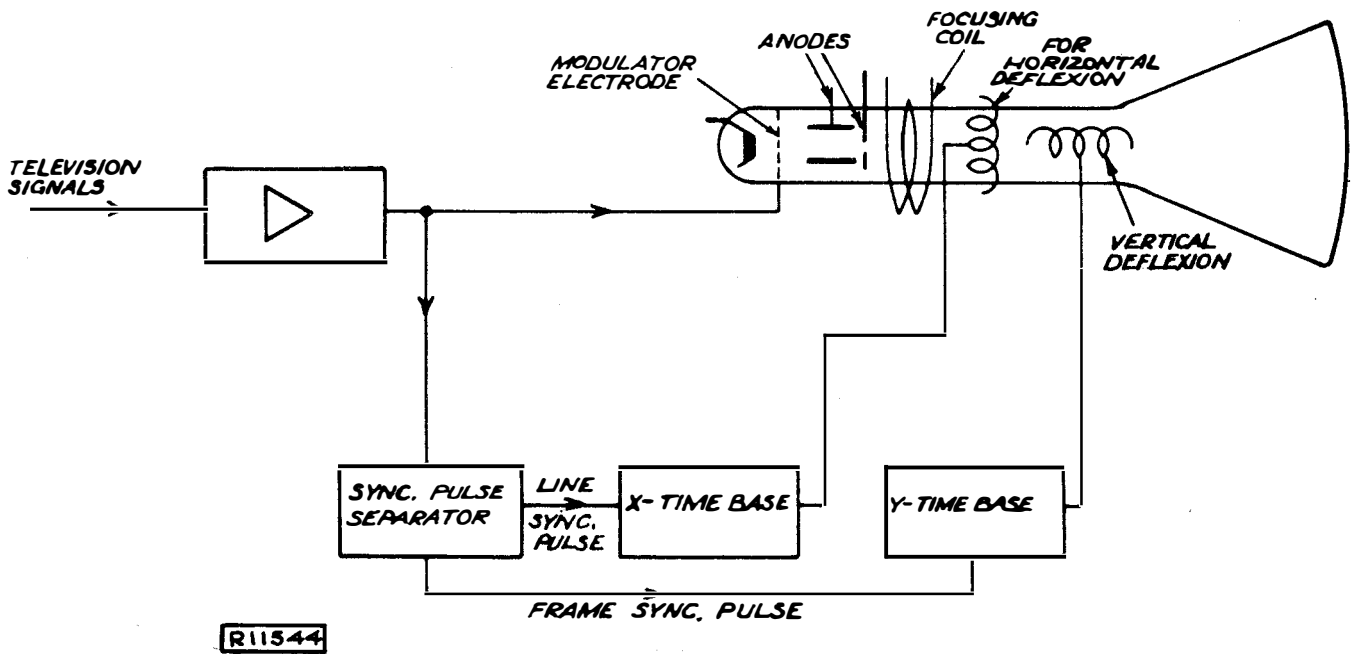


Fig. 11-8 Application of the C.R.T. in a television showing in block form the extraction of X and Y time base synchronizing pulses from the received signal

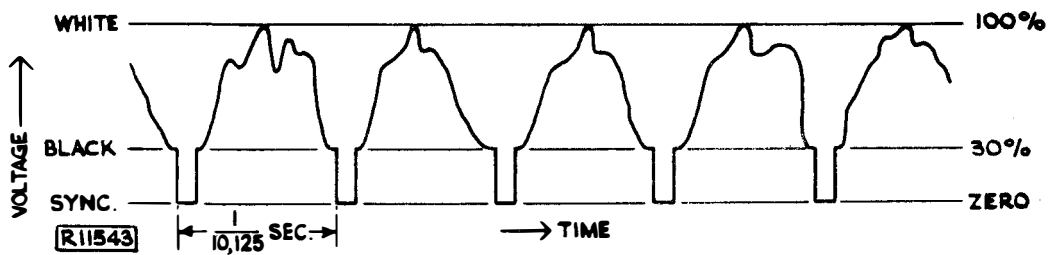


Fig. 11-9 Typical television signal. The portion from zero to 30% is used to synchronize the line and frame whilst that from 30% to 100% is used to modulate the electron stream

	Material	Activator	Chemical Composition	Fluorescent Colour	After-glow (seconds)
1	Zinc oxide	none	ZnO	Violet	
2	Zinc silicate	none	ZnO+SiO <sub>2</sub>	Blue	
3	Zinc silicate	Manganese	(ZnO+SiO <sub>2</sub> ):Mn	Blue-green	Medium 0.03-0.05
4	Zinc beryllium silicate	Manganese	(ZnO+BeO+SiO <sub>2</sub> ):Mn	Green to orange	Medium 0.05
5	Zinc sulphide	none	ZnS	Light blue	
6	Zinc sulphide	Silver	ZnS:Ag	Blue-violet	Medium 0.05
7	Zinc sulphide	Copper	ZnS:Cu	Green	Long > 1
8	4 and 6	as above		White	Short 0.005
9	Zinc sulphide	Silver with a nickel quencher	ZnS:Ag:Ni	Blue	Very short 10μs
10	Zinc cadmium sulphide	Silver	(ZnS+CdS):Ag	White	
11	Zinc cadmium sulphide	Copper	(ZnS+CdS):Cu	Yellow	Long > 1
12	Zinc borate	Manganese	(ZnO+B <sub>2</sub> O <sub>3</sub> ):Mn	Yellow-orange	
13	Zinc aluminate	Chromium	(ZnO+Al <sub>2</sub> O <sub>3</sub> ):Cr	Red	
14	Zinc germanate	Manganese	(ZnO+GeO <sub>2</sub> ):Mn	Yellow-green	
15	Zinc beryllium zirconium silicate	Manganese	[ZnO+BeO+(Ti-Zr-Th-O)+SiO <sub>2</sub> ]:Mn	White	
16	Calcium tungstate	none	CaWO <sub>4</sub>	Blue	Very short 5μs

Fig. 11-10 Characteristics of some luminescent screen materials